# Spherical Splines
for
# Hermite Interpolation and Surface Design

by

Jianbao Wu

(Under the direction of Ming Jun Lai)

## Abstract

The following dissertation consists of two parts. Throughout this dissertation, we assume that the spherical triangulation $\Delta$ could be a part of a sphere with or without holes, or the whole sphere $\mathbb{S}^2$. In the first part, given a set of function values and derivatives at scattered data locations over a spherical surface, we first use the minimal energy method to find a Hermite interpolation on the spherical spline spaces over a spherical triangulation $\Delta$ of the scattered data locations. We show that the minimal energy method produces a unique spherical Hermite interpolation spline of the given scattered data with derivatives. Also we show that the Hermite interpolatory surface converges to a given sufficiently smooth function $f$ in $L_2$ and $L_\infty$ norm if the values are obtained from this $f$. That is, the surface of the spherical Hermite interpolation spline resembles the given set of scattered data values and derivatives. Some numerical results are given to demonstrate our method. In the second part, for any integer $r \geq 0$, we first give a method of $C^r$ hole filling by the minimal energy quasi-Hermite interpolation method and delicate care of $C^r$ related boundaries. Then we present a method to deal with point cloud with $C^r$ continuity by using the minimal energy Hermite interpolation method or minimal energy quasi-Hermite interpolation method, and our surface can

interpolate these points and their derivatives if they are given. Several numerical experiments are presented to show our methods.

INDEX WORDS: Approximation, Approximation Order by Splines, Spherical Triangulation, Hermite Interpolation on-the-sphere, quasi-Hermite Interpolation on-the-sphere, Multivariate Splines, Homogeneous Splines, Spherical Splines, Geometric Continuity, Hole Filling, Data Fitting, Minimal Energy Method, Lagrange Multiplier Method, Matrix Iterative Method, Computer-Aided Geometry Design, Geophysics, Surface Modeling, Computer Graphics, Geodesy, Global Warming.

# Spherical Splines
for
# Hermite Interpolation and Surface Design

by

Jianbao Wu

M.S., Zhejiang University, 1992

B.S., Yunnan University, 1989

A Dissertation Submitted to the Graduate Faculty
of The University of Georgia in Partial Fulfillment
of the
Requirements for the Degree

Doctor of Philosophy

Athens, Georgia

2007

# Spherical Splines
for
# Hermite Interpolation and Surface Design

by

Jianbao Wu

Approved:

Major Professor: Ming Jun Lai

Committee: E. Azoff
C. McCrory
R. Varley
P. Wenston

Electronic Version Approved:

Maureen Grasso
Dean of the Graduate School
The University of Georgia
August 2007

## Dedication

Dedicated to my grandmother Guizhi Liu and my father Shengwen Wu

# Acknowledgments

First, I would like to thank my major professor Dr. Ming-Jun Lai for challenging me over the past graduate school years. I greatly appreciate the support and friendship from other members of my advisory committee, Dr. Edward A. Azoff, Dr. Clinton G. McCrory, Dr. Robert Varley, and Dr. Paul Wenston. Also I want to thank all the faculty, stuff, fellow students and friends who supported and helped me over these years. Especially thanks to Dr. David E. Galewski, Dr. Akos Magyar, Dr. Jingzhi Tie, Dr. Shuzhou Wang, Dr. Jie Zhou and Ms. Bree Ettinger for their support and kind help.

I deeply appreciate my father-in-law, my mother-in-law, sisters-in-law and brothers-in-law for their love and encouragement. I thank all ACCC(Athens Chinese Christian Church) members who have been my family here in Athens, with their concern and help. Especially thanks to Dr. Zhulu Lin and his wife Dr. Siew hoon Lim for their unselfish help over several years, Mrs. Alma Henderson in her eighties for her teaching Sunday school over these years. Also, I thank Mr. Liang Ouyang from the Church of the Nations for his help in faith.

I would like to thank my family, my wife Yang and my son John who has been the source of strength in my life. Especially I appreciate my wife Yang for her patience, sacrifices and support.

Finally, I greatly thank God for his grace, blessing and abundant love.

Table of Contents

## List of Figures

## List of Tables

# Chapter 1

# Introduction

Spline surfaces have been studied for more than 40 years, and have become very important tools in approximation theory and numerical analysis, cf. [14], [3] and [37]. They have found many applications in CAGD(computer-aided geometric design) which is concerned with the approximation and representation of curves and surfaces that arise when these objects have to be processed by a computer, CG(computer graphics), CAD(computer-aided design), signal processing, numerical solution of ordinary differential equations and partial differential equations, financial engineering etc., cf. [14], [3], [37], [9], [33], [36] and [15]. By far the most important spline surfaces are polynomial spline surfaces like classical Bézier patches defined on triangular and rectangular domains, B-spline surfaces defined on rectangular domains in terms of tensor product form and their extensions on higher dimension domains, and spherical splines defined on sphere. Interpolation and approximation are the main research interests. Many important achievements have been obtained, for example, the de Casteljau algorithm, subdivision algorithms and smoothness conditions connecting two surface patches, cf. [14], [13], [20], [3]. In particular, the most recent and important achievement is *ALW* method which enables us to use spline functions of any degree $d$ and any smoothness $r$ with $d \geq 3r + 2$ over a triangulation for numerical solution of partial differential equations and scattered data interpolation, cf. [9]. These results have been documented in [Lai & Schumaker'07] monograph, cf. [37].

The theory of spherical splines on triangulations of the sphere $\mathbb{S}^2$ in $\mathbb{R}^3$ have been developed by P. Alfeld, M. Neamtu, and L. L. Schumaker in a series of papers [3]-[5]. Spherical

splines are an interesting example for surfaces defined on surfaces and have important applications in geophysics and metrology which involve approximations of functions defined on the sphere, cf. [13] and [37]. Many theories of bivariate polynomial splines on planar triangulations carry over, but there are several significant differences because the sphere which is a closed manifold much different from planar domains. For example, the summation of barycentric coordinates is greater than one for any interior points while it is always one as in planar domains, computation of the derivatives of functions defined on sphere, integration of spherical splines over spherical triangulation and calculable spherical Sobolev space seminorms. In [40], M. Neamtu, and L. L. Schumaker studied approximation bounds of spherical splines on functions in Sobolev spaces on the sphere, where a spherical spline of degree $d$ is a $C^r$ function whose pieces are the restrictions of homogeneous polynomials of degree $d$ to the sphere. The bounds are expressed in terms of approximate seminorms defined with the help of a natural radial projection, and are obtained using appropriate quasi-interpolation operators. The derivatives of a Bézier-Bernstein polynomial defined on the sphere can be obtained by calculating the restriction of derivatives of its homogeneous extension to $\mathbb{R}^3$ on sphere $\mathbb{S}^2$.

Scattered data fitting has been studied widely. For planar domain case, Hermite interpolants in a triangulation of a planar domain was studied in [20], and the energy minimization method for scattered data Hermite interpolation has been studied recently in [48]. For spherical domain, minimal energy Lagrange interpolation using spherical splines was first studied in [4], then studied in [11] with a modification of energy functional, where triangulations in these papers are the whole sphere. In this dissertation, we first study the minimal energy method for Hermite interpolation problem on the sphere $\mathbb{S}^2$ in $\mathbb{R}^3$. The notion of spherical Hermite interpolation with first order directional derivatives was introduced in [22]. We use a general notation of Hermite interpolation discussed in [20] and [48] with a change of derivatives with respect to latitude and longitude direction. The Hermite interpolation problem does have an important practical application. In 2007, a satellite called GOCE (Gravity

field and steady-state Ocean Circulation Explorer) will be launched to collect gravitational vectors over sampling points around the Earth. Together with the geopotential data from CHAMP (CHAllenging Minisatellite Payload) which is a German small satellite mission for geoscientific and atmospheric research and its applications, we have location data and its derivatives up to second order for the geopotential function around the Earth, cf. [25]. The purpose of the satellite is to get a more accurate estimate of geopotential near the surface of the Earth. An important intermediate step is to estimate the geopotential very accurately at the orbital level of the satellite, cf. [12]. This motivates us to use spherical spline surfaces to solve Hermite interpolation problem over scattered data on the sphere, and make them resemble the shape of the given data values and approximate the geopotential very accurately.

On the second part of this dissertation, we study hole filling and $C^r$ scattered data smooth fitting with centralizable data. Scattered data interpolation and hole filling are important research questions and there are many papers about the planar domain case, e.g.,cf. [14], [16], [32], [34], [30] and [31]. For spherical domains, we use the minimal energy method for quasi-Hermite interpolation (cf. Definition 3.1.1) to deal with hole filling problem. Mainly we use this method to find a spherical spline surface satisfying Hermite interpolation conditions only at the vertices of boundary edges of curved polygon holes.

We always assume that the spherical triangulation $\Delta$ is a part of a sphere with or without holes, or the whole sphere throughout this dissertation. Our main contributions lie in the following.

- Given a set of scattered data with derivatives, we use minimal energy method to construct Hermite interpolation on spherical spline spaces over a spherical triangulation $\Delta$ of the scattered data locations. Then we show that the minimal energy method produces a unique Hermite spherical interpolation spline of given scattered data with derivatives. Finally we show that the Hermite interpolation spline converges to a given sufficiently smooth function $f$ in $L_2$ and $L_\infty$ if the values are obtained from this $f$.

Hence the surface of the Hermite spherical spline interpolation resembles the given set of derivatives.

- For any integer $r \geq 0$, we first give a method of $C^r$ hole filling using the minimal energy quasi-Hermite interpolation over a spherical triangulation of polygonal holes on the sphere. Then we implement several numerical experiments for $r = 0,\ 1,\ $ and $\ 2$ to demonstrate our method.

- For any integer $r \geq 0$, we deal with centralizable point cloud by using the minimal energy Hermite interpolation method or the quasi-Hermite interpolation method to get a surface with global $C^r$ continuity. Our surface can interpolate data locations and derivatives up to $r$th order if they are given. Also we implement experiments for $r = 0,\ 1,\ $ and $\ 2$ to show our method.

The organization of dissertation is as follows. Chapter 2 presents the basic topics of spherical splines as preliminaries. Chapter 3 addresses the minimal energy method for Hermite interpolation. Chapter 4 is devoted to surface design based on spherical splines, and it includes hole filling and $C^r$ scattered data fitting. The last chapter, Chapter 5, focuses on numerical experiments to support our methods and theories in Chapter 3 and Chapter 4.

# Chapter 2

# Preliminaries

In this chapter, we review well-established notations and theory in spline spaces defined on triangulations of the unit sphere $\mathbb{S}^2$ in $\mathbb{R}^3$. The spaces are natural analogs of the bivariate spline spaces discussed in [37], and are made up of pieces of trivariate homogeneous polynomials restricted to $\mathbb{S}^2$. Thus, they are piecewise spherical harmonics. As we shall see, virtually the entire theory of bivariate polynomial splines on planar triangulation carries over, although there are several significant differences. Spherical splines are an interesting example of surfaces defined on surfaces, and the sphere is a closed manifold much different from planar domain, cf. [13]. We divide this chapter into three sections, and discuss the basic theory of spherical splines and approximation properties of spherical splines.

## 2.1 Spherical triangulations and radial projection

In this section we introduce some basic notation, definitions and lemmas used throughout this dissertation. These contents including proof can be found in [40], [37] and [10]. Let $\mathbb{S}^2$ denote the unit sphere in $\mathbb{R}^3$. Given two points $u, v$ on $\mathbb{S}^2$ that are not **antipodal**, i.e., they do not lie on a line through the origin. Then the points $u$,$v$ divide the great circle passing through $u$,$v$ into two circular **arcs**. We write $\widehat{uv}$ for the shorter of the arcs. Its length is just the geodesic distance between $u$,$v$. Now let us give definitions for a spherical triangle, spherical triangulation and a regular spherical triangulation.

Definition 2.1.1. *Given three points $v_1, v_2$ and $v_3$ on the unit sphere $\mathbb{S}^2$ which lie strictly in one hemisphere. Then we define the associated* **spherical triangle** $\tau := < v1, v2, v3 >$ *to*

*be the set of points on* $\mathbb{S}^2$ *that lie in the region bounded by the three circular arcs* $\widehat{v_1v_2}$, $\widehat{v_2v_3}$ *and* $\widehat{v_3v_1}$, *which are called edges of the spherical triangle* $\tau$. *And the points* $v_1, v_2$ *and* $v_3$ *are called vertices of* $\tau$. *We say* $\tau$ *is* **non-degenerate** *if* $\tau$ *has nonzero area.*

DEFINITION 2.1.2. *A set of spherical triangles* $\Delta := \{T_i\}_1^N$ *is called a* **spherical triangulation** *provided that the intersection of two triangles in* $\Delta$ *is empty, or is a common vertex or common edge. We write* $\Omega := \bigcup_i^N T_i$ *for associated domain. If* $\Omega = \mathbb{S}^2$, *then we say that* $\Delta$ **covers** $\mathbb{S}^2$.

In this dissertation, we are interested in cases where $\Delta$ covers $\mathbb{S}^2$ and where $\Delta$ does not cover $\mathbb{S}^2$. Note that the hole filling problem is the second case. To state results on the relationship between the number $\#\mathcal{V}$ of vertices, number $\#E$ of edges, and number $\#T$ of triangles in a spherical triangulation, we have to distinguish between the cases when $\Delta$ covers $\mathbb{S}^2$ and when it does not. First we consider the case when $\Delta$ does not cover $\mathbb{S}^2$.

DEFINITION 2.1.3. *Let* $\Delta$ *be a spherical triangulation of a domain* $\Omega \subset \mathbb{S}^2$. *Then we say that* $\Delta$ *is* **shellable** *provided it consists of a single triangle, or if it can be obtained from a shellable triangulation of* $\tilde{\Delta}$ *by adding one triangle* $T$ *such that* $T$ *intersects* $\tilde{\Delta}$ *precisely along one or two edges. We say that* $\Delta$ *is* **regular** *provided that* $\Delta$ *is shellable, or it can be obtained from a shellable triangulation* $\tilde{\Delta}$ *by removing one or more shellable subtriangulations, all of whose vertices are interior vertices of* $\tilde{\Delta}$.

It is easy to show that for regular spherical triangulation that does not cover $\mathbb{S}^2$, exactly the same **Euler relations** as in the planar case hold.

THEOREM 2.1.4. *(Euler relations that* $\Delta$ *does not cover* $\mathbb{S}^2$, *cf. [37] ) Let* $\Delta$ *be a regular triangulation, and* $\#V_B$, $\#V_I$, $\#E_B$, $\#H$ *and* $\#T$ *denote the number of boundary vertices, interior vertices, boundary edges, holes and triangles respectively. Then we have*

*1)* $\#E_B = \#V_B$,

*2)* $\#E_I = 3\,\#V_I + V_B - 3 + 3\#H$,

*3)* $\#T = 2\#V_I + \#V_B - 2 + 2\#H$.

For case that $\Delta$ is regular and covers the whole unit sphere $\mathbb{S}^2$, we can state the following properties of $\Delta$( cf. [37]).

1) For $\Delta$ to exist the cardinality of $\mathcal{V}$ must be at least 4.

2) The number $\#E$ of edges of $\Delta$ is related to the number of triangles as $\#E = 3\#T/2$.

3) The number of vertices $\#\mathcal{V}$ and the number of triangles $\#T$ are related as $\#E = 3(\#\mathcal{V} - 2)$.

4) The number of vertices $\#\mathcal{V}$ and the number of triangles $\#T$ are related as $\#T = 2(\#\mathcal{V} - 2)$.

To study spherical spline space we need a notion of the size of a spherical partition.

Given a spherical triangle $\tau$ let $|\tau|$ denote the diameter of the smallest spherical cap containing $\tau$ and let $\rho_\tau$ denote the diameter of the largest spherical cap contained in $\tau$. Then

$$|\Delta| = \max\{|\tau|, \quad \tau \in \Delta\}$$

$$\rho_\Delta = \min\{\rho_\tau, \quad \tau \in \Delta\}$$

are correspondingly the diameter of the largest triangle in $\Delta$ and the diameter of the smallest spherical cap inscribed in $\Delta$.

Definition 2.1.5. *Let $\beta$ be a positive real number. A triangulation $\Delta$ is said to be $\beta$-***quasi-uniform** *provided that*

$$\frac{|\Delta|}{\rho_\Delta} \leq \beta.$$

It is well-known that in the planar case, the smallest angle of a quasi-uniform triangulation is bounded below by $1/\beta$, see [35]. We make use of a concept of a natural **radial projection** developed in [40] to relate properties of planar quasi-uniform triangulations to the spherical ones. It will be clear from our construction that we need to bound triangulation size. In order to use the results of [40], we need to choose this bound to be 1.

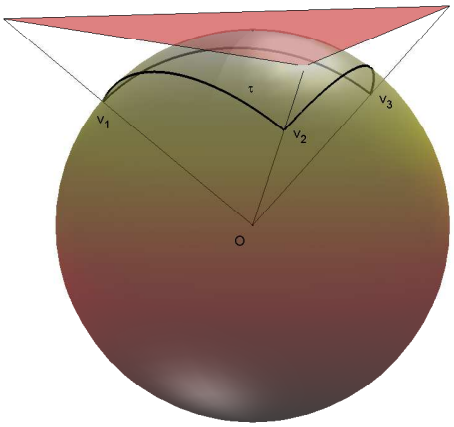


Figure 2.1: Radial mapping of a spherical triangle to a planar triangle.

DEFINITION 2.1.6. *(cf. [40]) Fix a spherical triangle $\tau$ with $|\tau| \leq 1$. Define $r_\tau$ to be the center of a spherical cap of smallest possible radius containing $\tau$, and let $\mathbf{T}_\tau$ be the tangent plane touching $\mathbb{S}^2$ at $r_\tau$ . We define the* **radial projection** *$R_\tau$ from $\mathbf{T}_\tau$ into $\mathbb{S}^2$ by*

$$w := R_\tau \bar{w} := \frac{\bar{w}}{|\bar{w}|} \in \mathbb{S}^2, \bar{w} \in \mathbf{T}_\tau.$$

*Since $R_\tau$ is one-to-one, $R_\tau^{-1}$ is well-defined. Let $\bar{\tau}$ be the image of $\tau$ under $R_\tau^{-1}$.*

Let $\rho_{\bar{\tau}}$ and $|\bar{\tau}|$ be diameters of the inscribed and outscribed circles of $\bar{\tau}$ correspondingly. It is not too difficult to check that

$$\begin{aligned} |\tau| \leq |\bar{\tau}| \leq K_1|\tau|, \\ K_2^{-1}\rho_\tau \leq \rho_{\bar{\tau}} \leq K_2\rho_\tau, \end{aligned} \tag{2.1.1}$$

for some positive constants $K_1$ and $K_2$ (cf. [40]). However we make use of the following

LEMMA 2.1.7. *(cf. [10]) Let $\tau$ be a spherical triangle with $|\tau| \leq 1$. Let $\bar{\tau}$ denote the image of $\tau$ under the map $R_\tau^{-1}$. Then*

$$2\tan\frac{|\tau|}{2} = |\bar{\tau}| \tag{2.1.2}$$

*and*

$$2\tan\frac{\rho_\tau}{2} \leq \rho_{\bar{\tau}}. \tag{2.1.3}$$

PROOF. By the definition of $R_\tau$ the center of the smallest spherical cap containing $\tau$ is the center of the circle outscribing $\bar{\tau}$. Let $\bar{v}$ be one of the vertices of $\bar{\tau}$. The center of the unit sphere $O$, $\bar{v}$ and $r_\tau$ form a right triangle with the leg $Or_\tau$ of length 1, the leg $\bar{v}r_\tau$ having length $\frac{|\bar{\tau}|}{2}$ and the angle $\angle\bar{v}Or_\tau$ having radian measurement $\frac{|\tau|}{2}$. Then (2.1.2) follows immediately.

The largest spherical cap $\sigma$ contained in $\tau$ is mapped onto an ellipse $\epsilon$ in the plane $\mathbf{T}_\tau$ which is contained in $\bar{\tau}$. The largest circle $\bar{\sigma}$ contained in $\bar{\tau}$ has a radius $\frac{\rho_{\bar{\tau}}}{2}$ greater than or equal to $r_\epsilon$ which is the radius of the largest circle contained in the ellipse. Let $o$ be the center of $\sigma$ and $v$ be any point on the boundary $\delta\sigma$ of the cap. Let $\bar{o}$ and $\bar{v}$ be the images of $o$ and $v$ under $R_\tau^{-1}$ respectively. Then $r_\epsilon$ can defined by $r_\epsilon := \min_{v\in\delta\sigma}\{|\bar{o}-\bar{v}|\}$. Note now that

$$|\bar{o}-\bar{v}| \geq \tan|o-v|, \forall v \in \delta\sigma.$$

Therefore

$$\frac{\rho_{\bar{\tau}}}{2} \geq r_\epsilon \geq \tan\frac{\rho_\tau}{2}$$

and we have (2.1.3). □

Since great circles are mapped into straight lines under the inverse of the radial projection $R_\tau$, any cluster of spherical triangles $\omega$ with $|\omega| \leq 1$ is mapped into a planar triangulation $\bar{\omega}$.

LEMMA 2.1.8. *(cf. [10], [37]) Let $\Delta$ be a $\beta$-quasi-uniform triangulation of the unit sphere with $|\Delta| \leq 1$. Let $\Theta_\Delta$ denote the smallest angle of $\Delta$. There exists a constant $A_1$ such that*

$$\Theta_\Delta \geq \frac{1}{A_1\beta}. \tag{2.1.4}$$

PROOF. Fix a spherical triangle $\tau \in \Delta$ and construct the radial projection $R_\tau$. By Lemma 2.1.7 we have

$$\frac{|\bar{\tau}|}{\rho_{\bar{\tau}}} \leq \frac{\tan\frac{|\tau|}{2}}{\tan\frac{\rho_\tau}{2}} \leq 2\tan\frac{1}{2}\,\beta.$$

Since $\bar{\tau}$ is a planar triangle, its every angle is bounded below by $\frac{1}{A_1\beta}$ with $A_1 := 2\tan\frac{1}{2}$. Since the corresponding spherical angles are even greater (2.1.4) follows. □

We will need another lemma comparing areas $A_\tau$ of spherical triangles to the size parameters $|\Delta|$ and $\rho_\Delta$ characterizing spherical triangulations.

LEMMA 2.1.9. *(cf. [10], [37])For every spherical triangle $\tau \in \Delta$ with $|\Delta| \leq 1$*

$$\frac{\pi\rho_\Delta^2}{5} \leq A_\tau \leq \frac{\pi|\Delta|^2}{4}. \tag{2.1.5}$$

PROOF. The area $A_\tau$ of a spherical triangle is bounded above by the area of the smallest spherical cap containing $\tau$. The diameter of this cap is $|\tau|$. Without loss of generality we assume that the center of this cap is located at the north pole. Then

$$A_\tau \leq \int_0^{2\pi}\int_0^{|\tau|/2} \sin\eta d\eta d\theta = 2\pi(1-\cos(|\tau|/2)) \leq \pi\frac{|\Delta|^2}{4}.$$

Similarly, $A_\tau$ is bounded below by the area of the largest spherical cap contained in $\tau$, which by the definition has a diameter $\rho_\tau$. Therefore

$$A_\tau \geq 2\pi(1-\cos(\rho_\tau/2)) \geq \frac{\pi\rho_\Delta^2}{5}.$$

□

Another result that we need concerning $\beta$-quasi-uniform triangulations is a bound on the number of triangles $n_k$ in the $k$-th disk around $\tau$. We denote the union of all triangles in $\Delta$ that share the vertex $v$ by $\mathrm{star}^1(v)$. Define recursively

$$\mathrm{star}^\ell(v) := \cup\{\mathrm{star}^1(w) : w \text{ is a vertex of } \mathrm{star}^{\ell-1}(v)\}, \ell > 1,$$

and

$$\mathrm{star}^\ell(\tau) := \cup\{\mathrm{star}^\ell(w) : w \text{ is a vertex of } \tau\}, \ell > 1.$$

LEMMA 2.1.10. *(cf. [37])Suppose $\Delta$ is a $\beta$-quasi-uniform triangulation such that $|\Delta| \leq 1$. Then for any triangle $\tau \in \Delta$ and any $k \geq 0$ the number $n_k$ of triangles in star$^k(\tau)$ is*

$$n_k \leq \frac{5\beta^2}{4}(2k+1)^2, \tag{2.1.6}$$

*and*

$$n_k \geq \frac{2}{\pi\beta^2}(2k+1)^2. \tag{2.1.7}$$

PROOF. Note that star$^k(\tau)$ is contained in a spherical cap of radius $R = (2k+1)\frac{|\Delta|}{2}$ and area $A_R = 2\pi(1-\cos R)$. By Lemma 2.1.9 we have

$$\frac{\pi\rho_\Delta^2}{5} \leq A_\tau.$$

Then

$$n_k\frac{\pi\rho_\Delta^2}{5} \leq A_R = 2\pi(1-\cos R) \leq \pi R^2.$$

Therefore

$$n_k \leq \frac{5\beta^2(2k+1)^2}{4}.$$

On the other hand, star$^k(\tau)$ contains a spherical cap of radius $r = (2k+1)\frac{\rho_\Delta}{2}$ and area $A_r = 2\pi(1-\cos r)$. Then by Lemma 2.1.9

$$2r^2 \leq 2\pi(1-\cos r) = A_r \leq n_k\frac{\pi|\Delta|^2}{4},$$

therefore

$$n_k \geq \frac{2(2k+1)^2}{\pi\beta^2}.$$

□

## 2.2 SPHERICAL POLYNOMIALS

In this section, we introduce the key buildings for spherical splines. Throughout this dissertation, we write $v$ for a point on the unit sphere $\mathbb{S}^2$ in $\mathbb{R}^3$, when there is no confusion. At times we will also use $v$ to denote the corresponding unit vector. Before introducing spherical polynomials, first we need to discuss spherical barycentric coordinates.

### 2.2.1 Spherical barycentric coordinates

In this subsection we define an analog of planar barycentric coordinates on the sphere and analyze some of their basic properties as well as two important differences as compared to planar barycentric coordinates. We start by introducing a special set of coordinates in $\mathbb{R}^3$ which will be used later to construct barycentric coordinates on the sphere, see [3].

Definition 2.2.1. *(cf. [3]) Let $V := \{\mathbf{v_1}, \mathbf{v_2}, \mathbf{v_3}\}$ be a basis for $\mathbb{R}^3$. We call*

$$\mathcal{T} := \{v \in \mathbb{R}^3 : \mathbf{v} = b_1\mathbf{v_1} + b_2\mathbf{v_2} + b_3\mathbf{v_3},\ b_i \geq 0\} \tag{2.2.1}$$

*the trihedron generated by $V$. Each $\mathbf{v} \in \mathbb{R}^3$ can be written in the form*

$$\mathbf{v} = b_1\mathbf{v_1} + b_2\mathbf{v_2} + b_3\mathbf{v_3}. \tag{2.2.2}$$

*We call $b_1, b_2, b_3$ the* **trihedral coordinates** *of $v$ with respect to $V$.*

Equation (2.2.2) defining the trihedral coordinates can be written as a system of three equations for $b_i$'s:

$$\begin{bmatrix} v_1^x & v_2^x & v_3^x \\ v_1^y & v_2^y & v_3^y \\ v_1^z & v_2^z & v_3^z \end{bmatrix} \begin{bmatrix} b_1 \\ b_2 \\ b_3 \end{bmatrix} = \begin{bmatrix} v^x \\ v^y \\ v^z \end{bmatrix},$$

where $v^x$ denotes the $x$-coordinate of $\mathbf{v}$, etc. The matrix above is nonsingular since $\mathbf{v_1}, \mathbf{v_2}, \mathbf{v_3}$ are linearly independent. Using Crammer's rule we immediately have

$$b_1 = \frac{\det(v, v_2, v_3)}{\det(v_1, v_2, v_3)},\ b_2 = \frac{\det(v_1, v, v_3)}{\det(v_1, v_2, v_3)},\ b_3 = \frac{\det(v_1, v_2, v)}{\det(v_1, v_2, v_3)}, \tag{2.2.3}$$

where

$$\det(v_1, v_2, v_3) = \det \begin{bmatrix} v_1^x & v_2^x & v_3^x \\ v_1^y & v_2^y & v_3^y \\ v_1^z & v_2^z & v_3^z \end{bmatrix}$$

and so forth. Equations above show that the $b_i$'s are ratios of volumes of tetrahedra.

The concept of homogeneity plays a very important role in the construction of spherical spline functions. Let us present a formal definition and relate it to trihedral coordinates.

DEFINITION 2.2.2. *(cf. [3], [4], [37])Given an arbitrary integer d,a trivariate function F is said to be* **homogeneous of degree** *d provided that for every real number* $\alpha \neq 0$,

$$F(\alpha v) = \alpha^d F(v), \quad v \in \mathbb{R}^3 \backslash \{0\}. \tag{2.2.4}$$

*Let*

$$\mathcal{H}_d := \{p \in \mathcal{P}_d : p \text{ is homogeneous of degree } d\},$$

*where* $\mathcal{P}_d$ *is the space of trivariate polynomials of degree d. Then we refer to* $\mathcal{H}_d$ *as the* **space of homogeneous trivariate polynomials of degree d**.

By definition, we have $b_i(\alpha v) = \alpha b_i(v)$ for all $\alpha \in \mathbb{R}$, $i = 1, 2, 3$, this implies that the $b_i$'s are homogeneous linear functions of $v$ of degree of homogeneity 1.

We summaries some additional properties of trihedral coordinates in the following

LEMMA 2.2.3. *(cf. [3])*

*1)* $\{b_i(v), i = 1, 2, 3\}$ *is a linearly independent set,*

*2) If* $\mathcal{L}$ *is the space of trivariate linear homogeneous polynomials, then* $\mathcal{L} = span\{b_1, b_2, b_3\}$,

*3)* $b_i(v_j) = \delta_{ij}, i, j = 1, 2, 3$,

*4)* $b_i(v) > 0$ *for all* $v$ *in the interior of trihedron* $\mathcal{T}$.

PROOF. 1) Suppose there are scalars $\alpha_1, \alpha_2, \alpha_3$ such that

$$\alpha_1 b_1(v) + \alpha_2 b_2(v) + \alpha_3 b_3(v) = 0, \forall v \in \mathbb{R}^3. \tag{2.2.5}$$

Define $\mathbf{v_0} := \alpha_1 \mathbf{v_1} + \alpha_2 \mathbf{v_2} + \alpha_3 \mathbf{v_3}$. By uniqueness of trihedral coordinates, we must have

$$\alpha_i = b_i(v_0), i = 1, 2, 3.$$

Then (2.2.5) implies

$$\sum_{i=1}^{3} \alpha_i^2 = 0,$$

and thus $\alpha_i = 0, i = 1, 2, 3$.

2) Since $b_i$'s are homogeneous linear functions, clearly

$$\text{span}\{b_1, b_2, b_3\} \subset \mathcal{L}$$

Let $P(x,y,z) = ax+by+cz+d \in \mathcal{L}$. Since $P(x,y,z)$ is linearly homogeneous $P(\alpha x, \alpha y, \alpha z) = \alpha P(x,y,z), \forall \alpha \in \mathbb{R}$. Choose $\alpha \neq 1$. Then we must have

$$\alpha(ax+by+cz)+d = \alpha(ax+by+cz)+\alpha d$$

and thus $d = 0$. Then $P(x,y,z) = ax+by+cz$, and $\mathcal{L} = \text{span}\{x,y,z\}$. Since $x,y,z$ are linearly independent $\dim(\mathcal{L}) = 3$. Since $b_1, b_2, b_3$ are linearly independent and $\dim(\text{span}\{b_1,b_2,b_3\}) = 3$, $\mathcal{L} = \text{span}\{b_1,b_2,b_3\}$.

3) Consider for some $v_j, j = 1,2,3$,

$$\mathbf{v_j} = \sum_{i=1}^{3} b_i(v_j)\mathbf{v_i}.$$

Then

$$(b_j(v_j)-1)\mathbf{v_j} + \sum_{i=1, i\neq j}^{3} b_i(v_j)\mathbf{v_i} = 0.$$

Since $\mathbf{v_i}$'s are linearly independent we must have

$$b_j(v_j) = 1$$

$$b_i(v_j) = 0, i \neq j.$$

4) If $b_i(v) = 0$ for some $i$, then $\mathbf{v} = \sum_{j=1,j\neq i}^{3} b_j(v)\mathbf{v_j}$. Hence $\mathbf{v} \in \text{span}\{b_j, j \neq i\}$, thus $v$ is not in the interior of $\mathcal{T}$. Thus if $v$ is in the interior of $\mathcal{T}$ we must have $b_i(v) \neq 0$ for all $i$. By the definition of $\mathcal{T}$ $b_i(v) > 0$ for $i = 1,2,3$, and all $v$ in the interior of $\mathcal{T}$. □

THEOREM 2.2.4. *(cf. [3]) Let $R$ be any nonsingular matrix. Then*

$$b_i^R(Rv) = b_i(v), \ i = 1,2,3, \tag{2.2.6}$$

*where $b_i^R$ are the trihedral coordinates of $Rv$ with respect to $\{R\mathbf{v_1}, R\mathbf{v_2}, R\mathbf{v_3}\}$.*

PROOF. Multiplying (2.2.2) by $R$, we have

$$R\mathbf{v} = b_1 R\mathbf{v_1} + b_2 R\mathbf{v_2} + b_3 R\mathbf{v_3}.$$

Since $R$ is nonsingular matrix, so $det(R) \neq 0$. Using Crammer's rule we immediately have

$$b^R{}_1(Rv) = \frac{\det(Rv, Rv_2, Rv_3)}{\det(Rv_1, Rv_2, Rv_3)} = \frac{det(R)\det(v, v_2, v_3)}{det(R)\det(v_1, v_2, v_3)},$$

$$b^R{}_2(Rv) = \frac{\det(Rv_1, Rv, Rv_3)}{\det(Rv_1, Rv_2, Rv_3)} = \frac{det(R)\det(v_1, v, v_3)}{det(R)\det(v_1, v_2, v_3)},$$

$$b^R{}_3(Rv) = \frac{\det(Rv_1, Rv_2, Rv)}{\det(Rv_1, Rv_2, Rv_3)} = \frac{det(R)\det(v_1, v_2, v)}{det(R)\det(v_1, v_2, v_3)}$$

where

$$\det(v_1, v_2, v_3) = \det \begin{bmatrix} v_1^x & v_2^x & v_3^x \\ v_1^y & v_2^y & v_3^y \\ v_1^z & v_2^z & v_3^z \end{bmatrix}$$

Therefore, $b^R{}_1(Rv) = b_1(v),\ b^R{}_2(Rv) = b_2(v),\ b^R{}_3(Rv) = b_3(v)$. □

THEOREM 2.2.5. *(cf. [3]) The three planes spanned by pairs of the* $\mathbf{v_i}$*'s divide* $\mathbb{R}^3$ *into eight trihedra. The functions* $b_1, b_2, b_3$ *have constant signs on each of the eight trihedra. In particular,* $v \in \mathcal{T}$ *if and only if* $b_i \geq 0,\ i = 1, 2, 3$.

PROOF. Let $\mathcal{T}^{ijk}$ denote a trihedron generated by $\{(-1)^i\mathbf{v_1}, (-1)^j\mathbf{v_2}, (-1)^k\mathbf{v_3}\}$, $i, j, k \in \{0, 1\}$. Note that $\mathcal{T}^{000} = \mathcal{T}$ and each of the eight trihedra can be described this way. Fix $i, j, k$. We show that for all $v$ in the interior of $\mathcal{T}^{ijk}$ $b_1^{000}$ ($b_1(v)$ with respect to $\mathcal{T}$) has a constant sign.

Let $b_1^{ijk}$ be the first trihedral coordinate of $v$ in the interior of $\mathcal{T}^{ijk}$ with respect to $\mathcal{T}^{ijk}$. Note that by Lemma 2.2.3, $b_1^{ijk}(v) > 0$ for any such $v$. Then

$$b_1^{ijk}(v) = \frac{\det(v, (-1)^j v_2, (-1)^k v_3)}{\det((-1)^i v_1, (-1)^j v_2, (-1)^k v_3)}$$

$$= (-1)^i \frac{\det(v, v_2, v_3)}{\det(v_1, v_2, v_3)} = (-1)^i b_1^{000}(v).$$

Since $b_1^{ijk}(v) > 0$ by above $b_1^{000}$ has a constant sign in the interior of $\mathcal{T}^{ijk}$. □

Now we introduce spherical barycentric coordinates and relate their properties to the set of trihedral coordinates. We also describe the two important differences between planar barycentric coordinates and spherical barycentric coordinates.

DEFINITION 2.2.6. *(cf. [3]) Assume intersection of $\mathbb{S}^2$ with the trihedron $\mathcal{T}$ generated by $V$ is a spherical triangle $\tau$, then the* **spherical barycentric coordinates of a point $v$ on $\mathbb{S}^2$ relative to $\tau$** *are the unique real numbers $b_1, b_2, b_3$ such that*

$$\mathbf{v} = b_1\mathbf{v_1} + b_2\mathbf{v_2} + b_3\mathbf{v_3}. \tag{2.2.7}$$

The spherical barycentric coordinates of a point $v$ with respect to $\tau$ are exactly the same as the trihedral coordinates of $v$ with respect to $\mathcal{T}$. This implies they have the following properties:

LEMMA 2.2.7. *(cf. [3], [37]) For any non-degenerate spherical triangle $\tau :=< v_1, v_2, v_3 >$, we have*

1) *$b_i(v_j) = \delta_{ij}, i, j = 1, 2, 3$,*

2) *The $b_i$ are ratios of volumes of tetrahedra,i.e., $b_1$ is the ration of the signed volume of the tetrahedra $t_1 :=< 0, v, v_2, v_3 >$ and $t :=< 0, v_1, v_2, v_3 >$, with a similar interpretation,*

3) *For all $v$ in the interior of $\tau$, $b_i(v) > 0$,*

4) *If a point $v$ lies on an edge of $\tau$, then one of its spherical barycentric coordinates vanishes, i.e., $b_i$ vanishes on the edge of $\tau$ opposite to $v_i$ for all $i = 1, 2, 3$. The remaining two spherical barycentric coordinates are ratios of sines of geodesic distances, rather then ratios of geodesic distances,*

5) *If the edges of a spherical triangle $\tau$ are extended to great circles, the sphere is divided into eight regions. The spherical barycentric coordinates $b_1, b_2, b_3$ have constant signs on each of these eight regions,*

*6) Spherical barycentric coordinates are infinitely differentiable functions of $v$,*

*7) The spherical barycentric coordinates of a point $v$ on the sphere relative to one spherical triangle $\tau$ can be computed from those relative to another spherical triangle by matrix multiplication,*

*8) The spherical barycentric coordinates of a point $v$ are* **rotation invariant**, *i.e., they depend only on the relative positions of $v$ and $v_1, v_2, v_3$ to each other,*

*9) The span of the spherical barycentric coordinates $b_1(v), b_2(v), b_3(v)$ relative to any triangle is always the three-dimensional linear space obtained by restricting the space $\mathcal{L}$ of linear homogeneous polynomials on $\mathbb{R}^3$ to the sphere $\mathbb{S}^2$,and is thus independent of the triangle,*

*10) In contrast to the usual barycentric coordinates on the planar triangles which always sum to 1, $b_1(v) + b_2(v) + b_3(v) > 1$, if $v \in \tau$ and $v \neq v_1, v_2, v_3$. And this is most significant difference as compared to planar case.*

PROOF. Apply Lemma 2.2.3, Theorem 2.2.4 and Theorem 2.2.5. □

We now show that spherical barycentric coordinates can also be expressed in terms of certain natural angles associated with the geometry. Let $\mathbf{n_i}$ denote the unit normal vectors to the planes $P_i := \text{span}(V \backslash \mathbf{v_i}), i = 1, 2, 3$. The orientation of these vectors is chosen to be consistent with the orientation of the vectors $\mathbf{v_i}$ relative to $P_i$, i.e.,

$$\text{sgn det}(v_1, v_2, v_3) = \text{sgn det}(n_1, v_2, v_3) =$$

$$\text{sgn det}(v_1, n_2, v_3) = \text{sgn det}(v_1, v_2, n_3).$$

For a point $v \in \mathbb{S}^2$, let the angles $\alpha_i,\ \beta_i$, be defined by the dot products

$$\sin \alpha_i := \mathbf{v} \cdot \mathbf{n_i}, \qquad \sin \beta_i := \mathbf{v_i} \cdot \mathbf{n_i}, \quad i = 1, 2, 3.$$

The $\alpha_i$ represent oriented angles between the vector $\mathbf{v}$ and the planes $P_i$, while the $\beta_i$ are the analogous angles between $\mathbf{v_i}$ and $P_i$. For nontrivial spherical triangles, $\det(v_1, v_2, v_3) \neq 0$,

and therefore $\sin\beta_i \neq 0, i = 1, 2, 3$.

THEOREM 2.2.8. *(cf. [3]) The spherical barycentric coordinates of a point $v \in \mathbb{S}^2$ with respect to a triangle $\tau$ are given by*

$$b_i(v) = \frac{\sin\alpha_i}{\sin\beta_i}, \ i = 1, 2, 3. \tag{2.2.8}$$

PROOF. Let $\mathbf{i}, \mathbf{j}, \mathbf{k}$ denote the unit coordinate vectors and $\|\cdot\|$ the usual Euclidean norm. Define

$$\mathbf{d_1} := \det \begin{bmatrix} \mathbf{i} & v_2^x & v_3^x \\ \mathbf{j} & v_2^y & v_3^y \\ \mathbf{k} & v_2^z & v_3^z \end{bmatrix},$$

$$\mathbf{d_2} := \det \begin{bmatrix} v_1^x & \mathbf{i} & v_3^x \\ v_1^y & \mathbf{j} & v_3^y \\ v_1^z & \mathbf{k} & v_3^z \end{bmatrix},$$

$$\mathbf{d_3} := \det \begin{bmatrix} v_1^x & v_2^x & \mathbf{i} \\ v_1^y & v_2^y & \mathbf{j} \\ v_1^z & v_2^z & \mathbf{k} \end{bmatrix}.$$

Then $\mathbf{n_i} = \mathbf{d_i}/\|\mathbf{d_i}\|$, and thus

$$\frac{\sin\alpha_i}{\sin\beta_i} = \frac{\mathbf{v}\cdot\mathbf{n_i}}{\mathbf{v_i}\cdot\mathbf{n_i}} = \frac{\mathbf{v}\cdot\mathbf{d_i}/\|\mathbf{d_i}\|}{\mathbf{v_i}\cdot\mathbf{d_i}/\|\mathbf{d_i}\|} = \frac{\mathbf{v}\cdot\mathbf{d_i}}{\mathbf{v_i}\cdot\mathbf{d_i}}. \tag{2.2.9}$$

It is easy to check that

$$\mathbf{v_i}\cdot\mathbf{d_i} = \det(v_1, v_2, v_3), \ i = 1, 2, 3,$$

and that

$$\mathbf{v}\cdot\mathbf{d_1} = \det(v, v_2, v_3),$$

$$\mathbf{v}\cdot\mathbf{d_2} = \det(v_1, v, v_3),$$

$$\mathbf{v}\cdot\mathbf{d_3} = \det(v_1, v_2, v).$$

Then by (2.2.9) and the property (2.2.3) of trihedral coordinates we get (2.2.8). □

LEMMA 2.2.9. *(cf. [2]) Let $C$ be the unit circle in $\mathbb{R}^2$ centered at the origin, and let $A$ be a circular arc with vertices $v_1 \neq v_2$ which are not antipodal. Let $b_1, b_2$ denote the circular barycentric coordinates of $v \in C$ relative to $A$. Then*

$$\begin{aligned} b_1(v) &= \frac{\sin(\theta_2 - \theta)}{\sin(\theta_2 - \theta_1)}, \\ b_2(v) &= \frac{\sin(\theta - \theta_1)}{\sin(\theta_2 - \theta_1)}, \end{aligned} \tag{2.2.10}$$

*where $\theta,\ \theta_1,\ \theta_2$ are the polar coordinates of $\mathbf{v}, \mathbf{v_1}, \mathbf{v_2}$ respectively.*

PROOF. Since

$$\mathbf{v_1} = (\cos\theta_1, \sin\theta_1)^T$$

$$\mathbf{v_2} = (\cos\theta_2, \sin\theta_2)^T$$

$$\mathbf{v} \ = (\cos\theta \ , \sin\theta \ )^T$$

and

$$\mathbf{v} = b_1\mathbf{v_1} + b_2\mathbf{v_2},$$

the circular barycentric coordinates of $v$ are solving the system:

$$\begin{bmatrix} \cos\theta_1 & \cos\theta_2 \\ \sin\theta_1 & \sin\theta_2 \end{bmatrix} \begin{bmatrix} b_1 \\ b_2 \end{bmatrix} = \begin{bmatrix} \cos\theta \\ \sin\theta \end{bmatrix}.$$

We immediately get the result. □

THEOREM 2.2.10. *(cf. [3]) For each $i = 1, 2, 3$, let $C_i$ be the great circle passing through the points $v \in \mathbb{S}^2$ and $v_i \in V$, and let $y_i$ denote the intersection of $C_i$ with the edge of $\tau$ opposite to $v_i$. Then the spherical barycentric coordinates of $v$ can be computed as*

$$b_i = \frac{\sin\delta_i}{\sin(\delta_i + \gamma_i)}, i = 1, 2, 3, \tag{2.2.11}$$

*where $\delta_i$ is the signed geodesic distance (measured along $C_i$) from $y_i$ to $v$, and $\gamma_i$ is the signed geodesic distance from $v$ to $v_i$.*

PROOF. It suffices to prove (2.2.11) for $i = 1$. By Lemma 2.2.9 if $v \in C_1$ it can be expressed relatively to $y_1$ and $v_1$ as:

$$\mathbf{v} = \frac{\sin \delta_1}{\sin(\delta_1 + \gamma_1)}\mathbf{v_1} + \frac{\sin \gamma_1}{\sin(\delta_1 + \gamma_1)}\mathbf{y_1}.$$

By the same lemma we can write $\mathbf{y_1}$ as a linear combination of $\mathbf{v_2}$ and $\mathbf{v_3}$ only. Then by the uniqueness of barycentric coordinates

$$b_1 = \frac{\sin \delta_1}{\sin(\delta_1 + \gamma_1)}.$$

Similarly, we can show the result for $i = 2, 3$. □

### 2.2.2 Homogeneous Bernstein-Bézier polynomials

Since the spherical polynomials are the restriction to $\mathbb{S}^2$ of certain homogeneous trivariate polynomials, we first study the homogeneous Bernstein-Bézier polynomials. Let $\mathcal{P}_d$ denote the space of polynomials of total degree $d$ on $\mathbb{R}^3$. Recall that the dimension of $\mathcal{P}_d$ is $\binom{d+3}{3}$ and that the set of classical Bernstein polynomials

$$B^d_{ijkl}(v) := \frac{d!}{i!j!k!\ell!} b_1^i b_2^j b_3^k b_4^\ell, \qquad i + j + k + \ell = d \tag{2.2.12}$$

forms a basis for $\mathcal{P}_d$ (cf. [3]).

Let $\mathcal{H}_d$ denote the space of polynomials of degree $d$ which are homogeneous of degree $d$.

LEMMA 2.2.11. *(cf. [3], [37]) The space $\mathcal{H}_d$ is an $\binom{d+2}{2}$ dimensional subspace of $\mathcal{P}_d$. Moreover, if we choose $v_4$ to be the origin in the above construction of the Bernstein polynomials, then the set $\{B^d_{ijk0} : i + j + k = d\}$ forms a basis for $\mathcal{H}_d$.*

PROOF. Let $f, g \in \mathcal{H}_d$, and $\alpha \in \mathbb{R}$. Then

(i) $(f + g)(\alpha v) = f(\alpha v) + g(\alpha v) = \alpha f(v) + \alpha g(v) = \alpha(f + g)(v)$

(ii) $\forall \beta \in \mathbb{R},\ \beta f(\alpha v) = \beta\alpha f(v) = \alpha(\beta f)(v)$.

Thus $\mathcal{H}_d$ is a subspace of $\mathcal{P}_d$.

Let $f = \sum_{0\le i+j+k\le d} c_{ijk}x^iy^iz^k$ be in $\mathcal{H}_d$. Since $f$ is homogeneous of degree $d$ we must have for all $\alpha \in \mathbb{R}$

$$\alpha^d \sum_{0\le i+j+k\le d} c_{ijk}x^iy^iz^k = \sum_{0\le i+j+k\le d} \alpha^{i+j+k}c_{ijk}x^iy^iz^k$$

and thus

$$\sum_{0\le i+j+k\le d} (\alpha^d - \alpha^{i+j+k})c_{ijk}x^iy^iz^k = 0.$$

Since $\{x^i, y^i, z^k, 0 \le i+j+k \le d\}$ is a linearly independent set

$$(\alpha^d - \alpha^{i+j+k})c_{ijk} = 0 \tag{2.2.13}$$

Choose $\alpha \neq 1$. Then (2.2.13) implies

$$c_{ijk} = 0,\ \forall i+j+k \neq d,$$

and

$$f = \sum_{i+j+k=d} c_{ijk}x^iy^iz^k.$$

It follows that $\{x^i, y^i, z^k,\ i+j+k=d\}$ spans $\mathcal{H}_d$ and thus $\dim(\mathcal{H}_d) = \binom{d+2}{2}$.

Next, we show that the set $\{B^n_{ijk0} : i+j+k=d\}$ forms a basis for $\mathcal{H}_d$. Since $\{B^d_{ijkl} : i+j+k+\ell = d\}$ is a linearly independent set, so is $\{B^d_{ijk0} : i+j+k=d\}$. Each $B^d_{ijk0}$ is a homogeneous polynomial of degree $d$, thus

$$\text{span}\{B^d_{ijk0} : i+j+k=d\} \subset \mathcal{H}_d.$$

Since

$$\dim\{\text{span}\{B^d_{ijk0} : i+j+k=d\}\} = \binom{d+2}{2} = \dim(\mathcal{H}_d)$$

we complete the proof. □

For convenience, we drop the last subscript and introduce the following definition.

Definition 2.2.12. *(cf. [3])Let $\mathcal{T}$ be a trihedron generated by $\{v_1, v_2, v_3\}$, and let $b_1(v)$, $b_2(v)$, $b_3(v)$ denote the trihedral coordinates as functions of $v \in \mathbb{R}^3$. Given an integer $d \ge 0$,*

*we define the* **homogeneous Bernstein-Bézier basis polynomials of degree** $d$ *on* $\mathcal{T}$ *to be the set of polynomials*

$$B^d_{ijk}(v) := \frac{d!}{i!j!k!} b_1^i(v) b_2^j(v) b_3^k(v), \qquad i+j+k=d. \tag{2.2.14}$$

*We call*

$$P(v) := \sum_{i+j+k=d} c_{ijk} B^d_{ijk}(v) \tag{2.2.15}$$

*a* **homogeneous Bernstein-Bézier (HBB-) polynomial of degree** $d$.

Many properties of classical, planar, Bernstein-Bézier polynomials hold for HBB-polynomials. We present several important results.

The first one is the classical de Casteljau algorithm to evaluate $P$ at points in $\mathbb{R}^3$ :

THEOREM 2.2.13. *(de Casteljau algorithm , cf. [3]) Suppose we want to evaluate the HBB-polynomial at a point $w$ with trihedral coordinates $b_1, b_2, b_3$.*

*Set* $c^0_{ijk} := c_{ijk},\ i+j+k=d.$

*For* $\ell = 1$ *to* $d$

*For* $i+j+k = d-\ell$

$c^\ell_{ijk} := b_1 c^{\ell-1}_{i+1,j,k} + b_2 c^{\ell-1}_{i,j+1,k} + b_3 c^{\ell-1}_{i,j,k+1}$.

*Then* $P(w) = c^d_{000}$.

PROOF. Let $B^0_{000}(w) = 1$. Suppose

$$c^{\ell-1}_{ijk} = \sum_{r+s+t=\ell-1} c_{i+r,j+s,k+t} B^{\ell-1}_{rst}(w)$$

for some $\ell$ and all $i, j, k$ such that $i+j+k = d-\ell+1$. By the definition

$$c^\ell_{ijk} = b_1 c^{\ell-1}_{i+1,j,k} + b_2 c^{\ell-1}_{i,j+1,k} + b_3 c^{\ell-1}_{i,j,k+1} = b_1 \sum_{r+s+t=\ell-1} c_{i+1+r,j+s,k+t} B^{\ell-1}_{rst} +$$

$$b_2 \sum_{r+s+t=\ell-1} c_{i+r,j+1+s,k+t} B^{\ell-1}_{rst} + b_3 \sum_{r+s+t=\ell-1} c_{i+r,j+s,k+1+t} B^{\ell-1}_{rst} =$$

$$\sum_{r+s+t=\ell-1} (b_1 c_{i+1+r,j+s,k+t} + b_2 c_{i+r,j+1+s,k+t} + b_3 c_{i+r,j+s,k+1+t}) \frac{(\ell-1)!}{r!s!t!} b_1^r b_2^s b_3^t =$$

$$\sum_{r+s+t=\ell-1} c_{i+1+r,j+s,k+t} b_1^{r+1} b_2^s b_3^t \frac{(\ell-1)!}{r!s!t!} + \sum_{r+s+t=\ell-1} c_{i+r,j+1+s,k+t} b_1^r b_2^{s+1} b_3^t \frac{(\ell-1)!}{r!s!t!} +$$

$$\sum_{r+s+t=\ell-1} c_{i+r,j+s,k+1+t} b_1^r b_2^s b_3^{t+1} \frac{(\ell-1)!}{r!s!t!} =$$

$$\sum_{r+1+s+t=\ell} \frac{r+1}{\ell} c_{i+1+r,j+s,k+t} b_1^{r+1} b_2^s b_3^t \frac{\ell!}{(r+1)!s!t!} +$$

$$\sum_{r+1+s+t=\ell} \frac{s+1}{\ell} c_{i+r,j+1+s,k+t} b_1^r b_2^{s+1} b_3^t \frac{\ell!}{r!(s+1)!t!} +$$

$$\sum_{r+1+s+t=\ell} \frac{t+1}{\ell} c_{i+r,j+s,k+1+t} b_1^r b_2^s b_3^{t+1} \frac{\ell!}{r!s!(t+1)!} =$$

$$\sum_{r'+s+t=\ell} \frac{r'}{\ell} c_{i+r',j+s,k+t} b_1^{r'} b_2^s b_3^t \frac{\ell!}{r'!s!t!} + \sum_{r+s'+t=\ell} \frac{s'}{\ell} c_{i+r,j+s',k+t} b_1^r b_2^{s'} b_3^t \frac{\ell!}{r!s'!t!} +$$

$$\sum_{r+s+t'=\ell} \frac{t'}{\ell} c_{i+r,j+s,k+t'} b_1^r b_2^s b_3^{t'} \frac{\ell!}{r!s!t'!} = \sum_{r+s+t=\ell} \frac{r+s+t}{\ell} c_{i+r,j+s,k+t} B_{rst}^\ell =$$

$$\sum_{r+s+t=\ell} c_{i+r,j+s,k+t} B_{rst}^\ell \quad .$$

Then

$$c_{000}^d = \sum_{r+s+t=d} c_{r,s,t} B_{rst}^d(w) = P(w).$$

□

The second important result is the subdivision algorithm to show how to write $p$ in HBB-polynomials on each of the subtriangles. This result is the analog of the classical subdivision algorithm for bivariate BB-polynomials.

THEOREM 2.2.14. *(Subdivision algorithm, cf. [3], [37]) Let $\{c_{ijk}^\ell\}$ be the coefficients produced by de Casteljau algorithm using trihedral coordinates $b_1, b_2, b_3$ of a point $w \in \mathcal{T}$ with vertices $\{v_1, v_2, v_3\}$. Then*

$$P(v) = \begin{cases} \sum_{i+j+k=d} c_{0,j,k}^i B_{ijk;1}^d(v), & v \in \mathcal{T}_1 = \{w, v_2, v_3\} \\ \sum_{i+j+k=d} c_{i,0,k}^j B_{ijk;2}^d(v), & v \in \mathcal{T}_2 = \{v_1, w, v_3\} \\ \sum_{i+j+k=d} c_{i,j,0}^k B_{ijk;3}^d(v), & v \in \mathcal{T}_3 = \{v_1, v_2, w\}, \end{cases} \tag{2.2.16}$$

*where $B_{ijk;\nu}^d$ are Bernstein-Bézier polynomials associated with the trihedron $\mathcal{T}_\nu$, $\nu = 1, 2, 3$.*

PROOF. Suppose $v \in \mathcal{T}_1$, and

$$P(v) = \sum_{i+j+k=d} c_{i,j,k} B^d_{ijk}(v) \tag{2.2.17}$$

with respect to $\mathcal{T}$, and

$$P(v) = \sum_{i+j+k=d} c_{i,j,k;1} B^d_{ijk;1}(v)$$

with respect to $\mathcal{T}_1$. We claim that $c_{ijk;1} = c^i_{0,j,k}$. The trihedral coordinates of $w$ with respect to $\mathcal{T}$ are determined by

$$w = a_1 v_1 + a_2 v_2 + a_3 v_3.$$

The trihedral coordinates of $v$ with respect to $\mathcal{T}$ are determined by

$$v = b_1 v_1 + b_2 v_2 + b_3 v_3$$

and with respect to $\mathcal{T}_1$ are determined by

$$v = c_1 w + c_2 v_2 + c_3 v_3.$$

Then

$$v = c_1(a_1 v_1 + a_2 v_2 + a_3 v_3) + c_2 v_2 + c_3 v_3 =$$

$$c_1 a_1 v_1 + (c_1 a_2 + c_2) v_2 + (c_1 a_3 + c_3) v_3.$$

The uniqueness of barycentric coordinates implies that

$$b_1 = c_1 a_1,$$

$$b_2 = c_1 a_2 + c_2,$$

$$b_3 = c_1 a_3 + c_3.$$

By (2.2.17)

$$P(v) = \sum_{i+j+k=d} c_{ijk} \frac{d!}{i!j!k!} b_1^i b_2^j b_3^k =$$

$$\sum_{i+j+k=d} c_{ijk} \frac{d!}{i!j!k!} c_1^i a_1^i (c_1 a_2 + c_2)^j (c_1 a_3 + c_3)^k.$$

Using binomial expansion and rearranging the terms we get

$$P(v) = \sum_{i+j+k=d} c_{ijk} \frac{d!}{i!j!k!} c_1^i a_1^i ( \sum_{r+s=j} \frac{j!}{r!s!} c_1^r a_2^r c_2^s )( \sum_{\ell+m=k} \frac{k!}{\ell!m!} c_1^l a_3^l c_3^m ) =$$

$$\sum_{i+j+k=d} \sum_{r+s=j} \sum_{\ell+m=k} c_{ijk} \frac{d!}{i!r!s!\ell!m!} c_1^{i+r+\ell} c_2^s c_3^m a_1^i a_2^r a_3^\ell =$$

$$\sum_{i+j+k=d} \sum_{r+s=j} \sum_{\ell+m=k} c_{ijk} \frac{(i+r+\ell)!}{i!r!\ell!} B^d_{i+r+\ell,s,m;1} a_1^i a_2^r a_3^\ell =$$

$$\sum_{i+j+k=d} \sum_{r+s=j} \sum_{\ell+m=k} c_{i,r+s,\ell+m} \frac{(i+r+\ell)!}{i!r!\ell!} a_1^i a_2^r a_3^l B^d_{i+r+\ell,s,m;1} =$$

$$\sum_{i+j+k=d} \sum_{r+s=j} \sum_{\ell+m=k} c_{i,r+s,\ell+m} B^{i+r+\ell}_{i,r,\ell} B^d_{i+r+\ell,s,m;1}.$$

Introducing a new index of summation $p = i + r + \ell$, and since

$$\sum_{i+r+\ell=p} c_{i,r+s,\ell+m} B^{i+r+\ell}_{i,r,\ell} = c^{i+r+\ell}_{0,s,m}$$

we have

$$P(v) = \sum_{p+s+m=d} ( \sum_{i+r+\ell=p} c_{i,r+s,\ell+m} B^p_{i,r,m} ) B^d_{p,s,m;1} =$$

$$\sum_{p+s+m=d} C^p_{0,s,m} B^d_{p,s,m;1}.$$

A similar proof works for $v \in \mathcal{T}_2$ and for $v \in \mathcal{T}_3$. □

The third important result is smoothness conditions for joining two HBB-polynomials. The following theorem establishes necessary and sufficient conditions for two HBB-polynomials to join together smoothly across a plane trough the origin in the sense that the polynomials and their usual directional derivatives as trivariate functions are continuous as we cross the plane.

THEOREM 2.2.15. *(Smoothness conditions, cf. [3])Let $\mathcal{T}$ and $\hat{\mathcal{T}}$ be trihedra generated by vertices $V = \{\mathbf{v_1}, \mathbf{v_2}, \mathbf{v_3}\}$ and $\hat{V} = \{\mathbf{v_2}, \mathbf{v_3}, \mathbf{v_4}\}$. Let*

$$P(v) = \sum_{i+j+k=d} c_{ijk} B^d_{ijk}(v)$$

*and*

$$\hat{P}(v) = \sum_{i+j+k=d} \hat{c}_{ijk} \hat{B}^d_{ijk}(v),$$

*where* $\{B^d_{ijkl}\}$ *and* $\{\hat{B}^d_{ijkl}\}$ *are the Bernstein-Bézier basis functions associated with* $\mathcal{T}$ *and* $\hat{\mathcal{T}}$. *Then* $P$ *and* $\hat{P}$ *and all of their derivatives up to order* $m$ *agree on the face shared by* $\mathcal{T}$ *and* $\hat{\mathcal{T}}$ *if and only if*

$$\hat{c}_{ijk} = \sum_{r+s+t=i} c_{r,j+s,k+t} B^i_{rst}(v_4) \tag{2.2.18}$$

*for all* $i = 0, ..., m$ *and all* $j, k$ *such that* $i + j + k = d$.

Proof. Suppose

$$Q(v) = \sum_{i+j+k+\ell=d} C_{ijkl} B^d_{ijkl}(v) \tag{2.2.19}$$

and

$$\hat{Q}(v) = \sum_{i+j+k+\ell=d} \hat{C}_{ijkl} \hat{B}^d_{ijkl}(v), \tag{2.2.20}$$

where

$$C_{ijkl} := \begin{cases} c_{ijk}, \ if \ \ell = 0 \\ 0, \ \text{otherwise} \end{cases} \tag{2.2.21}$$

and

$$\hat{C}_{ijkl} := \begin{cases} \hat{c}_{ijk}, \ if \ \ell = 0 \\ 0, \ \text{otherwise} \end{cases} \tag{2.2.22}$$

and $B^d_{ijkl}(v)$ are the usual BB-polynomials of degree $d$ associated with the trihedron with vertices $\{v_1, v_2, v_3, 0\}$ and $\hat{B}^d_{ijkl}(v)$ are those associated with the trihedron with vertices $\{v_4, v_2, v_3, 0\}$. It is well-known that these polynomials join with $C^m$ continuity if and only if

$$\hat{C}_{ijkl} = \sum_{r+s+t+u=i} C_{r,j+s,k+t,\ell+u} B^i_{rstu}(v_4), \ i = 0, ..., m. \tag{2.2.23}$$

In view of (2.2.21) and (2.2.22) we can choose $\ell = u = 0$. In this case, (2.2.23) holds if and only if (2.2.18) holds. But $P = Q$ and $\hat{P} = \hat{Q}$, proof is complete. □

### 2.2.3 Spherical Bernstein-Bézier polynomials

The spherical Bernstein-Bézier polynomials are the restriction of HBB-polynomials on the sphere. In this subsection, we discuss the existence of homogeneous extensions for functions defined on the sphere, the directional derivatives of spherical functions, the smoothness conditions to join two SBB-polynomials, and the calculation of integration on the sphere. Let us first present the definition of SBB-polynomials.

Definition 2.2.16. *(cf. [3]) The restriction of an HBB-polynomial of degree $d$ to the points on the unit sphere is called a* **spherical Bernstein-Bézier (SBB-) polynomial of degree** *$d$.*

Now we state the existence of homogeneous extensions.

Lemma 2.2.17. *(cf. [4]) Suppose $f$ is a function defined on $\mathbb{S}^2$ and let $t \in \mathbb{R}$. Then*

$$F_t(v) := \|v\|^t f(v/\|v\|) \tag{2.2.24}$$

*is the unique homogeneous extension of $f$ of degree $t$ to all of $\mathbb{R}^3\backslash\{0\}$, i.e., $F_t|_{\mathbb{S}^2} = f$, and $F_t$ is homogeneous of degree $t$.*

Proof. The assertion is an immediate consequence of the definition. □

Many properties of SBB-polynomials follow naturally from the properties of HBB-polynomials.

Theorem 2.2.18. *(cf. [4]) The polynomials $\{B^d_{ijk}, i+j+k=d\}$ restricted to $\mathbb{S}^2$ are linearly independent.*

Proof. Suppose

$$P(v) = \sum_{i+j+k=n} c_{ijk} B^d_{ijk}(v) = 0$$

for all $v \in \mathbb{S}^2$. By Lemma 2.2.17 there exists the unique homogeneous extension of $P(v)$ to all of $\mathbb{R}^3$ of degree $d$. Then $P(v) = 0$ for all $v \in \mathbb{R}^3$. The linear independence of the $B^d_{ijk}$'s implies that $c_{ijk} = 0, i+j+k = d$ and thus the $B^d_{ijk}$'s restricted to $\mathbb{S}^2$ are linearly independent. □

de Casteljau and subdivision algorithms can also be applied to the polynomials restricted on the sphere. Now we turn to a question how to compute derivatives of spherical functions and in particular SBB-polynomials. Let us define what we mean by the derivatives of a spherical function.

DEFINITION 2.2.19. *(cf. [4])We define the* **directional derivative** $D_g f$ *of* $f$ *at a point* $v \in \mathbb{S}^2$ *by*

$$D_g f(v) := D_g F(v) = g^T \nabla F(v), \tag{2.2.25}$$

*where* $F$ *is some homogeneous extension of* $f$*, and* $\nabla F$ *is the gradient of the trivariate function* $F$*.*

While a polynomial of degree $d$ has a natural homogeneous extension to $\mathbb{R}^3$, a general function $f$ on $\mathbb{S}^2$ has infinitely many different extensions. The value of its derivative may depend on which extension we take. The following lemma shows that we get the same value for derivatives no matter what degree extension we take.

LEMMA 2.2.20. *(cf. [4]) Suppose* $f$ *is a function on* $\mathbb{S}^2$ *and* $g$ *is a tangent vector to* $\mathbb{S}^2$ *at a point* $v$*. Then the value of* $D_g f(v)$ *can be computed from (2.2.25) using any homogeneous extension of* $f$*.*

PROOF. Let $F$ be a homogeneous extension of $f$, and let $C$ be a $C^1$ smooth curve on $\mathbb{S}^2$ passing through the point $v$, parameterized by a parameter $\theta$ such that $C(\theta) = v$ and $C'(\theta) = g$ for $\theta = 0$. By the chain rule we obtain

$$\frac{df(C(\theta))}{d\theta}|_{\theta=0} = \frac{dF(C(\theta))}{d\theta}|_{\theta=0} = g^T \nabla F(v) = D_g F(v).$$

This shows that $D_g F(v)$ does not depend on the degree of homogeneity of $F$ since the left-hand side clearly depends only on $f = F|_{\mathbb{S}^2}$. □

Let us continue with directional derivatives of barycentric coordinates.

LEMMA 2.2.21. *(cf. [4]) Let $g$ be a given unit vector in $\mathbb{R}^3$. Then*

$$D_g b_i = b_i(g). \tag{2.2.26}$$

PROOF. Let $\tau = \{v_1, v_2, v_3\}$ and $v \in \mathbb{S}^2$. By (2.2.25), we have

$$\begin{aligned}
D_g b_1 &= g^T \nabla b_1 = g^T \nabla \Big( \frac{1}{det(v_1, v_2, v_3)} det\Big( \begin{bmatrix} x \\ y \\ z \end{bmatrix}, v_2, v_3 \Big) \Big) \\
&= \frac{1}{det(v_1, v_2, v_3)} \Big( g_1 det\Big( \begin{bmatrix} 1 \\ 0 \\ 0 \end{bmatrix}, v_2, v_3 \Big) + g_2 det\Big( \begin{bmatrix} 0 \\ 1 \\ 0 \end{bmatrix}, v_2, v_3 \Big) \\
&\quad + g_3 det\Big( \begin{bmatrix} 0 \\ 0 \\ 1 \end{bmatrix}, v_2, v_3 \Big) \Big) \\
&= \frac{\det(g, v_2, v_3)}{\det(v_1, v_2, v_3)} = b_1(g),
\end{aligned}$$

$$\begin{aligned}
D_g b_2 &= g^T \nabla b_2 = g^T \nabla \Big( \frac{1}{det(v_1, v_2, v_3)} det\Big( \begin{bmatrix} x \\ y \\ z \end{bmatrix}, v_2, v_3 \Big) \Big) \\
&= \frac{1}{det(v_1, v_2, v_3)} \Big( g_1 det\Big( v_1, \begin{bmatrix} 1 \\ 0 \\ 0 \end{bmatrix}, v_3 \Big) + g_2 det\Big( v_1, \begin{bmatrix} 0 \\ 1 \\ 0 \end{bmatrix}, v_3 \Big) \\
&\quad + g_3 det\Big( v_1, \begin{bmatrix} 0 \\ 0 \\ 1 \end{bmatrix}, v_3 \Big) \Big) \\
&= \frac{\det(v_1, g, v_3)}{\det(v_1, v_2, v_3)} = b_2(g),
\end{aligned}$$

and

$$\begin{aligned} D_g b_3 &= g^T \nabla b_3 = g^T \nabla \left( \frac{1}{det(v_1, v_2, v_3)} det\left( v_1, v_2, \begin{bmatrix} x \\ y \\ z \end{bmatrix} \right) \right) \\ &= \frac{1}{det(v_1, v_2, v_3)} \left( g_1 det\left( v_1, v_2, \begin{bmatrix} 1 \\ 0 \\ 0 \end{bmatrix} \right) + g_2 det\left( v_1, v_2, \begin{bmatrix} 0 \\ 1 \\ 0 \end{bmatrix} \right) \right. \\ &\quad \left. + g_3 det\left( v_1, v_2, \begin{bmatrix} 0 \\ 0 \\ 1 \end{bmatrix} \right) \right) \\ &= \frac{\det(v_1, v_2, g)}{\det(v_1, v_2, v_3)} = b_3(g). \end{aligned}$$

So the proof is complete. □

PROPOSITION 2.2.22. *(cf. [4]) Suppose $P$ is an SBB-polynomial. Then*

$$D_g P(v) = b^T(g) \nabla_b P, \tag{2.2.27}$$

*where*

$$\nabla_b := (\frac{\partial}{\partial b_1}, \frac{\partial}{\partial b_2}, \frac{\partial}{\partial b_3})^T. \tag{2.2.28}$$

PROOF. By the definition, we have

$$\begin{aligned} D_g P(v) &= g^T \nabla P(v) = g^T \begin{bmatrix} \frac{\partial P}{\partial b_1}\frac{\partial b_1}{\partial x} + \frac{\partial P}{\partial b_2}\frac{\partial b_2}{\partial x} + \frac{\partial P}{\partial b_3}\frac{\partial b_3}{\partial x} \\ \frac{\partial P}{\partial b_1}\frac{\partial b_1}{\partial y} + \frac{\partial P}{\partial b_2}\frac{\partial b_2}{\partial y} + \frac{\partial P}{\partial b_3}\frac{\partial b_3}{\partial y} \\ \frac{\partial P}{\partial b_1}\frac{\partial b_1}{\partial z} + \frac{\partial P}{\partial b_2}\frac{\partial b_2}{\partial z} + \frac{\partial P}{\partial b_3}\frac{\partial b_3}{\partial z} \end{bmatrix} \\ &= \begin{bmatrix} g_1\frac{\partial b_1}{\partial x} + g_2\frac{\partial b_2}{\partial y} + g_3\frac{\partial b_3}{\partial z} \\ g_1\frac{\partial b_1}{\partial x} + g_2\frac{\partial b_2}{\partial y} + g_3\frac{\partial b_3}{\partial z} \\ g_1\frac{\partial b_1}{\partial x} + g_2\frac{\partial b_2}{\partial y} + g_3\frac{\partial b_3}{\partial z} \end{bmatrix}^T \begin{bmatrix} \frac{\partial P}{\partial b_1} \\ \frac{\partial P}{\partial b_2} \\ \frac{\partial P}{\partial b_3}. \end{bmatrix} \end{aligned}$$

So we get

$$D_g P(v) = g^T \begin{bmatrix} \frac{\partial b_1}{\partial x} & \frac{\partial b_2}{\partial x} & \frac{\partial b_3}{\partial x} \\ \frac{\partial b_1}{\partial y} & \frac{\partial b_2}{\partial y} & \frac{\partial b_3}{\partial y} \\ \frac{\partial b_1}{\partial z} & \frac{\partial b_2}{\partial z} & \frac{\partial b_3}{\partial z} \end{bmatrix} \begin{bmatrix} \frac{\partial P}{\partial b_1} \\ \frac{\partial P}{\partial b_2} \\ \frac{\partial P}{\partial b_3} \end{bmatrix}$$

Therefore,

$$D_g P(v) = \begin{bmatrix} g^T \nabla b_1 \\ g^T \nabla b_2 \\ g^T \nabla b_3 \end{bmatrix}^T \nabla_b P = \begin{bmatrix} b_1(g) \\ b_2(g) \\ b_3(g) \end{bmatrix}^T \nabla_b P.$$

□

We now turn to the problem of computing higher derivatives of SBB-polynomials. Let $c^0_{ijk} := c_{ijk}$ be the Bézier coefficients of $P$ of degree $d$, and let $g_1, ..., g_m$, $1 \le m \le d$, be a set of direction vectors. For each $1 \le \ell \le m$, let $c^\ell_{ijk}, i+j+k = d-\ell$, be the intermediate values obtained in carrying out de Casteljau algorithm using $b(g_\ell)$. That is, $c^\ell_{ijk}$ is obtained from the recursion

$$c^\ell_{ijk} = b_1(g_\ell)c^{\ell-1}_{i+1,j,k} + b_2(g_\ell)c^{\ell-1}_{i,j+1,k} + b_3(g_\ell)c^{\ell-1}_{i,j,k+1}, \ell = 1, ..., m.$$

It follows that $c^\ell_{ijk}$ depend on the vectors $g_1, ..., g_\ell$, but not on their ordering.

THEOREM 2.2.23. *(cf. [4]) For any $0 \le m \le d$,*

$$D_{g_1,...,g_m} P(v) := D_{g_1} \cdots D_{g_m} P(v) = \frac{d!}{(d-m)!} \sum_{i+j+k=d-m} c^m_{ijk} B^{d-m}_{ijk}(v). \tag{2.2.29}$$

PROOF. By Lemma 2.19, for $i+j+k = d$,

$$D_{g_1} B^d_{ijk}(v) = \frac{d!}{i!j!k!}[ib_1^{i-1}b_2^j b_3^k D_{g_1} b_1 + jb_1^i b_2^{j-1} b_3^k D_{g_1} b_2 + kb_1^i b_2^j b_3^{k-1} D_{g_1} b_3] =$$

$$d[B^{d-1}_{i-1,j,k}(v)b_1(g_1) + B^{d-1}_{i,j-1,k}(v)b_2(g_1) + B^{d-1}_{i,j,k-1}(v)b_3(g_1)].$$

Substituting this in

$$D_{g_1} P(v) = \sum_{i+j+k=d} c_{ijk} D_{g_1} B^d_{ijk}(v)$$

and rearranging terms we get (2.2.29) for $m = 1$. The general result follows by induction. □

Now we consider derivatives at the vertices of triangles. It is clear from the properties of trihedral coordinates that the values of an SBB-polynomial $P$ at the vertices of its domain triangle are given by $P(v_1) = c_{d00}, P(v_2) = c_{0d0}, P(v_3) = c_{00d}$. The derivatives of $P$ at the vertices of $\tau$ also have a simple form.

PROPOSITION 2.2.24. *(cf. [4]) For all* $0 \leq m \leq d$,

$$\begin{aligned} D_{g_1,\ldots,g_m} P(v_1) &= \frac{d!}{(d-m)!} c^m_{d-m,0,0}, \\ D_{g_1,\ldots,g_m} P(v_2) &= \frac{d!}{(d-m)!} c^m_{0,d-m,0}, \\ D_{g_1,\ldots,g_m} P(v_3) &= \frac{d!}{(d-m)!} c^m_{0,0,d-m}. \end{aligned} \tag{2.2.30}$$

PROOF. Consider $P(v_1)$. By Theorem 2.2.23

$$D_{g_1,\ldots,g_m} P(v_1) = \frac{d!}{(d-m)!} \sum_{i+j+k=d-m} c^m_{ijk} B^{d-m}_{ijk}(v_1),$$

where

$$B^{d-m}_{ijk}(v_1) = \frac{(d-m)!}{i!j!k!} b_1(v_1)^i b_2(v_1)^j b_3(v_1)^k = \frac{(d-m)!}{i!j!k!} 1^i 0^j 0^k = 1,$$

if $i = d-m, j = 0, k = 0$ and is 0 otherwise. Thus

$$D_{g_1,\ldots,g_m} P(v_1) = \frac{d!}{(d-m)!} c^m_{d-m,0,0}.$$

□

Let us consider the question when two polynomials on adjoining surface triangles join smoothly across a common edge $e$.

THEOREM 2.2.25. *(cf. [3], [37]) Suppose* $Q$ *and* $\hat{Q}$ *are polynomials as in (2.2.19) and (2.2.20) and let* $\tau$ *and* $\hat{\tau}$ *be the surface triangles with a common edge* $e$*. Then the restrictions of* $Q$ *and* $\hat{Q}$ *to* $\mathbb{S}^2$*,* $P$ *and* $\hat{P}$*, along with their derivatives up to order* $m$ *join continuously along* $e$*, i.e., for every point* $v \in e$ *and every curve* $c \in \hat{S}$ *crossing* $e$ *at* $v$*,*

$$D^j_c P(v) = D^j_c \hat{P}(v), \qquad j = 0, \ldots, m, \tag{2.2.31}$$

*if and only if*

$$\hat{c}_{ijk} = \sum_{r+s+t=i} c_{r,j+s,k+t} B^i_{rst}(v_4), \tag{2.2.32}$$

*for all* $i = 0, ..., m$ *and all* $j, k$ *such that* $i + j + k = d$.

PROOF. Suppose (2.2.31) holds for all $v \in e$ and for all $c \in \mathbb{S}^2$ crossing $e$ at $v$. Since $P$ and $\hat{P}$ are polynomials of degree $d$, by Lemma 2.2.17 there exist unique homogeneous extensions of degree $d$ which thus must be our $Q$ and $\hat{Q}$. Since $Q|_{\mathbb{S}^2} = P$ and $\hat{Q}|_{\mathbb{S}^2} = \hat{P}$

$$D^j_c Q(v) = D^j_c \hat{Q}(v), \qquad j = 0, ..., m, \tag{2.2.33}$$

for every point $v \in e$ and every curve $c \in \mathbb{S}^2$ crossing $e$ at $v$. Now we claim that (2.2.33) holds for any $v$ on the common face of tetrahedra corresponding to $\tau$ and $\hat{\tau}$. Let $v$ belong to the common face of $\mathcal{T}$ and $\hat{\mathcal{T}}$. Clearly, if $v \neq 0$, there exist $v' \in e$ and $\lambda \in R$, such that $v = \lambda v'$. Since $Q$ and $\hat{Q}$ are homogeneous of degree $d$

$$Q(v) = Q(\lambda v') = \lambda^d Q(v'),$$

and similarly for $\hat{Q}$. Then we have

$$D^j_c Q(v) = \lambda^d D^j_c Q(v') = \lambda^d D^j_c \hat{Q}(v') = D^j_c \hat{Q}(v), \qquad j = 0, ..., m.$$

By the Theorem 2.2.15

$$\hat{c}_{ijk} = \sum_{r+s+t=i} c_{r,j+s,k+t} B^i_{rst}(v_4).$$

For the other direction, suppose (2.2.32) holds. Then by Theorem 2.15 $Q(v)$ and $\hat{Q}(v)$ join smoothly across the common face, i.e.,

$$D^j Q(v) = D^j \hat{Q}(v), \qquad j = 0, ..., m, \tag{2.2.34}$$

for any $v$ on the face. This condition holds for any curve on the common face and thus for the edge $e$ as well. Since $Q(v)|e = P(v)$ and $\hat{Q}(v)|e = \hat{P}(v)$ (2.2.34) holds for the restrictions. In particular,

$$\nabla P(v) = \nabla \hat{P}(v), \qquad v \in e.$$

Now let $c$ be a curve on the sphere-like surface $\mathbb{S}^2$, then by the chain rule

$$\nabla P(v) = \nabla c D_c P(v) = \nabla c D_c \hat{P}(v) = \nabla \hat{P}(v),$$

and so on. Thus we have the result for any $v \in e$ and any curve $c$ crossing $e$ at $v$. □

For many practical applications it is necessary to compute integrals of piecewise polynomial functions. Evaluating integrals of spherical polynomials is considerably more difficult than in the planar case. Recall that for planar triangles, the integral of a Bernstein basis polynomial of degree $d$ is equal to the area of the corresponding triangle divided by $d+1$, see [37]. Thus, the value of the integral does not depend on the particular basis polynomial or on the precise shape of the triangle. Unfortunately, this wonderful and attractive property does not carry over to spherical polynomials. In general, for two different triangles, the values of the integrals are different unless the two triangles are similar. Moreover, the integrals of the Bernstein basis polynomials of degree $d$ associated with a single triangle are also different in general.

To compute integrals in this case we propose a mapping of a surface triangle $\tau$ to a planar triangle $\bar{\tau}$ by means of radial projection defined in Section 2.1. This will enable us to use a standard integration technique for planar triangles.

LEMMA 2.2.26. *(cf. Proposition 4.1 in [4]) Let $\tau$ be a spherical triangle and $\bar{\tau}$ its radial projection as in Section 2.1. Suppose $|\tau| \leq 1$ and $R_\tau$ denotes the radial projection defined by $R_\tau \bar{\omega} := \frac{\bar{\omega}}{|\bar{\omega}|}$ for $\bar{\omega} \in \bar{\tau}$. If $\sigma$ and $\bar{\sigma}$ denote the Lebesgue measures on $\tau$ and $\bar{\tau}$ correspondingly then*

$$\int_\tau f(\omega) d\sigma(\omega) = \int_{\bar{\tau}} f(R_\tau \bar{\omega}) |\bar{\omega}|^{-3} d\bar{\sigma}(\bar{\omega}). \tag{2.2.35}$$

PROOF. Without loss of generality assume that the tangent plane $\mathbf{T}_\tau$ is $z = 1$. Recall that $\frac{\bar{\omega}}{|\bar{\omega}|} = \omega$, and for $\omega = (x, y, z)$ we can write $\bar{\omega} = (x', y', 1)$ with $x' = x/z$ and $y' = y/z$. Then $d\bar{\sigma} = dx'dy'$. For the spherical measure recall that $d\sigma = \sin\phi d\phi d\theta$, where $\phi$ and $\theta$ are spherical coordinates of $\omega$ defined by

$$x = \cos\theta \sin\phi$$

$$y = \sin\theta \sin\phi$$

$$z = \cos\phi.$$

Therefore

$$x' = \cos\theta \tan\phi$$

$$y' = \sin\theta \tan\phi.$$

We can compute the partial derivatives

$$\begin{aligned}
\frac{\partial x'}{\partial \theta} &= -\sin\theta \tan\phi, \\
\frac{\partial x'}{\partial \phi} &= \cos\theta \sec^2\phi, \\
\frac{\partial y'}{\partial \theta} &= \cos\theta \tan\phi, \\
\frac{\partial y'}{\partial \phi} &= \sin\theta \sec^2\phi.
\end{aligned}$$

Then, by definition, we have

$$|\frac{\partial(x', y')}{\partial(\theta, \phi)}| = \left| det\begin{pmatrix} -sin\theta tan\phi & cos\theta sec^2\phi \\ cos\theta tan\phi & sin\theta \sec^2\phi \end{pmatrix} \right|$$

Therefore,

$$\begin{aligned}
|\frac{\partial(x', y')}{\partial(\theta, \phi)}| &= |-\sin^2\theta \tan\phi \sec^2\phi - \cos^2\theta \sec^2\phi \tan\phi| \\
&= \tan\phi \sec^2\phi = \frac{\sin\phi}{\cos^3\phi}
\end{aligned}$$

and hence using $\cos\phi = z = |\bar{\omega}|^{-1}$ we get (2.2.35). □

### 2.2.4 Non-homogeneous spherical polynomials

In this subsection, we define non-homogeneous spherical polynomials and trace their properties to the properties outlined above for homogeneous polynomials, see [29].

In Theorem 1 of [29] it is shown that $\mathcal{P}_d = \mathcal{H}_d \oplus \mathcal{H}_{d-1}$, i.e., $\mathcal{H}_d \oplus \mathcal{H}_{d-1}$ restricted to the unit sphere is identical to the space $\mathcal{P}_d$ of trivariate non-homogeneous polynomials of degree $d$

restricted to the unit sphere. Therefore the set $\{B^d_{ijk},\ i+j+k=d\}\cup\{B^{d-1}_{ijk},\ i+j+k=d-1\}$ forms a basis for $\mathcal{P}_d$. We call spherical polynomials in $\mathcal{P}_d$ **non-homogeneous spherical polynomials**, and we can express a non-homogeneous spherical polynomial $P$ in terms of BB-basis functions as

$$P(v)=\sum_{i+j+k=d} a_{ijk}B^d_{ijk}(v)+\sum_{i+j+k=d-1} c_{ijk}B^{d-1}_{ijk}(v).$$

With this definition it is easy to see that the methods of evaluating values (de Casteljau's algorithm), taking derivatives and computing integrals with homogeneous polynomials can be easily applied to non-homogeneous polynomials.

## 2.3 Approximation of Spherical Splines

In this section, we discuss how well smooth functions defined on $\mathbb{S}^2$ can be approximated by spherical polynomials and spherical splines. It consists of two subsections, first one is Spherical Sobolev Spaces and Seminorms, the second one is Approximation by Spherical Polynomials.

### 2.3.1 Spherical Sobolev Spaces and Seminorms

In this subsection we introduce notations of spherical Sobolev spaces and seminorms that annihilate spherical polynomials, also state some relating results, see [40]. To define Sobolev-type norms and seminorms for functions on the unit sphere, we need to use a concept of a homogeneous extension. Recall that a trivariate function $f(v)$ is homogeneous of degree $n$ if

$$f(\alpha v)=\alpha^n f(v), \forall v\in\mathbb{R}^3\backslash\{0\}, \alpha\neq 0. \tag{2.3.1}$$

Also recall that by Lemma 2.2.17, every spherical function $f$ has a unique homogeneous extension of degree $n$ to $\mathbb{R}^3\backslash\{0\}$ defined by

$$f_n(u)=|u|^n f\left(\frac{u}{|u|}\right). \tag{2.3.2}$$

Let $\Omega$ be a domain on $\mathbb{S}^2$ such that $|\Omega| \leq 1$, and let $\bar{\Omega}$ denote the image of $\Omega$ under the inverse radial projection as defined in Section 2.1. We will be relating properties of a spherical function $f$ defined on $\Omega$ to the properties of its homogeneous extension $f_n$ restricted to $\bar{\Omega}$, and we denote such a restriction by $\bar{f}_n$, i.e., $\bar{f}_n := f_n|_{\bar{\Omega}}$.

Fix $1 \leq p \leq \infty$. Assume $k$ is a nonnegative integer and $B$ is an open set in $\mathbb{R}^2$. Recall that the corresponding classical Sobolev space $W^{k,p}(B)$ is the space of functions on $B$ whose derivatives up to order $k$ belong to $L_p(B)$ [1]. A norm on $W^{k,p}(B)$ can be defined as

$$\|g\|_{k,p,B} := \sum_{\gamma_1+\gamma_2 \leq k} ||D_\xi^{\gamma_1} D_\eta^{\gamma_2} g\|_{p,B}, \tag{2.3.3}$$

where $D_\xi^{\gamma_1} D_\eta^{\gamma_2} = \frac{\partial^{\gamma_1+\gamma_2}}{\partial \xi^{\gamma_1} \partial \eta^{\gamma_2}}$.

Definition 2.3.1. *([40]) Suppose that $\{(\Gamma_j, \phi_j)\}$ is an atlas for $\Omega$. Let $\{\alpha_j\}$ be a* **partition of unity** *subordinate to the atlas. We define* **spherical Sobolev spaces** *$W^{k,p}(\Omega)$ as follows:*

$$W^{k,p}(\Omega) := \{f : (\alpha_j f) \circ \phi_j^{-1} \in W^{k,p}(\phi_j(\Gamma_j)), \textit{for all } j\}. \tag{2.3.4}$$

*with norm $||f||_{k,p,\Omega} := \sum_j ||(\alpha_j f) \circ \phi_j^{-1}||_{W^{k,p}(\phi_j(\Gamma_j))}$.*

Then the Sobolev space $W^{k,p}(\Omega)$ is just the space of all functions f defined on $\Omega$ for which $||f||_{k,p,\Omega}$ is finite. It is well known that this definition does not depend on the choice of the atlas and the partition of unity, in the sense that other choices will give rise to the same space with a norm that is equivalent to the above one, see [7] and [39]. Now we give definition of Sobolev-type seminorm on the sphere.

Definition 2.3.2. *Let $\Omega \subset \mathbb{S}^2$, and let $f \in W^{k,p}(\Omega)$ for some $k \geqslant 0$ and $1 \leq p \leq \infty$. Then we define* **Sobolev-type seminorm** *of $f$ on $W^{k,p}(\Omega)$ to be*

$$|f|_{k,p,\Omega} := \sum_{|\alpha|=k} \|D^\alpha f_{k-1}\|_{p,\Omega}, \tag{2.3.5}$$

*where $\|D^\alpha f_{k-1}\|_{p,\Omega}$ is understood as the $L_p$-norm of the restriction of the trivariate function $D^\alpha f_{k-1}$ to $\Omega$. For $k = 0$, the above seminorm reduces to the usual $L_p -$ norm*

$$|f|_{0,p,\Omega} = ||f||_{L^p(\Omega)}.$$

Let us present several elementary facts of concerning homogeneous extensions and semi-norms to end this subsection.

LEMMA 2.3.3. *(cf. [40]) 1) Let $k, n \in \mathbb{Z}_+$, and suppose $f$ is a function defined on $\Omega$, with $|\Omega| \leq 1$. Then $f \in W^{k,p}(\Omega)$ if and only if $\bar{f}_n \in W^{k,p}(\bar{\Omega})$.*
*2)Let $f \in W^{k,p}(\Omega)$ for some $k \geq 1$ with $|\Omega| \leq 1$. Then $(D^\alpha f_{k-1})|_\Omega \in L_p(\Omega)$ for all multi-indices $\alpha$ such that $|\alpha| = k$.*
*3) Let $\Omega \subsetneq \mathbb{S}^2$ with $|\Omega| \leq 1$. Suppose $f \in W^{k,p}(\Omega)$ and let $\bar{f}_m$ and $\bar{f}_n$ be two homogeneous extensions of $f$ restricted to $\bar{\Omega}$. Then*

$$||\bar{f}_m||_{k,p,\bar{\Omega}} \leq C_3||\bar{f}_n||_{k,p,\bar{\Omega}},$$

*for some constant $C_3$ depending only on $k$, $m$, and $n$. This implies that the Sobolev norm of $\bar{f}_n = f_n|_{\bar{\Omega}}$ does not depend in an essential way on the degree $n$ of the homogeneous extension of $f$ that is used to define $f_n$.*

PROPOSITION 2.3.4. *(cf. [40]) Let $\Omega \subset \mathbb{S}^2$ with $|\Omega| \leq 1$. Then there exist positive constants $C_1, C_2$ depending only on $k$ and $p$ such that for every $f \in W_{k,p}(\Omega)$*

$$C_1|f|_{k,p,\Omega} \leq |\bar{f}_{k-1}|_{k,p,\bar{\Omega}} \leq C_2|f|_{k,p,\Omega}. \tag{2.3.6}$$

Our last proposition shows that the semi-norm defined by (2.3.5)annihilates certain homogeneous polynomials.

PROPOSITION 2.3.5. *(cf. [40]) Suppose $\Omega$ is an open connected subset of $\mathbb{S}^2$. Let $f \in W^{k,p}(\Omega)$ and $k \geq 2$. $|f|_{k,p,\Omega} = 0$ if and only if $f$ is a homogeneous spherical polynomial of degree $k-1$.*

### 2.3.2 Approximation Order of Spherical Polynomials

In this subsection, we mainly discuss the error bounds of spherical spline approximation. First we presents some important inequalities, then local approximation, finally the local stable basis, existence of Quasi-interpolant, and approximation order of spherical splines.

Given a homogeneous trivariate polynomial $P$ in BB form (2.2.15), let $c$ be a vector of its coefficients. Let $\|c\|_{\infty,\tau}$ and $\|c\|_{p,\tau}$ denote its $\ell_\infty$ and $\ell_p$ norms on a spherical triangle $\tau$ respectively. Then we have following lemma.

LEMMA 2.3.6. *(cf. [40], [10]) Any homogeneous polynomial $P$ of degree $d$ in Bernstein-Bézier form (2.2.15) with respect to a spherical triangle $\tau$ with $|\tau| \leq 1$ satisfies the property*

$$A_1 \ \|c\|_{\infty,\tau} \leq \|P\|_{\infty,\tau} \leq A_2 \|c\|_{\infty,\tau} \tag{2.3.7}$$

*and*

$$A_3 A_\tau^{1/p} \ \|c\|_{p,\tau} \leq \|P\|_{p,\tau} \leq A_2 A_\tau^{1/p} \|c\|_{p,\tau} \tag{2.3.8}$$

*for any $1 \leq p < \infty$. Here $A_1, A_2$ are positive constants independent of $\tau$, $P$ and $p$. $A_3$ depends $d$, $p$ and the smallest angle of $\tau$.*

PROOF. Proof of (2.3.7) can be found in [40]. For (2.3.8) fix $1 \leq p < \infty$. By Lemma 4.4 in [40] there exists a positive constant $K_3$ depending on $d$, $p$ and the smallest angle $\Theta_\tau$ of $\tau$ such that

$$A_\tau^{-1/p} \|P\|_{p,\tau} \leq \|P\|_{\infty,\tau} \leq K_3 A_\tau^{-1/p} \|P\|_{p,\tau}. \tag{2.3.9}$$

Then using (2.3.7) and $\|c\|_{p,\tau} \leq \binom{d+2}{2} \|c\|_{\infty,\tau}$ we get

$$\frac{A_\tau^{1/p}}{K_3} A_7 \binom{d+2}{2}^{-1/p} \|c\|_{p,\tau} \leq \frac{A_\tau^{1/p}}{K_3} A_1 \|c\|_{\infty,\tau} \leq \frac{A_\tau^{1/p}}{K_3} \|P\|_{\infty,\tau} \leq \|P\|_{p,\tau}.$$

Similarly, by (2.3.9)

$$\|P\|_{p,\tau} \leq A_\tau^{1/p} \|P\|_{\infty,\tau} \leq A_2 A_\tau^{1/p} \|c\|_{\infty,\tau} \leq A_2 A_\tau^{1/p} \|c\|_{p,\tau}.$$

Therefore we obtain (2.3.8) with $A_3 := \frac{A_1}{K_3} \binom{d+2}{2}^{-1/p}$. □

Next we need **Markov-type inequality** for spherical polynomials.

LEMMA 2.3.7. *(cf. [40], [10]) Let $P$ be a trivariate homogeneous polynomial of degree $d$ defined on a spherical triangle $\tau$ with $|\tau| \leq 1$. There exist constants $A_4$ depending on $d$ and*

$\Theta_\tau$ *only, and* $A_5$ *depending on* $d$*, such that*

$$|P|_{k,\infty,\tau} \leq \frac{A_{10}}{(\tan\frac{\rho_\tau}{2})^k}\|P\|_{\infty,\tau}, \tag{2.3.10}$$

*and*

$$|P|_{k,p,\tau} \leq \frac{A_5}{(\tan\frac{\rho_\tau}{2})^k}\|P\|_{p,\tau} \tag{2.3.11}$$

*for* $1 \leq p < \infty$*. Here* $\rho_\tau$ *is a the diameter of the largest spherical cap contained in* $\tau$*.*

Proof. For the first equation in (2.3.11) we modify the proof of Proposition 4.3 in [40] by replacing (2.1.1) with (2.1.3). To prove (2.3.10) we apply Lemma 4.4 in [40] to both sides of (2.3.11) to get

$$|P|_{k,\infty,\tau} \leq \frac{A_{11}K}{(\tan\frac{\rho_\tau}{2})^k}\|P\|_{\infty,\tau}$$

for some $K$ depending on $d-k$ and $\Theta_\Delta$. □

Now we express a bound on the values of certain spherical functions in terms of its 2nd Sobolev semi-norm over a spherical triangle.

Lemma 2.3.8. *(cf. [10], [37]) Let* $\tau$ *be a spherical triangle such that* $|\tau| \leq 1$ *and suppose* $f \in W^{2,p}(\tau)$ *vanishes at the vertices of* $\tau$*, that is* $f(v_i) = 0, i = 1, 2, 3$*. Then for all* $v \in \tau$*,*

$$|f(v)| \leq A_6 \left(\tan\frac{|\tau|}{2}\right)^2 |f|_{2,\infty,\tau}, \tag{2.3.12}$$

*for some positive constants* $A_6$ *independent of* $f$ *and* $\tau$*. Moreover, if* $f$ *is a homogeneous polynomial of degree* $d$*, then*

$$|f(v)| \leq A_7 A_\tau^{-1/p} \left(\tan\frac{|\tau|}{2}\right)^2 |f|_{2,p,\tau} \tag{2.3.13}$$

*for some positive constants* $A_7$ *dependent only on* $d$*,* $p$ *and the smallest angle in* $\tau$*.*

Proof. Let $R_\tau$ be the radial projection defined before. Let $\bar{v}_i, i = 1, 2, 3$ denote the vertices of a planar triangle $\bar{\tau}$, which is the image of $\tau$ under the inverse of $R_\tau$ and $\bar{v} = R_\tau^{-1}v$ for $v \in \tau$. Recall that $|\bar{\tau}| = 2\tan\frac{|\tau|}{2}$ by Lemma 2.1.7

Let $f_\delta(v) = |v|^\delta f\left(\frac{v}{|v|}\right)$ be the homogeneous extension of $f$ to $\mathbb{R}^3\backslash\{0\}$ of degree $\delta = 0$ or 1, and let $\bar{f}_\delta$ denote its restriction to the planar triangle $\bar{\tau}$. By Lemma 3.2 in [40], $\bar{f}_\delta$ belongs to $W^{2,p}(\bar{\tau})$. Note also that $\bar{f}_\delta(\bar{v}_i) = |\bar{v}_i|^\delta f_\delta(\frac{\bar{v}_i}{|\bar{v}_i|}) = |\bar{v}_i|^\delta f(\frac{\bar{v}_i}{|\bar{v}_i|}) = |\bar{v}_i|^\delta f(v_i) = 0, i = 1, 2, 3.$ Therefore by Lemma 6.1 in [26], we have for every $\bar{v} \in \bar{\tau}$

$$|\bar{f}_\delta(\bar{v})| \leq 12|\bar{\tau}|^2 |\bar{f}_\delta|_{2,\infty,\bar{\tau}}. \tag{2.3.14}$$

Since $f(v) = f(\frac{\bar{v}}{|\bar{v}|}) = \frac{\bar{f}_\delta(\bar{v})}{|\bar{v}|^\delta}$ and $|\bar{v}|^\delta \geq 1$ for all $\bar{v} \in \bar{\tau}$,

$$|f(v)| \leq |\bar{f}_\delta(\bar{v})| \leq 48 \left(\tan\frac{|\tau|}{2}\right)^2 |\bar{f}_\delta|_{2,\infty,\bar{\tau}},$$

by (2.3.14). By Proposition 2.3.4 we get (2.3.12) with $A_6 = 48K_6$.

If $f$ is a homogeneous polynomial, then its second derivatives are homogeneous polynomials and by (2.3.9) we have

$$|f|_{2,\infty,\tau} \leq K_8 A_\tau^{-1/p} |f|_{2,p,\tau}$$

and

$$|f|'_{2,\infty,\tau} \leq K_8 A_\tau^{-1/p} |f|'_{2,p,\tau}$$

for some $K_8$ depending on $d$, $p$ and the smallest angle in $\tau$. Hence

$$|f(v)| \leq 48K_6 \left(\tan\frac{|\tau|}{2}\right)^2 |f|_{2,\infty,\tau} \leq A_7 A_\tau^{-1/p} \left(\tan\frac{|\tau|}{2}\right)^2 |f|_{2,p,\tau}$$

This completes the proof with $A_7 = 48K_6K_8$. □

Definition 2.3.9. *Let $\Delta$ a regular spherical triangulation which is a part of sphere with or without holes or the whole sphere. For $d \geq 1$ and $r \geq 0$, two integers with $d \geq 3r + 2$, we define $S_d^{-1}(\Delta)$ to be the space of homogeneous splines of degree $d$ and smoothness $-1$, i.e.*

$$S_d^{-1}(\Delta) := \{s : s|_\tau \in \mathcal{H}_d, \forall \tau \in \Delta\}.$$

*And we define $C^r$* **spline spaces with degree** *$d$ as*

$$S_d^r(\Delta) := S_d^{-1}(\Delta) \cap C^r(\mathbb{S}^2).$$

Although the construction of stable basis is a delicate process, as pointed out in [18], the construction presented there for the bivariate analog of $S_d^r(\Delta)$ also carries over to the spherical spline spaces $S_d^r(\Delta)$. We shall briefly outline the construction after presenting some definitions, and also use the spline spaces that have a local basis to solve the interpolation problem on the sphere.

Let

$$\mathcal{D} := \cup_{\tau\in\Delta}\{\xi_{ijk}^{\tau}, i+j+k=d\}, \tag{2.3.15}$$

with $\xi_{ijk}^{\tau} := \frac{iu+jv+kw}{d}$ for $\tau =< u, v, w >$ be the set of **domain points** associated with $\Delta$ and $d$. It is well known that each spline in $S_d^0(\Delta)$ is uniquely determined by associating one Bézier coefficient with each domain point. A subset $\mathcal{M} \subset \mathcal{D}$ is called a **minimal determining set** for $S_d^r(\Delta)$ if the values of the coefficients of $s \in S_d^r(\Delta)$ associated with domain points in $\mathcal{M}$ uniquely determine all of the coefficients of $s$.

Definition 2.3.10. *(cf. [40], [37]) A basis $\{B_\xi\}_{\xi\in\mathcal{M}}$ for a space $\mathcal{S}$ of splines on a triangulation $\Delta$ is a* **stable local basis**, *if there exists an integer $\ell$ and constants $0 < C_1 < C_2 < \infty$ depending only on $d$ and the smallest angle $\theta_\Delta$ in the triangulation $\Delta$ such that*

*1) for each $\xi \in \mathcal{M}$, $supp(B_\xi) \subseteq star^{\ell}(v_\xi)$ for some $v_\xi$ of $\Delta$,*

*2) for all $\{c_\xi\}_{\xi\in\mathcal{M}}$,*

$$C_1 max_{\xi\in\mathcal{M}}|c_\xi| \le \|\sum_{\xi\in\mathcal{M}} c_\xi B_\xi\|_{\infty,\mathbb{S}^2} \le C_2 max_{\xi\in\mathcal{M}}|c_\xi|. \tag{2.3.16}$$

The construction of a stable local basis using the Bernstein-Bézier representation of splines in $S_d^r(\Delta)$ when $d \ge 3r+2$ is outlined in [40] with a reference to [18]. Now let us show it. Given a minimal determining set, we can construct a basis $\{B_\xi\}_{\xi\in\mathcal{M}}$ for $S_d^r(\Delta)$ by requiring

$$\mu_\eta B_\xi = \delta_{\xi,\eta}, \quad \eta \in \mathcal{M}, \tag{2.3.17}$$

where $\mu_\eta$ is the linear functional which picks the coefficient associated with the domain point $\eta$. In particular, $B_\xi$ has the property that the coefficient associated with $\xi$ is 1 while the coefficients associated with all other points in $\mathcal{M}$ are zero. The remaining coefficients of $B_\xi$ are computed using smoothness conditions.

For any given spline space $S_d^r(\Delta)$, there are many possible choices for a minimal determining set $\mathcal{M}$. A choice of $\mathcal{M}$ presented in [18] leads to a basis with the following properties, where for each $\xi$, $\Omega_\xi := \text{supp}(B_\xi)$ and $\tau_\xi$ is the triangle in which $\xi$ lies.

PROPOSITION 2.3.11. *(cf. [40]) Let $\{B_\xi\}_{\xi\in\mathcal{M}}$ be the basis for $S_d^r(\Delta)$ corresponding to the minimal determining set $\mathcal{M}$ described in [18]. Then there exist constants $C_3, ..., C_9$ depending only on $d, p$ and the minimal angle in $\Delta$ such that for each $\xi \in \mathcal{M}$,*

*1) there exists a vertex $v_\xi \in \Delta$ such that $\Omega_\xi \subseteq star^3(v_\xi)$,*

*2) $\|B_\xi\|_{\infty,\mathbb{S}^2} \le C_3$,*

*3) $|\mu_\xi s| \le C_4\|s\|_{\infty,\tau_\xi}$, for all $s \in S_d^r(\Delta)$,*

*4) $|\mu_\xi s| \le C_5 A_{\tau_\xi}^{-1/p}\|s\|_{p,\tau_\xi}$, for all $s \in S_d^r(\Delta)$, and for every $\tau \in \Delta$,*

*5) $\|B_\xi\|_{p,\tau} \le C_6 A_\tau^{1/p}$,*

*6) $\#I_\tau \le C_7$, where $I_\tau := \{\xi : \tau \subset \Omega_\xi\}$,*

*7) $|B_\xi|_{k,\infty,\tau} \le C_8\rho_\tau^{-k}$, for all $0 \le k \le d$*

*8) $|B_\xi|_{k,p,\tau} \le C_9\rho_\tau^{-k}A_\tau^{1/p}$, for all $0 \le k \le d$.*

The proof of the above lemma can be found in [40]. Furthermore, the analysis of the proof of 8) of the above lemma leads to a refinement of 8) as follows. Using (2.1.1) instead of (2.1.3) in [40] one gets

$$|B_\xi|_{k,p,\tau} \le C_9 \left(\tan\frac{\rho_\tau}{2}\right)^{-k} A_\tau^{1/p} \tag{2.3.18}$$

with $C_9 = A_7C_6$, see [10].

It was shown in [40] that with the basis defined above one can construct a quasi-interpolation operator $Q : L_p(\mathbb{S}^2) \to S_d^r(\Delta)$ which achieves the optimal approximation property. Indeed, extend the linear functionals $\mu_\xi$ to all of $L_p(\mathbb{S}^2)$ using Hahn-Banach theorem. Then for every $f \in L_p(\tau_\xi)$,

$$|\mu_\xi f| \le C_5 A_{\tau_\xi}^{-1/p} \|f\|_{p,\tau_\xi}, \xi \in \mathcal{M}. \tag{2.3.19}$$

This inequality implies that for each $\xi$, the carrier of the extended functional $\mu_\xi$ is contained in $\tau_\xi$, i.e., if $f \equiv 0$ on $\tau_\xi$, then $\mu_\xi f = 0$. With (2.3.18) in mind we modify the proof of Proposition 5.2 in [40] accordingly to get the following

PROPOSITION 2.3.12. *(cf. [40]) For each $f \in L_p(\mathbb{S}^2)$, let*

$$Qf := \sum_{\xi \in \mathcal{M}} (\mu_\xi f) B_\xi. \tag{2.3.20}$$

*Then $Qg = g$ for all $g \in \mathcal{H}_d(\mathbb{S}^2)$. Moreover, there exists a constant $C_{10}$ depending only on $d, p$ and the smallest angle in $\Delta$ such that for each triangle $\tau \in \Delta$,*

$$|Qf|_{k,p,\tau} \le C_{10} \left(\tan \frac{\rho_\tau}{2}\right)^{-k} \|f\|_{p,\Omega_\tau}, \tag{2.3.21}$$

*where $\Omega_\tau := \cup_{\xi \in I_\tau} \Omega_\xi$ and $I_\tau := \{\xi : \tau \subset \Omega_\xi\}$.*

Theorem 4.2 in [40] states the existence of a spherical polynomial of degree $d$ approximating $f \in W^{d+1,p}(\tau)$ for $|\tau| \le 1$ satisfying

$$|f - s|_{k,p,\tau} \le K_9' |\tau|^{d+1-k} |f|_{d+1,p,\tau}.$$

for some positive constant $K_9$ depending on $d$, $p$ and the smallest angle of $\tau$. With a little modification in the proof we can see that in fact

$$|f - s|_{k,p,\tau} \le K_9 (\tan \frac{|\tau|}{2})^{d+1-k} |f|_{d+1,p,\tau} \tag{2.3.22}$$

for a positive constant $K_9$ depending on $d, p$ and the smallest angle of $\tau$. Using this inequality we can prove the following result on local approximation.

THEOREM 2.3.13. *(cf. [40], [10], [37]) Suppose $\tau \in \Delta$ is a spherical triangle with $|\tau| \leq 1$. Let $f \in W^{m+1,p}(\tau)$ for $0 \leq m \leq d$ such that $(d-m) \bmod 2 = 0$. There exists a spherical homogeneous polynomial $s$ of degree $d$ such that for every $0 \leq k \leq m$*

$$|f-s|_{k,p,\tau} \leq C_{11} \left(\tan \frac{|\tau|}{2}\right)^{m+1-k} |f|_{m+1,p,\tau}. \tag{2.3.23}$$

*Here $C_{11}$ is a constant that depends on $p, m$ and $\theta_\Delta$. Moreover*

$$|f-s|_{k,p,\Omega_\tau} \leq C_{11} \left(\tan \frac{|T'|}{2}\right)^{m+1-k} |f|_{m+1,p,\Omega_\tau}. \tag{2.3.24}$$

*Here $T'$ is the largest triangle in $\Omega_\tau$, i.e. $|T| = max\{|T| : T \in \Omega_\tau\}$.*

PROOF. Fix $m$. By Theorem 4.2 in [40], there exists a spherical homogeneous polynomial $s'$ of degree $m$ such that for every $0 \leq k \leq m$

$$|f-s'|_{k,p,\tau} \leq C_{11}|\tau|^{m+1-k}|f|_{m+1,p,\tau}. \tag{2.3.25}$$

If we slightly modify the proof of Theorem 4.2 [40], i.e. replace (2.1.1) by (2.1.2), we can get

$$|f-s'|_{k,p,\tau} \leq C_{11} \left(\tan \frac{|\tau|}{2}\right)^{m+1-k} |f|_{m+1,p,\tau}. \tag{2.3.26}$$

Since $(d-m) \bmod 2 = 0$, $s = |v|^{d-m}s'$ is a homogeneous spherical polynomial of degree $d$. Since on the unit sphere $s' \equiv s$, their $(k-1)$-st extensions are the same, and we have (2.3.23). To get (2.3.24), sum (2.3.23) over triangles in $\Omega_\tau$. We are done. □

Finally we describe a theorem on approximation order of spherical splines to end this chapter.

THEOREM 2.3.14. *([40], [10], [37]) Let $\Delta$ be a $\beta$-quasi-uniform spherical triangulation with $|\Delta| \leq 1$. Let $1 \leq p \leq \infty$, $d \geq 3r+2$, and $0 \leq k \leq d$. Then there exists a constant $C_{12}$ depending only on $d, p$ and the smallest angle in $\Delta$, such that*

$$|f-Qf|_{k,p,\tau} \leq C_{12} \left(\tan \frac{|T'|}{2}\right)^{m+1-k} |f|_{m+1,p,\Omega_\tau}, \tag{2.3.27}$$

*for all $f \in W^{m+1,p}(\mathbb{S}^2)$ and all $\tau \in \Delta$. Moreover, there exists a constant $C_{13}$ such that*

$$|f-Qf|_{k,p,\mathbb{S}^2} \leq C_{13} \left(\tan \frac{|\Delta|}{2}\right)^{m+1-k} |f|_{m+1,p,\mathbb{S}^2}, \tag{2.3.28}$$

*for all* $f \in W^{m+1,p}(\mathbb{S}^2)$ *and all* $0 \le k \le d$ *such that* $Qf \in W^{k,p}(\mathbb{S}^2)$. *Here* $m$ *is taken between* $0$ *and* $d$ *with* $(d-m)$ *mod* $2 = 0$.

PROOF. Let $\tau \in \Delta$ with $|\tau| \le 1$. By Theorem 2.3.13 there exists a spherical homogeneous polynomial $s$ of degree $d$ such that (2.3.23) holds. By the linearity of $Q$ and the fact that $Q$ reproduces polynomials of degree $d$ we can write

$$|f - Qf|_{k,p,\tau} \le |f - s|_{k,p,\tau} + |Q(f-s)|_{k,p,\tau}.$$

We now consider the last term in the above inequality. By (2.3.21)

$$|Q(f-s)|_{k,p,\tau} \le C_{10} \left(\tan \frac{\rho_\tau}{2}\right)^{-k} \|f - s\|_{p,\Omega_\tau}.$$

Since $\Delta$ is assumed to be $\beta$-quasi-uniform $|\rho_\tau| \ge \frac{|T'|}{\beta}$ and therefore

$$\tan \frac{\rho_\tau}{2} \ge \tan \frac{|T'|}{2\beta} \ge \frac{1}{\beta^2} \tan \frac{|T'|}{2}.$$

By Theorem 2.3.13

$$\begin{aligned} |Q(f-s)|_{k,p,\tau} &\le C_{10}C_{11}(\beta)^{2k} \left(\tan \frac{|T'|}{2}\right)^{-k} \left(\tan \frac{|T'|}{2}\right)^{m+1} |f|_{m+1,p,\Omega_\tau} \\ &\le C_{10}C_{11}(\beta)^{2k} \left(\tan \frac{|T'|}{2}\right)^{m+1-k} |f|_{m+1,p,\Omega_\tau}. \end{aligned}$$

Therefore we get (2.3.27) with $C_{12} = C_{11}(1 + C_{10}\beta^{2k})$.

To prove (2.3.28), we sum (2.3.27) over all triangles in $\Delta$.

$$\begin{aligned} |f - Qf|_{k,p,\mathbb{S}^2} &= \sum_{\tau \in \Delta} |f - Qf|_{k,p,\tau} \le C_{12} \left(\tan \frac{|\Delta|}{2}\right)^{m+1-k} \sum_{\tau \in \Delta} |f|_{m+1,p,\Omega_\tau} \\ &\le C_{12} \left(\tan \frac{|\Delta|}{2}\right)^{m+1-k} \sum_{\tau \in \Delta} \sum_{\tau' \subset \Omega_\tau} |f|_{k,p,\tau'} \\ &= C_{12} \left(\tan \frac{|\Delta|}{2}\right)^{m+1-k} \sum_{\tau' \in \Delta} \#\{\tau : \tau' \subset \Omega_\tau\} |f|_{m+1,p,\tau'} \\ &\le C_{12}K_{10} \left(\tan \frac{|\Delta|}{2}\right)^{m+1-k} \sum_{\tau' \in \Delta} |f|_{m+1,p,\tau'}. \end{aligned}$$

Here $K_{10} := \max\{\#\{\tau : \tau' \subset \Omega_\tau\}, \tau' \in \Delta\}$ which is bounded by Lemma 2.1.10. Therefore (2.3.28) holds with $C_{13} = C_{12}K_{10}$. We are done. □

# Chapter 3

## Spherical Hermite Interpolation

In this chapter, we study spherical Hermite interpolation problem. Given a set of scattered data with derivative values, we use the minimal energy method to find Hermite interpolation on spherical spline spaces over a spherical triangulation of the scattered data locations. Note that the spherical triangulation is a part of a sphere with or without holes, or the whole sphere. We show that the minimal energy method produces a unique Hermite spherical spline interpolation for a given scattered data with derivative values. Also we show that the Hermite interpolation spline converges to a given sufficiently smooth function $f$ if the values are obtained from this $f$. That is, the surface of the Hermite interpolation spherical spline resembles the given set of derivative values. We organize this chapter as the following. In section 1, we give an overview of spherical Hermite interpolation. In section 2, we discuss the existence and uniqueness of the Hermite data interpolatory splines with minimal energy. In section 3, we study the approximation properties of spline interpolants. In section 4, we give a computational method for minimal energy spherical Hermite interpolatory splines.

### 3.1 Overview

Definition 3.1.1. *Let $\mathbb{S}^2$ denote a unit sphere in $\mathbb{R}^3$ and $\mathcal{V} = \{v_i = (x_i, y_i, z_i)\}_{i=1}^n$ be a set of scattered points on $\mathbb{S}^2$. Suppose that we are given the following data values*

$$f_i^{\alpha,\beta}, 0 \leq \alpha + \beta \leq l, i = 1, \cdots, n,$$

*where $l \geq 0$. Then the* **Hermite interpolation problem on-the-sphere** *is to find a smooth function $s \in C^m(\mathbb{S}^2)$ such that*

$$D_\phi^\alpha D_\theta^\beta s(v_i) = f_i^{\alpha,\beta}, 0 \leq \alpha + \beta \leq l, i = 1, \ldots, n. \tag{3.1.1}$$

*where $D_\phi^\mu$ and $D_\theta^\nu$ are the derivative along latitude and longitude direction respectively, and in general we need $m \geq l$. If we only interpolate partial values defined in (3.1.1), then we call this kind of interpolation problem as* **quasi-Hermite interpolation on-the-sphere**, *and we shall use this notion in Chapter 4 for hole filling problem and point cloud(scattered data) problem. For $C^r(r \geq 0)$ hole filling problem, we may only interpolate the derivatives up to the $r$-th order at vertices of boundary edges, that is, our surface is Hermite interpolation curve when it is restricted to boundary curves. For point cloud problem, we may only interpolate partial points or their derivatives.*

In case $l = 1$, this definition is similar to the Definition 8 in [22] where the Hermite interpolation problem is to find a function $s$ on the sphere such that $s$ interpolates location values and two first order independent direction derivatives. We have generalized this definition. Note that we have a fixed coordinate $(\phi, \theta)$ such that

$$x = \sin(\phi)\cos(\theta), y = \sin(\phi)\sin(\theta), z = \cos(\phi)$$

with $\phi \in [0, \pi]$ and $\theta \in [0, 2\pi]$. If we use three-dimensional coordinate system in $\mathbb{R}^3$, then we need to construct a smooth function $s \in C^m(\mathbb{S}^2)$ such that

$$D_x^\alpha D_y^\beta D_z^\gamma s(v_i) = f_i^{\alpha,\beta,\gamma}, 0 \leq \alpha + \beta + \gamma \leq l, i = 1, \ldots, n. \tag{3.1.2}$$

And this is a generalization of the planar case in [48]. It is easy to show these expressions are equivalent to each other exception polar points. We use polar system to avoid the computing trouble in polar points.

We shall use spherical spline functions to construct such an interpolative surface $s$. When $l = 0$, this is a standard Lagrange interpolation problem and it was studied in [4], [11], [22]. In this chapter, we consider $l \geq 1$. For $l \geq 1$, it is a classical Hermite interpolation problem. It has been studied in [4] with $l = 1$ by constructing $C^2$ macro-elements. As pointed in [37], it is also an analog of planar case with $l \gneq 1$ by constructing $C^{l+1}$ macro-elements. However, all the constructions require higher order derivative information than the given data. Also

derivatives at edges are needed in order to make these macro-elements smooth across common edges. Since such higher order derivatives and normal derivative information are not available in practice, we have to use other techniques to estimate the needed information. As in the case $l = 0$, one can use a minimal energy method to construct an interpolation spline. For Hermite interpolation problem, we can also use minimal energy technique.

The interpolation problem with $l \leq 2$ does have an important practical application. In the year 2007, a satellite called GOCE(Gravity field and steady-state Ocean Circulation Explorer) will be launched in December to collect gravitational vectors over sampling points around the Earth . Together the geopotential data from CHAMP(CHAllenging Minisatellite Payload which is a German small satellite mission for geoscientific and atmospheric research and applications), we have

$$g(v_i) \text{ up to a constant}, D_x g(v_i), D_y g(v_i), D_z g(v_i), i = 1, \ldots, n$$

and

$$D^2_{xx} g(v_i), D^2_{xy} g(v_i), D^2_{yy} g(v_i), i = 1, \ldots, n$$

will be available around the Earth for a large integer $n$, where $g$ denotes the geopotential function, cf. [25]. Let $(\phi_i, \theta_i)$ be the spherical coordinate for point $v_i$. Then the following

$$\begin{aligned} D_\phi g(v_i) &= D_x g(v_i)\cos(\phi_i)\cos(\theta_i) + D_y g(v_i)\cos(\phi_i)\sin(\theta_i) - D_z g(v_i)\sin(\phi_i) \\ D_\theta g(v_i) &= -D_x g(v_i)\sin(\phi_i)\sin(\theta_i) + D_y g(v_i)\sin(\phi_i)\cos(\theta_i) \end{aligned} \tag{3.1.3}$$

as well as $D^2_{\phi\phi} g(v_i), D^2_{\theta\phi} g(v_i), D^2_{\theta\theta} g(v_i)$ for all $i = 1, \ldots, n$ will be available. The purpose of the satellite is to get more accurate estimate of geopotential near the surface of the Earth. An important intermediate step is to estimate the geopotential very accurately at the orbital level of the satellite, cf. [12] and [25]. That is, we want $s$ to resemble the given data values. More precisely, if $f$ is sufficiently smooth over $\mathbb{S}^2$, we would like a spherical spline function $s \in S^r_d$ satisfying (3.1.1) and approximate $f$ very well in the following sense:

$$\|f - s\|_{L_\infty(\mathbb{S}^2)} \leq C(\tan\frac{|\triangle|}{2})^{l+1} \tag{3.1.4}$$

for a constant $C$ dependent on $f$, where $f$ is a sufficiently smooth function over $\mathbb{S}^2$. These spherical splines were introduced in [3] more than 10 years ago and were used for scattered data interpolation and fitting, e.g., [22] and [11]. Recall that space of spherical polynomial splines

$$S_d^r(\Delta) := \{s \in C^r(\Omega) : s|_T \in \mathcal{H}_d(\mathbb{S}^2), \forall T \in \Delta\},$$

where $d \geq 3r + 2$ and $\mathcal{H}_d$ is a homogeneous polynomial spaces on sphere with degree $d$, and $\Omega$ is the sphere domain bounded by $\Delta$ which is a triangulation of the sphere projection of data locations in $\mathbb{R}^3$ that could cover sphere $\mathbb{S}^2$ or could not cover $\mathbb{S}^2$.

For $d \geq 3r + 2$, the existence of Hermite interpolatory spline satisfying conditions (3.1.1) can be easily understood from [4], [40], [37]. For the proof of uniqueness, see next section. Next we are interested in how well the interpolatory spline resemble the given data. For only location interpolation(standard Lagrange interpolation spline problem), the approximation of spherical splines with the second order energy functional $E^2$ was studied in [10]. The researchers in [10] showed that the minimal energy interpolatory splines converges to values of the given location data when the number of data values increases and the size of triangulation decreases. Here we need to consider additional interpolation conditions except the location values. Also we are going to use the third order energy functional $E^3$. We want to attain an analog of planar case in [48]. But the main difficulty lies in that we do not have the planar counterpart of Taylor expansion on sphere. Our main theorems give the convergence rate of minimal energy interpolation under two different norms.

## 3.2 Existence and Uniqueness of Spherical Hermite Minimal Energy Interpolation

In this section we first give a brief review of energy functionals and then give the the proof of existence and uniqueness of minimal energy spherical Hermite interpolatory splines. Recall that an energy functional $E(f)$ is an expression for the amount of potential energy in a thin elastic plate $f$ that passes through the data points $\mathcal{V}$ over planar region. The potential

energy of the thin plate is given by

$$E = \int_\Omega [aH^2 + bK]\, dxdy, \tag{3.2.1}$$

where $H$ and $K$ are mean curvature and Gaussian curvature of the surface $S$ and $a$ and $b$ are constants which depend on the materials of the plate, cf. [43]. In particular,

$$H = \frac{\kappa_1 + \kappa_2}{2} = \frac{(1+f_x^2)f_{yy} - 2f_x f_y f_{xy} + (1+f_y^2)f_{xx}}{(1+f_x^2+f_y^2)^{\frac{3}{2}}}$$

and

$$K = \kappa_1\kappa_2 = \frac{f_{xx}f_{yy} - f_{xy}^2}{(1+f_x^2+f_y^2)^2},$$

where $\kappa_1$ and $\kappa_2$ are the principle curvatures of the surface of the plate. Suppose that $f_x \approx 0$ and $f_y \approx 0$ when the plate has small deflections. The potential energy $E$ can be simplified in the following form:

$$E(f) = \int_\Omega [a(f_{xx}+f_{yy})^2 - 2(1-\omega)(f_{xx}f_{yy} - f_{xy}^2)]\, dxdy,$$

where the parameter $\omega$ is a constant depending on the material at the hand, cf. [24]. For simplicity, we choose $a = 1$ and $\omega = 0$. That is,

$$\begin{aligned} E(f) &= \int_\Omega [f_{xx}^2 + 2f_{xy}^2 + f_{yy}^2]\, dxdy, & (3.2.2)\\ &= \int_\Omega \left[\sum_{k=0}^{2} \binom{2}{k} [(\frac{\partial}{\partial x})^k (\frac{\partial}{\partial y})^{2-k} f]^2\right] dxdy & (3.2.3) \end{aligned}$$

which is commonly used in the literature, cf. [21]. In [48] the following energy functional was taken:

$$E(f) = \int_\Omega \left[\sum_{k=0}^{\bar{l}+2} \binom{\bar{l}+2}{k} [(\frac{\partial}{\partial x})^k (\frac{\partial}{\partial y})^{\bar{l}+2-k} f]^2\right] dxdy.$$

For spherical domain, the energy functional in [4] was defined as

$$E(f) = \int_{\mathbb{S}^2} (\Delta^* f)^2\, d\mu,$$

where $\Delta^*$ is the Laplace-Beltrami operator, $\mu$ is the Lebesgue measure on $\mathbb{S}^2$, and the integral in this definition is taken over the unit sphere. Because the Laplace-Beltrami operator only

annihilates constants. In [11], the researchers introduced an alternative functional motivated by Sobolev-type seminorms defined in [40] (also see Section 2 in Chapter2) like the following

$$E_\delta(f) = \int_{\mathbb{S}^2} \sum_{|\gamma|=2} (D^\gamma f_\delta)^2 \, d\mu, \tag{3.2.4}$$

where and $\gamma = (\gamma_1, \gamma_2, \gamma_3)$ with $|\gamma| = \gamma_1 + \gamma_2 + \gamma_3$, $D^\gamma = D_x^{\gamma_1} D_y^{\gamma_2} D_z^{\gamma_3}$ is a standard differential operator, $f_\delta$ is the unique homogeneous extension of $f$ of degree $\delta$ to $\mathbb{R}^3 \backslash \{0\}$ defined by $f_\delta(v) = |v|^\delta f(\frac{v}{|v|})$. If the degree $d$ of homogeneous spline space is even, then $\delta$ is taken 0; if odd, $\delta$ is taken 1. After evaluating the second order partial derivatives, $D^\alpha f_\delta$ are restricted to $\mathbb{S}^2$ and are then integrated.

In this dissertation, we take some changes from the above functionals and use a generalized version of the energy functional $E(f)$ which can be represented as

$$E_\delta(s) = \int_\Omega \left[ \sum_{k=0}^{\bar{l}+2} \binom{\bar{l}+2}{k} [(\frac{\partial}{\partial x})^k (\frac{\partial}{\partial y})^{\bar{l}+2-k} s_\delta]^2 \right] dxdy, \tag{3.2.5}$$

where $\Omega$ is a connected domain bounded by a triangulation $\Delta$ of a part or whole sphere. For $s \in S_d^r(\Delta)$, we can use energy functional

$$E_\delta(s) = \sum_{\tau \in \Delta \subseteq \mathbb{S}^2} \int_\tau \sum_{|\alpha|=\bar{l}+2} |D^\alpha s_\delta|^2 \, d\mu. \tag{3.2.6}$$

It is equivalent to the following one.

$$E_\delta(s) = \sum_{\tau \in \Delta \subseteq \mathbb{S}^2} \int_\tau \left[ \sum_{k=0}^{\bar{l}+2} \binom{\bar{l}+2}{k} [(\frac{\partial}{\partial x})^k (\frac{\partial}{\partial y})^{\bar{l}+2-k} s_\delta]^2 \right] dxdy.$$

When $\bar{l} = 0$, we call the $E_\delta(s)$ in (3.2.6) as the **second order energy functional** $E_\delta^2$; When $\bar{l} = 1$, we call it the **third order energy functional** $E_\delta^3$. In this dissertation, we mainly focus on above two energy functionals. In general, we need $l \geq 1$ for $E^3$ and $l \geq 0$ for $E^2$.

To establish the existence and uniqueness of spherical splines in $S_d^r(\Delta)$ interpolating conditions (3.1.1) and minimizing (3.2.6), we need the following.

LEMMA 3.2.1. *Let $\Delta$ be a spherical triangulation of an interested domain and suppose $f \neq 0$. Then*

*1)* $E_0^2(f) = 0$ *if and only if* $f$ *is a constant,*

*2)* $E_1^2(f) = 0$ *if and only if* $f$ *is a trivariate homogeneous linear polynomial on* $\mathbb{S}^2$.

PROOF. The proof can be found in [11] □

LEMMA 3.2.2. *Let* $\Delta$ *be a spherical triangulation of an interested domain and suppose* $f \neq 0$. *Then*

*1)* $E_0^3(f) = 0$ *if and only if* $f$ *is a trivariate homogeneous linear polynomial on* $\mathbb{S}^2$,

*2)* $E_1^3(f) = 0$ *if and only if* $f$ *is a trivariate homogeneous quadratic polynomial on* $\mathbb{S}^2$.

PROOF. If $E_\delta^3(f) = 0$, then by definition, $D^\alpha f_\delta = 0$ on every triangle $\tau \in \Delta$ for $|\alpha| = 3$. Consider $\delta = 1$. Since $f_1$ is linear homogeneous, $D^\alpha f_1$ is homogeneous of degree $-2$, and therefore, by the uniqueness of homogeneous extensions, $(D^\alpha f_1|_\tau)_{-2} = D^\alpha f_1$. On the other hand, by definition, $(D^\alpha f_1|_\tau)_{-2}(v) = |v|^{-2}(D^\alpha f_1|_\tau)(\frac{v}{|v|})$. As we noted above, $D^\alpha f_1|_\tau = 0$, and therefore $D^\alpha f_1 = 0$ as well. Hence $f_1$ is a polynomial of degree at most 2. Since it is a homogeneous quadratic function, $f_1$ must be a homogeneous quadratic polynomial on $\mathbb{R}^3$. Therefore by uniqueness of homogeneous extensions, $f$ is a quadratic homogeneous polynomial on $\tau$. A similar proof works for $\delta = 0$. The other direction is trivial from definition (3.2.6). □

LEMMA 3.2.3. *Let* $g$ *be a trivariate homogeneous quadratic polynomial. If* $g$ *and its first order derivatives equal zero on three vertices of a non-degenerate triangle* $\tau :=< v_1, v_2, v_3 >$, *then* $g \equiv 0$ *on* $\tau$.

PROOF. Let $g(x, y, z) = ax^2 + by^2 + cz^2 + dxy + exz + fyz$, then taking partial derivatives with respect to $x, y, z$, we get

$$g_x(x, y, z) = 2ax + dy + ez, g_y(x, y, z) = 2by + dx + fz, g_z(x, y, z) = 2cz + ex + fy.$$

By assumption, we have

$$g(x_i, y_i, z_i) = ax_i^2 + by_i^2 + cz_i^2 + dx_iy_i + ex_iz_i + fy_iz_i = 0, i = 1, 2, 3$$

and

$$g_x(x_i, y_i, z_i) = 2ax_i + dy_i + ez_i = 0, i = 1, 2, 3,$$

$$g_y(x_i, y_i, z_i) = 2by_i + dx_i + fz_i = 0, i = 1, 2, 3,$$

$$g_z(x_i, y_i, z_i) = 2cz_i + ex_i + fy_i = 0, i = 1, 2, 3.$$

Therefore we have

$$\begin{bmatrix} x_1 & y_1 & z_1 \\ x_2 & y_2 & z_2 \\ x_3 & y_3 & z_3 \end{bmatrix} \begin{bmatrix} 2a \\ d \\ e \end{bmatrix} = \begin{bmatrix} 0 \\ 0 \\ 0 \end{bmatrix},$$

$$\begin{bmatrix} x_1 & y_1 & z_1 \\ x_2 & y_2 & z_2 \\ x_3 & y_3 & z_3 \end{bmatrix} \begin{bmatrix} d \\ 2b \\ f \end{bmatrix} = \begin{bmatrix} 0 \\ 0 \\ 0 \end{bmatrix},$$

and

$$\begin{bmatrix} x_1 & y_1 & z_1 \\ x_2 & y_2 & z_2 \\ x_3 & y_3 & z_3 \end{bmatrix} \begin{bmatrix} e \\ f \\ 2c \end{bmatrix} = \begin{bmatrix} 0 \\ 0 \\ 0 \end{bmatrix}.$$

Since triangle $\tau$ is non-degenerate, so $det(v_1, v_2, v_3) \neq 0$. Hence by Crammer rule we get that $a, b, c, d, e, f$ are all zeros. We are done. □

Let $\Delta$ be a triangulation of the domain of interest over the unit sphere. Assume that the data locations $v_i, i = 1, \cdots, n$ are vertices of $\Delta$. Let $S_d^r(\Delta)$ be the spherical spline space of degree $d \geq 3r + 2$ and $r \geq l$ over $\Delta$. To approximate $f$, we choose a linear space $\mathcal{S} \subseteq S_d^r(\Delta)$ of polynomial splines of degree $d$ defined on a triangulation $\Delta$ as above. For a given set of data $f_i^{\alpha,\beta}, 0 \leq \alpha + \beta \leq l, i = 1, \cdots, n$, let

$$U_f := \{s \in S_d^r(\Delta), D_\theta^\alpha D_\phi^\beta s(v_i) = f_i^{\alpha,\beta},\ i = 1, \cdots, n\,,\ 0 \leq \alpha + \beta \leq l\}. \tag{3.2.7}$$

When $d \geq 3r+2$, it is known that $U_f$ is not empty when $\mathcal{S}$ is big enough, cf. [4] and [40]. That is, there exists a spline $s_f \in S_d^r(\Delta)$ satisfying the interpolation conditions (3.1.1). We shall

use the energy functional $E$ defined in the previous section to find an Hermite interpolatory spline of good shape in the following sense: $S_f \in U_f$ and

$$E(S_f) = \min\{E(s), \quad s \in U_f\}. \tag{3.2.8}$$

Let us first show that $S_f$ exists and is unique. First of all, it is clear that $U_f$ is a nonempty convex set in a finite dimensional space $S_d^r(\Delta)$. Let

$$W = \{s \in S_d^r(\Delta),\ D_\theta^\alpha D_\phi^\beta s(v_i) = 0,\ 0 \le \alpha + \beta \le l,\ i = 1, \cdots, n, \}, \tag{3.2.9}$$

and

$$X := \{f \in B(\mathbf{S}) : f|_\tau \in C^3(\tau), \forall \tau \in \Delta\},$$

where $B(\mathbf{S})$ is the set of all bounded real-valued functions on the sphere $\mathbb{S}^2$. For each triangle $\tau \in \Delta$, let

$$\langle f, g\rangle_{E,\tau} := \int_\tau \sum_{|\alpha|=\bar{l}+2} D^\alpha f_\delta\ D^\alpha g_\delta.$$

Then

$$\langle f, g\rangle_E := \sum_{\tau \in \Delta \subseteq \mathbb{S}^2} \langle f, g\rangle_{E,\tau}$$

is a semidefinite inner product on $X$. Let $||f||_{E,\tau}$ and $||f||_E$ be the associated seminorms. We can see that $< \cdot, \cdot >$ is an inner product on the linear space $W$ defined in (3.2.9) and $E(s)^{\frac{1}{2}}$ is a norm on $W$.

LEMMA 3.2.4. *Let $E$ be defined as (3.2.6). Then $\|s\|_E := E(s)^{1/2} = \langle s, s\rangle_E^{\frac{1}{2}}$ is a norm on $W$ induced by energy functional.*

PROOF. Clearly, we have $\|s\|_E \ge 0$ and $\|\alpha s\|_E = \alpha \|s\|_E$ for any real number $\alpha$ by definition. Now let us show that triangle inequality is true. In fact, by Cauchy-Schwarz

inequality, we have

$$\begin{aligned}
\|s+t\|_E^2 &= \sum_{\tau\in\Delta\subseteq\mathbb{S}^2}\int_\tau \sum_{|\alpha|=\bar{l}+2} |D^\alpha(s_\delta+t_\delta)|^2\,d\mu \\
&= \sum_{\tau\in\Delta\subseteq\mathbb{S}^2}\int_\tau \sum_{|\alpha|=\bar{l}+2} |D^\alpha s_\delta + D^\alpha t_\delta|^2\,d\mu \\
&= \sum_{\tau\in\Delta\subseteq\mathbb{S}^2}\int_\tau \sum_{|\alpha|=\bar{l}+2} |(D^\alpha s_\delta)^2 + 2D^\alpha s_\delta D^\alpha t_\delta + (D^\alpha t_\delta)^2|\,d\mu \\
&\le \sum_{\tau\in\Delta\subseteq\mathbb{S}^2}\int_\tau \sum_{|\alpha|=\bar{l}+2} |D^\alpha s_\delta|^2 + 2|D^\alpha s_\delta D^\alpha t_\delta| + |D^\alpha t_\delta|^2\,d\mu \\
&\le E(s)+E(t)+2\Big(\sum_{\tau\in\Delta\subseteq\mathbb{S}^2}\int_\tau \sum_{|\alpha|=\bar{l}+2} |D^\alpha s_\delta|^2\,d\mu\Big)^{1/2}\Big(\sum_{\tau\in\Delta\subseteq\mathbb{S}^2}\int_\tau \sum_{|\alpha|=\bar{l}+2} |D^\alpha t_\delta|^2\,d\mu\Big)^{1/2} \\
&= E(s)+E(t)+2E(s)^{\frac{1}{2}}E(t)^{\frac{1}{2}} \\
&= (E(s)^{\frac{1}{2}}+E(t)^{\frac{1}{2}})^2 \\
&= (\|s\|_E+\|t\|_E)^2.
\end{aligned}$$

Hence

$$\|s+t\|_E \le \|s\|_E + \|t\|_E.$$

Finally we need to show that $\|s\|_E = 0$ implies $s \equiv 0$. Note that $\|s\|_E = 0$ implies that $s$ is a homogeneous polynomial of degree at most $\bar{l}+1$. The zero interpolation conditions at vertices $v_i, i = 1,2,3$ implies that $s \equiv 0$. Indeed if $E$ is the second order energy function, then $\bar{l} = 0$ and $s$ is a trivariate homogeneous function with degree at most 1. So we attain $s \equiv 0$ by Lemma 3.2.1. If $E$ is the third order energy function, then $\bar{l} = 1$ and $s$ is a trivariate homogeneous function with degree at most 2. Therefore we prove $s \equiv 0$ by Lemma 3.2.2 and Lemma 3.2.3. We are done. □

Let $s_f$ be any spline in the set $U_f$ defined above. It is easy to see that $U_f = s_f + W$. The minimization problem in (3.2.8) can be written as

$$E(S_f) = \min\{E(s_f+w), \quad w \in W\}.$$

Thus, the solution $S_f$ can be written as $S_f = s_f - Ps_f$, where $P$ is the linear projector $P : X \to W$ defined by

$$E(f - Pf) = \min_{w \in W} E(f + w),$$

for all $f \in X$. Since $W$ is a Hilbert space with respect to $\langle \cdot, \cdot \rangle_E$, $Pf$ is uniquely defined and is characterized by

$$\langle f - Pf, w \rangle_E = 0, \qquad \forall w \in W. \tag{3.2.10}$$

Moreover

$$\|Pf\|_E \leq \|f\|_E \tag{3.2.11}$$

for all $f \in X$. In fact, $\langle f - Pf, w \rangle_E = 0$ implies that $\langle Pf, w \rangle_E = \langle f, w \rangle_E$, so by Cauchy-Schwarz inequality we have

$$|\langle Pf, w \rangle_E| \leq |\langle f, w \rangle_E| \leq \|f\|_E \|w\|_E$$

Hence, if $\|w\|_E \neq 0$, then we have

$$|\langle Pf, \frac{w}{\|w\|_E} \rangle_E| \leq \|f\|_E.$$

By the definition of norm, we complete the proof of (3.2.11).

Therefore, there exists a unique $S_f \in U_f$ such that the energy norm $E(S_f)$ is minimal and we have proved the following theorem

THEOREM 3.2.1. *There exists a unique spline in $S_d^r(\Delta)$ minimizing (3.2.8)*

## 3.3 Approximation Power of Spherical Hermite Interpolation Splines

This section devotes to the study of convergence of minimal energy Hermite interpolatory splines. We have to assume that $\Delta$ is a triangulation of data locations $v_i, i = 1, \cdots, n$.

Note that $Ps_f$ is characterized by

$$\langle s_f - Ps_f, w \rangle_E = 0, \quad \text{for all } w \in W.$$

Here the inner product $\langle f, g\rangle_E$ is induced by the energy norm in the sense that $E(f) = \langle f, f\rangle_E$. By (3.2.11), we have

$$\|Ps_f\|_E \leq \|s_f\|_E. \tag{3.3.1}$$

LEMMA 3.3.1. *Let $T$ be a spherical triangle such that $|T| \leq 1$, and suppose that $D_\theta^\mu D_\phi^\nu f(v_i) = 0$ for $i = 1, 2, 3$ and $0 \leq \mu + \nu \leq l$ and $f \in C^{l+2}(T)$. Then for all $v \in T$,*

$$|f(v)| \leq K(\tan\frac{|T|}{2})^{l+2}|f|_{l+2,\infty,T} \tag{3.3.2}$$

*for some positive constant $K$ independent of $f$ and $T$, where $|f|_{l+2,\infty,T}$ denotes the maximal norm of the $(l+2)$th derivative of $f$ over $T$.*

PROOF. Let $R_T$ be the radial projection defined in [40]. Let $\bar{v}_i, i = 1, 2, 3$ denote the vertices of a planar triangle $\bar{T}$, which is the image of $T$ under the inverse of $R_T$ and $\bar{v} = R_T^{-1}v$ for $v \in T$. Recall from [10] that $|\bar{T}| = 2\tan\frac{|T|}{2}$.

Let $f_{l+1}(v) = |v|^{l+1}f(\frac{v}{|v|})$ be the homogeneous extension of $f$ to $R^3 \setminus \{0\}$ of degree $l+1$ and let $\bar{f}_{l+1}$ denote its restriction to the planar triangle $\bar{T}$. By Lemma 3.2 in [40], $\bar{f}_{l+1}$ belongs to $W_p^{l+2}(\bar{T})$. Note that $\bar{f}_{l+1}(\bar{v}_i) = |\bar{v}_i|^{l+1}f(v_i)$ and $D_\theta^\mu D_\phi^\nu f(v_i) = 0$ for $i = 1, 2, 3$ and $0 \leq \mu + \nu \leq l$, then $D_x^\alpha D_y^\beta \bar{f}(\bar{v}_i) = 0, \alpha + \beta = 0, \cdots, l, i = 1, 2, 3$. Therefore by Lemma 4.1 in [48], we have for every $\bar{v} \in \bar{T}$

$$|\bar{f}_{l+1}(\bar{v})| \leq C|\bar{T}|^{l+2}|\bar{f}_{l+1}|_{l+2,\infty,\bar{T}} \tag{3.3.3}$$

Since $f(v) = \frac{\bar{f}_{l+1}(\bar{v})}{|\bar{v}|^{l+1}}$ and $|\bar{v}| \geq 1$ for all $\bar{v} \in \bar{T}$,

$$|f(v)| \leq |\bar{f}_{l+1}(\bar{v})| \leq C(\tan\frac{|T|}{2})^{l+2}|\bar{f}_{l+1}|_{l+2,\infty,\bar{T}}$$

by (3.3.3). By Proposition 3.4 in [40], there exists a positive constant $K$ such that we get

$$|f(v)| \leq CK(\tan\frac{|T|}{2})^{l+2}|f|_{l+2,\infty,T}.$$

This completes the proof. □

We now are ready to establish an approximation property of $S_f$. Without loss of generality, we may assume that $\Delta$ is a triangulation of the entire unit sphere. Let us first have a quick review of Theorem 2.3.14 for the seminorm approximation properties of spherical spline space $S_d^r(\Delta)$ with $d \geq 3r+2$.

Note that when $p = \infty$, $Q_f$ can be chosen to be an interpolatory spline by Theorem 2.3.14. We first consider the standard $L_2$ norm approximation on the entire sphere $\mathbb{S}^2$.

THEOREM 3.3.1. *Suppose $S_d^r$ is a spline space defined on a $\beta$-quasi-uniform triangulation $\triangle$ with $|\triangle| \leq 1$, $d \geq 3r+2$ and $(d-l)$ mod $2 = 1$ for $l$ defined in (3.2.7). There exists a constant $C$ depending only on $d$ and $\beta$, such that the minimal energy interpolant $S_f$ defined in (3.2.8) satisfies*

$$\|f - S_f\|_{L_2(\mathbb{S}^2)} \leq C(\tan\frac{|\triangle|}{2})^{l+2}|f|_{l+2,\infty,\mathbb{S}^2} \tag{3.3.4}$$

*for all $f \in C^{r+2}(\mathbb{S}^2)$ and some $l$ with $r \geq l$.*

PROOF. Since $S_f = Q_f - PQ_f$, we have

$$||S_f - f||_{L_2(\mathbb{S}^2)} \leq ||Q_f - f||_{L_2(\mathbb{S}^2)} + ||PQ_f||_{L_2(\mathbb{S}^2)}.$$

and by using the above Lemma 3.3.1,

$$\begin{aligned}
||PQ_f||^2_{L_2(\mathbb{S}^2)} &= \sum_{T\in\Delta} ||PQ_f||^2_{L_2(T)} \\
&= \sum_{T\in\Delta} \int_T |PQ_f|^2 \, d\mu \\
&\leq \sum_{T\in\Delta} ||PQ_f||^2_{\infty,T} \int_T d\mu \\
&\leq \sum_{T\in\Delta} A_T ||PQ_f||^2_{\infty,T} \\
&\leq \sum_{T\in\Delta} A_T C(\tan\frac{|T|}{2})^{2l+4}|PQ_f|^2_{l+2,\infty,T} \\
&\leq \sum_{T\in\Delta} CC_1(\tan\frac{|T|}{2})^{2l+4}|PQ_f|^2_{l+2,2,T} \\
&\leq C_2(\tan\frac{|\Delta|}{2})^{2l+4}||PQ_f||^2_E \\
&\leq C_2(\tan\frac{|\Delta|}{2})^{2l+4}||Q_f||^2_E
\end{aligned}$$

by using (3.3.1). Here $A_T$ denotes the area of spherical triangle $T$. By the approximation property of $Q_f$ from Theorem 2.3.14 with $k = 0$, $p = \infty$ and $m = l + 1$, one has

$$\|f - Q_f\|_{\infty,\mathbb{S}^2} \leq C(\tan\frac{|\triangle|}{2})^{l+2}|f|_{l+2,\infty,\mathbb{S}^2}$$

and

$$|Q_f|_{l+2,\infty,\mathbb{S}^2} \leq K|f|_{l+2,\infty,\mathbb{S}^2}.$$

We have

$$||S_f - f||_{L_2(\mathbb{S}^2)} \leq C(\tan\frac{|\triangle|}{2})^{l+2}|f|_{l+2,\infty,\mathbb{S}^2}.$$

We are done. □

Next we study the error $S_f - f$ in the maximum norm.

THEOREM 3.3.2. *Suppose $S_d^r$ is a spline space defined on a $\beta$-quasi-uniform triangulation $\triangle$ with $|\triangle| \leq 1$, $d \geq 3r + 2$ and $(d - l)$ mod $2 = 1$ for $l$ defined in (3.2.7). There exists a constant $C$ depending only on $d$ and $\beta$, such that the minimal energy interpolant $S_f$ defined in (3.2.8) satisfies*

$$\|f - S_f\|_{L_\infty(\mathbb{S}^2)} \leq C(\tan\frac{|\triangle|}{2})^{l+1}|f|_{l+2,\infty,\mathbb{S}^2} \tag{3.3.5}$$

*for all $f \in C^{r+2}(\mathbb{S}^2)$.*

PROOF. Again we use $S_f = Q_f - PQ_f$ to have

$$||S_f - f||_{\infty,\mathbb{S}^2} \leq ||Q_f - f||_{\infty,\mathbb{S}^2} + ||PQ_f||_{\infty,\mathbb{S}^2}.$$

There exists a triangle $T_0 \in \Delta$ such that $||PQ_f||_{\infty,\mathbb{S}^2} = ||PQ_f||_{L_\infty(T_0)}$. By using Lemma 3.3.1,

$$||PQ_f||_{L_\infty(T_0)} \leq C|T_0|^{l+2}|PQ_f|_{l+2,\infty,T_0}.$$

Since $PQ_f$ is a spherical polynomial of degree $d$, $|PQ_f|_{l+2,\infty,T_0} \leq C|PQ_f|_{l+2,2,T_0}/|T_0| \leq C\|PQ_f\|_E/|T_0|$. By (3.3.1), $\|PQ_f\|_E \leq \|Q_f\|_E \leq 4\pi\|Q_f\|_{l+2,\infty,\mathbb{S}^2}$. Thus,

$$\|S_f - f\|_{\infty,\mathbb{S}^2} \leq \|Q_f - f\|_{\infty,\mathbb{S}^2} + C|\Delta|^{l+2}4\pi\|Q_f\|_{l+2,\infty,\mathbb{S}^2}/|T_0|.$$

By the approximation property of $Q_f$ from Theorem 2.3.14 with $k = 0$ and $m = l + 1$, we have

$$||S_f - f||_{L_\infty(\mathbb{S}^2)} \leq C(\tan \frac{|\triangle|}{2})^{l+1}|f|_{l+2,\infty,\mathbb{S}^2}.$$

Therefore we have proved the theorem. □

## 3.4 Computational Method for Spherical Hermite Interpolation Spline

In this section we describe how the minimal energy Hermite interpolation methods are implemented in practice. Given $\mathcal{V} := \{v \in \mathbb{S}^2\}$ a set of points on the unit sphere with real numbers $\{f(v),\ v \in \mathcal{V}\}$, we construct a regular spherical triangulation $\Delta$ which is a part of sphere with or without holes or the whole sphere. For $d \geq 1$ and $r \geq 0$, two integers with $d \geq 3r+2$, define $S_d^{-1}(\Delta)$ to be the space of homogeneous splines of degree $d$ and smoothness $-1$, i.e.

$$S_d^{-1}(\Delta) := \{s : s|_\tau \in \mathcal{H}_d, \forall \tau \in \Delta\}.$$

Then let

$$S_d^r(\Delta) := S_d^{-1}(\Delta) \cap C^r(\mathbb{S}^2).$$

It is understood from [4] and [40] that for $d \geq 3r + 2$ there is more than one interpolating spline in set $U_f$ defined by (3.2.7). A typical way to use the extra degrees of freedom is to minimize a functional $E(s)$ measuring smoothness of $s$. Let

$$E_\delta(s) = \sum_{\tau \in \Delta \subseteq \mathbb{S}^2} \int_\tau (\diamondsuit s_\delta)^T (\diamondsuit s_\delta) d\sigma, \tag{3.4.1}$$

where $\diamondsuit$ is a vector of second order differential operators defined for a trivariate function $h$ by

$$\diamondsuit h = \begin{bmatrix} D_{xx}^2 h \\ D_{yy}^2 h \\ D_{zz}^2 h \\ \sqrt{2} D_{xy}^2 h \\ \sqrt{2} D_{xz}^2 h \\ \sqrt{2} D_{yz}^2 h \end{bmatrix}, \tag{3.4.2}$$

or a vector of third order differential operators defined for a trivariate function $h$ by

$$\diamondsuit h = \begin{bmatrix} D^3_{xxx}h \\ D^3_{yyy}h \\ D^3_{zzz}h \\ \sqrt{3}D^3_{xxy}h \\ \sqrt{3}D^3_{xxz}h \\ \sqrt{3}D^3_{xyy}h \\ \sqrt{3}D^3_{xzz}h \\ \sqrt{3}D^3_{yyz}h \\ \sqrt{3}D^3_{yzz}h \\ \sqrt{6}D^3_{xyz}h \end{bmatrix}. \tag{3.4.3}$$

In (3.4.1) $s_\delta$ is the unique homogeneous extension of $s$ of degree $\delta$ to $\mathbb{R}^3 \setminus \{0\}$ defined by $s_\delta = |v|^\delta s(\frac{v}{|v|})$. As we discussed in Chapter 3 we use $\delta = 0$ or $\delta = 1$. After evaluation $\diamondsuit s_\delta$ is restricted to the unit sphere and then integrated. In case of second order energy functional we use (3.4.2) and in third order energy functional we use (3.4.3). By Theorem 3.2.1, there exists a unique minimal energy functional Hermite interpolation solution. Now we explain how to compute minimal energy interpolating spherical splines. We use a coefficient vector $\mathbf{c}$ to represent each spline function in $S_d^{-1}(\Delta)$

$$s|_\tau = \sum_{i+j+k=d} c^\tau_{ijk} B^{d,\tau}_{ijk}, \tau \in \Delta$$

$$\mathbf{c} := (c^\tau_{ijk}), i+j+k = d, \tau \in \Delta.$$

When $s \in S_d^r(\Delta)$,to ensure the $C^r$ continuity across each interior edge of $\Delta$, we impose smoothness conditions, i.e., the conditions in Theorem 2.2.25 for every edge of $\Delta$. Let $\mathbf{H}$ denote the smoothness matrix such that

$$\mathbf{Hc} = \mathbf{0}$$

if and only if $s \in S_d^r(\Delta)$.

To simplify the data management we linearize the triple indices of BB-coefficients $c_{ijk}$ and correspondingly the indices of BB-basis functions $B^d_{ijk}$. From the properties of SBB-polynomials, we have

$$c_{d00} = f(v_1), c_{0d0} = f(v_2), c_{00d} = f(v_3)$$

and

$$\begin{aligned}
\frac{\partial P}{\partial \theta}|_{v_1} &= d\left[\frac{\partial b_1}{\partial \theta}c_{d,0,0} + \frac{\partial b_2}{\partial \theta}c_{d-1,1,0} + \frac{\partial b_3}{\partial \theta}c_{d-1,0,1}\right] = \frac{\partial f}{\partial \theta}|_{v_1}, \\
\frac{\partial P}{\partial \phi}|_{v_1} &= d\left[\frac{\partial b_1}{\partial \phi}c_{d,0,0} + \frac{\partial b_2}{\partial \phi}c_{d-1,1,0} + \frac{\partial b_3}{\partial \phi}c_{d-1,0,1}\right] = \frac{\partial f}{\partial \phi}|_{v_1}, \\
\frac{\partial P}{\partial \theta}|_{v_2} &= d\left[\frac{\partial b_1}{\partial \theta}c_{1,d-1,0} + \frac{\partial b_2}{\partial \theta}c_{0,d,0} + \frac{\partial b_3}{\partial \theta}c_{0,d-1,1}\right] = \frac{\partial f}{\partial \theta}|_{v_2}, \\
\frac{\partial P}{\partial \phi}|_{v_2} &= d\left[\frac{\partial b_1}{\partial \phi}c_{1,d-1,0} + \frac{\partial b_2}{\partial \phi}c_{0,d,0} + \frac{\partial b_3}{\partial \phi}c_{0,d-1,1}\right] = \frac{\partial f}{\partial \phi}|_{v_2}, \\
\frac{\partial P}{\partial \theta}|_{v_3} &= d\left[\frac{\partial b_1}{\partial \theta}c_{1,0,d-1} + \frac{\partial b_2}{\partial \theta}c_{0,1,d-1} + \frac{\partial b_3}{\partial \theta}c_{0,0,d}\right] = \frac{\partial f}{\partial \theta}|_{v_3}, \\
\frac{\partial P}{\partial \phi}|_{v_3} &= d\left[\frac{\partial b_1}{\partial \phi}c_{1,0,d-1} + \frac{\partial b_2}{\partial \phi}c_{0,1,d-1} + \frac{\partial b_3}{\partial \phi}c_{0,0,d}\right] = \frac{\partial f}{\partial \phi}|_{v_3},
\end{aligned}$$

on each triangle $\tau \in \Delta$. We can calculate the derivatives up to $l$-th order, then assemble interpolation conditions into a matrix $\mathbf{I}$, according to the order in which the coefficient vector $\mathbf{c}$ is organized. Then $\mathbf{Ic} = \mathbf{F}$ is the linear system of equations such that a coefficient vector $\mathbf{c}$ solving it corresponds to a spline $s$ interpolating $f$ and its $l$-th order derivatives $f^{\alpha,\beta},\ \alpha + \beta = l$ at the data sites $\mathcal{V}$.

Next fix $\delta = d \bmod(2)$. The problem of minimizing (3.4.1) over $S^r_d(\Delta)$ can be formulated as follows:

$$\text{minimize } \mathbf{c}^T\mathbf{Ec}, \text{ subject to } \mathbf{Hc} = \mathbf{0} \text{ and } \mathbf{Ic} = \mathbf{F}.$$

Here the energy matrix $\mathbf{E}$ is defined as follows. $\mathbf{E} = \text{diag}(\mathbf{E}^\tau, \tau \in \mathbf{\Delta})$ is a diagonally block matrix. Each block $\mathbf{E}^\tau$ is associated with a triangle $\tau$ and contains the following entries

$$\mathbf{E}^\tau_{ij} := \int_\tau \diamondsuit(B_i)^T_\delta \diamondsuit(B_j)_\delta d\sigma, \tag{3.4.4}$$

where $B_i$ denotes a BB-polynomial basis function (2.2.12) of degree $d$ corresponding to the order of the linearized triple indices $(i, j, k), i + j + k = d$.

By the method of Lagrange multiplier method, let

$$L(\mathbf{c}, \eta, \gamma) := \frac{\mathbf{1}}{\mathbf{2}}\mathbf{c^T E c} + \eta^\mathbf{T}\mathbf{I c} + \gamma^\mathbf{T}\mathbf{H c}.$$

be a Lagrangian function. We need to find a local minimizer of $L(\mathbf{c}, \eta, \gamma)$. That is

$$\frac{\partial}{\partial \mathbf{c}} L(\mathbf{c}, \eta, \gamma) = \mathbf{0}, \ \frac{\partial}{\partial \eta}\mathbf{L}(\mathbf{c}, \eta, \gamma) = \mathbf{0}, \ \frac{\partial}{\partial \gamma}\mathbf{L}(\mathbf{c}, \eta, \gamma) = \mathbf{0}.$$

Hence, we have

$$\frac{1}{2}(\mathbf{E} + \mathbf{E^T})\mathbf{c} + \mathbf{I}^\mathbf{T}\eta + \mathbf{H}^\mathbf{T}\gamma = \mathbf{0}, \quad \mathbf{Ic} = \mathbf{0}, \quad \mathbf{Hc} = \mathbf{0}.$$

By the symmetry of matrix $\mathbf{E}$, we need to solve the linear system

$$\begin{bmatrix} \mathbf{E} & \mathbf{I^T} & \mathbf{H^T} \\ \mathbf{I} & 0 & 0 \\ \mathbf{H} & 0 & 0 \end{bmatrix} \begin{bmatrix} \mathbf{c} \\ \eta \\ \gamma \end{bmatrix} = \begin{bmatrix} 0 \\ \mathbf{F} \\ 0 \end{bmatrix}.$$

Here $\gamma$ and $\eta$ are vectors of Lagrange multiplier coefficients. Note that $\mathbf{E}$ is a singular matrix. Although we can use a least squares solution to the singular linear system above, we use the following iterative method introduced in [8] which is much more efficient to obtain the coefficient vector of spherical spline Hermite interpolation. For simplicity, let us consider the following singular linear system:

$$\begin{bmatrix} A & L^T \\ L & 0 \end{bmatrix} \begin{bmatrix} \mathbf{c} \\ \lambda \end{bmatrix} = \begin{bmatrix} \bar{F} \\ \bar{G} \end{bmatrix}.$$

It can be solved by using the following iterative method [8]

$$\begin{bmatrix} A & L^T \\ L & -\epsilon I \end{bmatrix} \begin{bmatrix} \mathbf{c}^{(\ell+1)} \\ \lambda^{(\ell+1)} \end{bmatrix} = \begin{bmatrix} \bar{F} \\ \bar{G} - \epsilon\lambda^{(\ell)} \end{bmatrix},$$

for $\ell = 0, 1, \ldots$, where $\epsilon > 0$ is a fixed number, e.g. $\epsilon = 10^{-4}$, $\lambda^{(\ell)}$ is iterative solution of a Lagrange multiplier coefficient vector with $\lambda^0 = 0$ and $I$ is the identity matrix. The above matrix iterative steps can in fact be rewritten as follows:

$$(A + \frac{1}{\epsilon} L^T L)\mathbf{c}^{(\ell+1)} = A\bar{F}\mathbf{c}^{(\ell)} + \frac{1}{\epsilon} L^T \bar{G}$$

with $\mathbf{c}^{(0)} = 0$. Note that the size of the above linear system is much smaller than of the original one. The iterations converge very quickly as shown in the following theorem. In our numerical experiments, a few iterations (less than 10) often suffice. A general convergence theorem is proved in [8]. To state the convergence result, we need the following definition.

DEFINITION 3.4.1. *(cf. [8])Let $A$ be a square matrix of size $n \times n$ and $L$ be a rectangular matrix of size $m \times n$. We say a matrix $A$ is positive definite with respect to $L$ if $\mathbf{c}^T A\mathbf{c} \geq 0$, and $A\mathbf{c} = 0$, $L\mathbf{c} = 0$ imply that $\mathbf{c} = 0$.*

THEOREM 3.4.1. *(cf. [8]) Suppose that $A$ is symmetric and positive definite with respect to $L$. Then the matrix $A + \frac{1}{\epsilon} L^T L$ is always invertible for any $\epsilon > 0$. Furthermore, there exists a constant $C$ such that*

$$\|\mathbf{c}^{(\ell+1)} - \mathbf{c}\| \leq C\epsilon \|\mathbf{c}^{(\ell)} - \mathbf{c}\|, \qquad \textit{for all } \ell \geq 0.$$

It is easy to see that $\mathbf{E}$ is symmetric and nonnegative definite with respect to $\mathbf{L} = (\mathbf{I}; \mathbf{H})$. Thus, the iterative method converges to the vector $c$, which is the coefficient vector of the unique interpolating spline minimizing (3.4.1). This furnishes a computational algorithm like the following.

**Algorithm of spherical Hermite minimal energy interpolation:**

step1. Find the center of data sets, and project them to the unit sphere $\mathbb{S}^2$.

step2. Triangulate the points on the unit sphere corresponding to the projection of data sets to get a triangulation $\Delta$.

step3. Calculate the function values and derivatives up to the $l$-th order($l \geq 0$ defined by (3.2.7)) on each vertex of triangulation $\Delta$, and assemble these conditions into matrix form $\mathbf{Ic} = \mathbf{F}$, here $\mathbf{c}$ denotes the coefficient vector.

step4. Assemble smoothness conditions into matrix form $\mathbf{Hc} = \mathbf{0}$.

step5. Compute all derivatives up to third order. Calculate the energy functional on the triangulation $\Delta$ and write it in form $\mathbf{c}^T\mathbf{Ec}$, where $\mathbf{E}$ (could be the second or third order energy functional) is a diagonal block matrix and each block element is the energy functional on each triangle $T \in \Delta$.

step6. Apply Lagrangian multiplier method to get the linear system

$$\begin{bmatrix} \mathbf{E} & \mathbf{I^T} & \mathbf{H^T} \\ \mathbf{I} & 0 & 0 \\ \mathbf{H} & 0 & 0 \end{bmatrix} \begin{bmatrix} \mathbf{c} \\ \eta \\ \gamma \end{bmatrix} = \begin{bmatrix} 0 \\ \mathbf{F} \\ 0 \end{bmatrix}.$$

step7. Solve the linear system in step 6 to get $\mathbf{c}$.

step8. Computing maximal and relative error.

We shall show our numerical results in chapter 5 to demonstrate effectiveness of our method.

# Chapter 4

## Surface Design Based on Spherical Splines

Holes filling and scattered data smooth fitting are important and difficult research fields in CAGD(Computer Aided Geometric Design), especially for high order continuity. They have been widely studied in planar domains for at least over twenty years. In this chapter, we study above problems in a spherical domain which is much different from a planar one and present them in two parts. In first part, we study the method to fill holes with $C^r(r \geq 0)$ continuity using spherical splines if the surrounding surface and mending surface have the same degree of $SBB$-polynomials. Otherwise we approximate the boundary information of holes. In some cases, we also need the mending surface to satisfy certain interpolation conditions, and we call this problem as hole filling and data fitting. This problem has not been studied in the literature before. In second part, we deal with point cloud using spherical splines to get a smooth and visually fair surface to interpolate the given data locations and their derivatives. Our surface is $C^r$ $(r \geq 0)$ globally continuous. We give examples of $C^0$, $C^1$ and $C^2$ continuity to demonstrate our methods.

### 4.1 Spherical Spline Method for Hole Filling

#### 4.1.1 Overview

In complex surface modeling and surface design, we often encounter a curved polygonal hole($N-$ sided hole) when assembling several surface patches together. Usually these given surface patches are spline surface patches. We have to find a mending surface patch to fill the hole such that the modified surface is $C^i$ or $G^i(i = 0,\ i = 1 \text{ or } 2)$ globally continuous. In some applications, the mending surface patch to fill the hole may be required to satisfy

certain interpolation conditions. In a planar domain, several researchers have already tested some ideas, e.g. rectangular patches, triangular patches, multisided patches, subdivision algorithm and etc. See, e.g., [Hahn'89], [Gregory'89], [Jones'88], [Zheng and Ball'97], [Chui and Lai'2000].

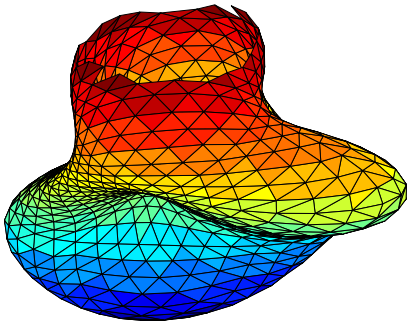

Figure 4.1: Data with one hole .

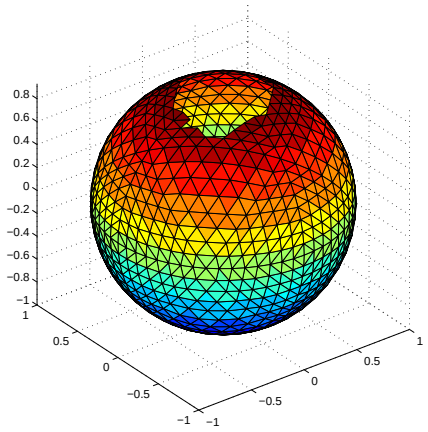


Figure 4.2: Projection of data with one hole onto the unit sphere.

We study the sphere case for the first time. One typical situation is that a given smooth surface is defined over the entire unit sphere except for a polygonal cap, see Fig. 4.1 and Fig. 4.2. Such a surface is said to have a hole. To fill the surface over the cap, we need to get a regular triangulation of holes which share common edges with the triangulation of surrounding surface over the boundary curves of holes. To get global $C^r$ $(r \geq 0)$ surface, we first use $C^r$ $(r \geq 0)$ smoothness conditions across interior edges of triangles in a triangulation

of holes to guarantee interior parts of holes $C^r$ $(r \geq 0)$ smoothness. Second, we deal with $C^r$ $(r \geq 0)$ related boundaries. We compute the values over a discrete set of points along the curve of the hole over the boundary of the cap and derivatives up to $r$-th order at vertices of boundary edges, also we use the smoothness conditions across boundary edges to determine the undetermined points from 1-th to $r$-th layers from boundary edges. After above processes, we have constructed a spherical spline surface with global $C^r$ $(r \geq 0)$continuity. And the original and resulting spherical spline surface form a visually smooth surface over the entire unit sphere if the discrete set of points are dense enough. See [16] for $C^1$ hole-filling using bivariate spline functions over planar domains. We shall present our numerical method for $C^r(r \geq 0)$ hole filling in next subsection.

In this chapter, we propose to use $C^r$ $(r \geq 0)$ spherical spline patches to handle the filling problem. Our filling spherical surface only matches the boundary values exactly for surrounding spherical spline patches which form a curved polygonal hole with the same degree of $SBB$-polynomials of filling holes, and it is a common assumption for exactly hole filling that a mending surface is the same type as its surrounding surface(cf. [34]). Otherwise, we need to approximate the boundary curve and derivative on the boundaries of holes.

### 4.1.2 Spherical Spline Method for Filling Curved Polygonal Holes

Now let us describe our new method for filling curved polygon hole on the sphere. For simplicity, we assume that there exists a domain $\Omega$ on the unit sphere $\mathbb{S}^2$ such that the projection of hole H onto $\mathbb{S}^2$ is $\Omega$. That is, the intersection of the spherical surface $\mathbb{S}^2$ and the line passing through the center of the sphere $\mathbb{S}^2$ and a point of the curve of the hole forms a boundary curve of a domain $\Omega$. Suppose that $\partial\Omega$ can be divided into a finite non-overlapping arc segments in great circle $p_1, \cdots, p_n$ such that $\partial\Omega = \bigcup_{i=1}^{n} p_i$ with $p_i \cap p_{i+1} = v_{i+1}$, $i = 1, \cdots, n-1$, and $p_n \cap p_1 = v_1$. That is, $\Omega$ is a circulated curved polygonal cap of $\mathbb{S}^2$.

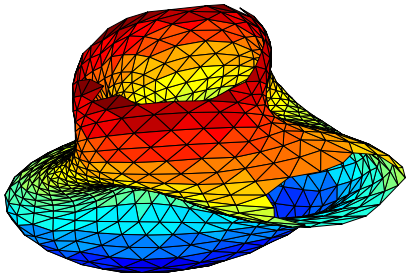

Figure 4.3: Data with two holes.

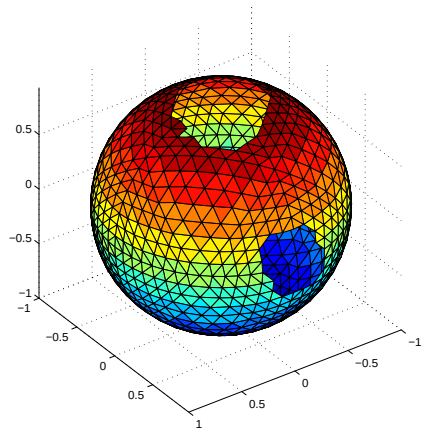


Figure 4.4: Projection of the data with two holes onto the unit sphere.

In a general situation, there maybe many disjoint holes, see Fig. 4.3 and Fig. 4.4 for two holes' case. But we deal with these holes with same procedure. So we only describe how to fill one hole.

We first partition the curved polygonal cap $\Omega$ into a collection $\Delta$ of spherical triangles. Let $V_b = \{v_1, \cdots, v_n\}$ be the collection of boundary vertices of sphere triangulation $\Delta$, $p_i = (\overline{v_i, v_{i+1}})$ be the boundary edges from starting point $v_i$ to ending point $v_{i+1}$, $i = 1, \cdots, n$ (note $v_{n+1} = v_1$) and calculate the $r-$th($r$=0,1,or 2) derivatives of surrounding surface at these vertices $v_i$, $i = 1, \ldots, n$. We evenly divide the chord connecting $v_i$ and $v_{i+1}$ by inserting $d-1$ ($d$ is the degree of SBB-polynomial) points and then project them to circulated edge $e_i$, denote these points on the $e_i$ by $i_b^j$ for $i = 1, \cdots, n$, $j = 1, \cdots, d-1$. Let $U_b = \bigcup i_b^j$,

and $V_{\partial\Omega} = V_b \bigcup U_b$. We evaluate the curve $\mathcal{C}$ of hole as well as derivatives of the points in $V_b$. For $r \geq 0$, to make mending patch smoothly connect the surrounding surface $h$ with $C^r$ continuity, we construct a spherical spline surface $S_f$ on $\Delta$ to interpolate the values on points in $V_{\partial\Omega}$ and derivatives up to $r$-th order at points of $V_b$, also we need $C^r$ conditions across the boundaries of surrounding surface. The $C^r$ related boundaries need delicate care.

For $C^0$ smoothness to connect the originally given surface $h$, we only need to interpolate the boundary values at the $nd$ distinct points on the boundary $\partial\Omega$.

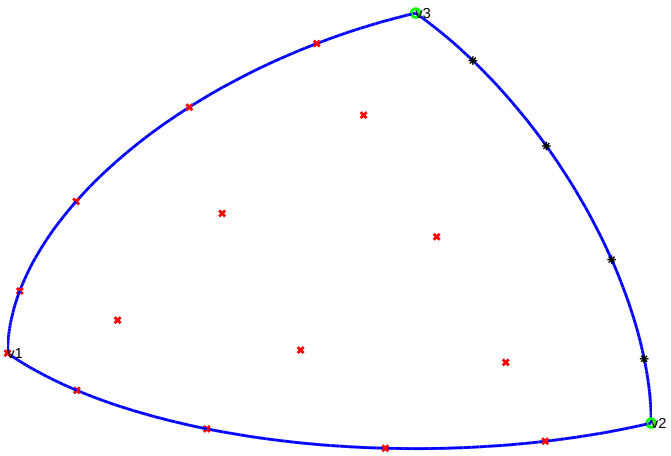


$*$ : inserted points

$\circ$ : interpolated vertices

$+$ : points determined by smoothness conditions across interior edges or minimal energy.

Figure 4.5: Domain points of $S_5^0$ for one triangle of mending surface with boundary edge $\widehat{v_2v_3}$ and vertex $v_1$ inside hole.

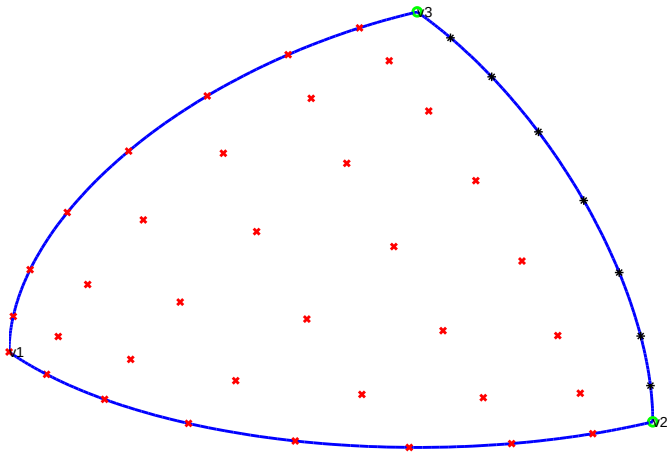


$*$ : inserted points

$\circ$ : interpolated vertices

$+$ : points determined by smoothness conditions across interior edges or minimal energy.

Figure 4.6: Domain points of $S_8^0$ for one triangle of mending surface with boundary edge $\widehat{v_2v_3}$ and vertex $v_1$ inside hole.

These points consist of $n$ distinct vertices $v_i, i = 1, \cdots, n$ and $(n-1)d$ distinct inserting points $i_b^j$ for $i = 1, \cdots, n,\ j = 1, \cdots, d-1$ on $n$ sides of the boundary $\partial\Omega$, see Fig. 4.5 and Fig. 4.6. Denote the values of $\mathcal{C}$ over the points in $V_{\partial\Omega}$ by a vector $\mathbf{f}_{bc0}$. Let $\mathbf{c}$ be the vector of spline coefficients in $SBB-$form as in Chapter3. By our construction, we have

$$i_b^j = \frac{v_i + \dfrac{j(v_{i+1} - v_i)}{d}}{\|v_i + \dfrac{j(v_{i+1} - v_i)}{d}\|},\ i = 1, \cdots, n,\ j = 1, \cdots, d-1.$$

We first compute the barycentric coordinates of $i_b^j$ for $i = 1, \cdots, n,\ j = 1, \cdots, d-1$ in the corresponding triangles of mending surface. Then we can write interpolation conditions on these points and vertices in matrix form:

$$\mathbf{I}_{bc0}\mathbf{c} = \mathbf{f}_{bc0}. \tag{4.1.1}$$

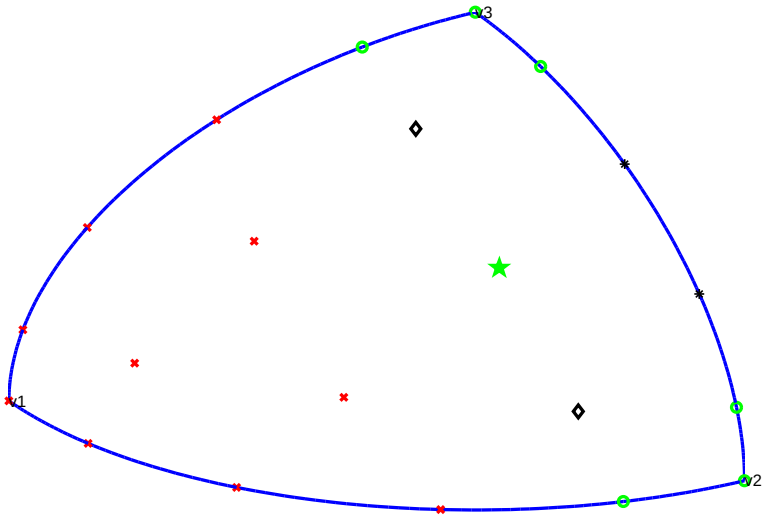


$*$ : inserted points

$\circ$ :points determined by quasi-Hermite interpolation

$+$ : points determined by smoothness conditions across interior boundary or minimal energy

$\diamond$ : points determined by $C^1$ smoothness conditions across boundary $\widehat{v_2v_3}$ and interior edges

$\bigstar$ : point determined by $C^1$ smoothness condition across boundary $\widehat{v_2v_3}$

Figure 4.7: Domain points of $S_5^1$ for one triangle of mending surface with boundary edge $\widehat{v_2v_3}$ and vertex $v_1$ inside hole.

For $C^1$ continuity, we need quasi-Hermite interpolation at vertices of boundary $\partial\Omega$, $C^0$ interpolation on the points $i_b^j$, $i = 1, \cdots, n,\ j = 2, \cdots, d-2$, and $C^1$ smoothness conditions on points denoted by $\diamond$ and $\bigstar$ in Fig. 4.7. We can express above $C^1-$ related boundary conditions in terms of coefficient vector $\mathbf{c}$ and assemble them into matrix form:

$$\mathbf{I}_{bc1}\mathbf{c} = \mathbf{f}_{bc1}. \tag{4.1.2}$$

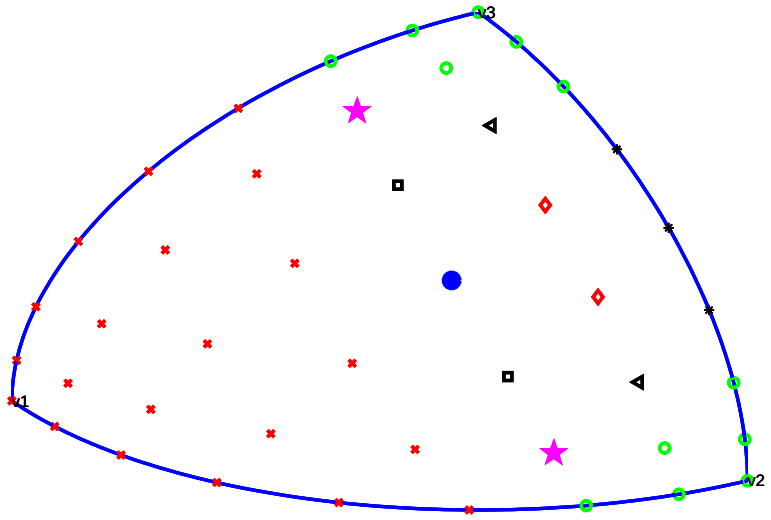


$*$ : inserted points

$\circ$ : points determined by quasi-Hermite interpolation

$+$ : points determined by smoothness conditions across interior boundary or minimal energy

$\diamond$ : points determined by $C^1$ smoothness conditions across boundary $\widehat{v_2v_3}$

$\bigstar$ : points determined by $C^2$ smoothness conditions across the boundary $\widehat{v_2v_3}$ and $C^1$ smoothness conditions across interior edges

$\triangle$ : points determined by $C^1$ smoothness conditions across the boundary $\widehat{v_2v_3}$ and $C^2$ smoothness conditions across interior edges

$\square$ : points determined by $C^2$ smoothness conditions across boundary edge $\widehat{v_2v_3}$ and interior edges

$\bullet$ : point determined by $C^2$ smoothness conditions across boundary edge $\widehat{v_2v_3}$

Figure 4.8: Domain points of $S_8^2$ for one triangle of mending surface with boundary edge $\widehat{v_2v_3}$ and vertex $v_1$ inside hole.

Similarly, for $C^2$ connection, we need quasi-Hermite interpolation at vertices of boundary $\partial\Omega$, $C^0$ interpolation on the points $i_b^j$, $i = 1, \cdots, n$, $j = 3, \cdots, d-3$, $C^1$ smoothness conditions on points shown in Fig. 4.7, and $C^2$ smoothness conditions on points demonstrated in Fig. 4.8. We also can express above $C^2-$ related boundary conditions in terms of coefficient

vector $\mathbf{c}$ and assemble them into matrix form:

$$\mathbf{I}_{bc2}\mathbf{c} = \mathbf{f}_{bc2}. \tag{4.1.3}$$

By the same process, we can express $C^r-$ related boundary ($r \geq 3$) connection conditions in terms of coefficient vector $\mathbf{c}$ and assemble them into matrix form:

$$\mathbf{I}_{bcr}\mathbf{c} = \mathbf{f}_{bcr}. \tag{4.1.4}$$

For simplicity, we denote all above $C^r(r \geq 0)$ boundary related conditions by $\mathbf{I}_{bc}\mathbf{c} = \mathbf{f}_{bc}$.

In some applications, we are also given some data inside the hole in addition to the given boundary of surface patches. Let us write the scattered data $\{(x_i, y_i, z_i), i = 1, \cdots, P\}$ over the $\Omega$ in matrix form: $\mathbf{I}_v\mathbf{c} = \mathbf{f}_v$. For convenience, we combine the interpolation conditions $\mathbf{I}_{bc}\mathbf{c} = \mathbf{f}_{bc}$ and $\mathbf{I}_v\mathbf{c} = \mathbf{f}_v$ together and denote them by $\mathbf{Ic} = \mathbf{f}$.

Let $U_f = \{s \in S_d^r(\Delta), \mathbf{Ic} = \mathbf{f}\}$ be the collection of all spherical splines in $S_d^r(\Delta)$ which interpolates the given data and satisfies $C^r-$ related boundary conditions. Now our method to fill the hole is to find $S_f \in S_d^r(\Delta)$ ($d \geq 3r + 2$ for $r \geq 0$) such that $S_f \in U_f$ and

$$E(S_f) = \min\{E(s), s \in U_f\}. \tag{4.1.5}$$

That is, we need to solve the following minimization problem:

$$\text{minimize } \mathbf{c}^T\mathbf{E}\mathbf{c}, \text{ subject to } \mathbf{Hc} = \mathbf{0} \text{ and } \mathbf{I}_{bc}\mathbf{c} = \mathbf{f}_{bc}, \mathbf{I}_v\mathbf{c} = \mathbf{f}_v, \tag{4.1.6}$$

where $\mathbf{E}$ is the energy functional matrix explained in Chapter 3, $\mathbf{I}_{bc}\mathbf{c} = \mathbf{f}_{bc}$ for $C^r-$ related boundary conditions explained above, and $\mathbf{H}$ for the smoothness conditions across the interior edges of triangles of mending surface. Since $U_f$ is not empty, it is easily understood there exists a minimal energy solution for our hole filling problems, see Section 3.2.

Energy functional $\mathbf{E}$ helps us to determine all the remaining coefficients in SBB polynomial representation and reduces the bumpiness of the surface. In [16], (4.1.6) was called the minimal energy filling and fitting problem. we shall solve spherical case using Lagrange multiplier method described in Chapter3.

By the method of Lagrange multiplier, let

$$L(\mathbf{c},\eta,\gamma) := \frac{\mathbf{1}}{\mathbf{2}}\mathbf{c^T E c} + \eta^{\mathbf{T}}\mathbf{I c} + \gamma^{\mathbf{T}}\mathbf{H c}.$$

be a Lagrangian function. We need to find a local minimizer of $L(\mathbf{c},\eta,\gamma)$. That is

$$\frac{\partial}{\partial \mathbf{c}}L(\mathbf{c},\eta,\gamma) = \mathbf{0},\ \frac{\partial}{\partial \eta}\mathbf{L}(\mathbf{c},\eta,\gamma) = \mathbf{0},\ \frac{\partial}{\partial \gamma}\mathbf{L}(\mathbf{c},\eta,\gamma) = \mathbf{0}.$$

Hence, we have

$$\frac{1}{2}(\mathbf{E}+\mathbf{E^T})\mathbf{c} + \mathbf{I^T}\eta + \mathbf{H^T}\gamma = \mathbf{0},\quad \mathbf{Ic} = \mathbf{0},\quad \mathbf{Hc} = \mathbf{0}.$$

By the symmetry of matrix $\mathbf{E}$, we need to solve the linear system

$$\begin{bmatrix} \mathbf{E} & \mathbf{I^T} & \mathbf{H^T} \\ \mathbf{I} & 0 & 0 \\ \mathbf{H} & 0 & 0 \end{bmatrix} \begin{bmatrix} \mathbf{c} \\ \eta \\ \gamma \end{bmatrix} = \begin{bmatrix} 0 \\ \mathbf{f} \\ 0 \end{bmatrix}.$$

Here $\gamma$ and $\eta$ are vectors of Lagrange multiplier coefficients. Note that the above coefficient matrix is a singular matrix. Although we can use a least squares solution to the singular linear system above, we use the iterative method introduced in [8] which is much more efficient to obtain the coefficient vector of spherical spline quasi-Hermite interpolation, also see the description in Chapter 3.

It is easy to see that $\mathbf{E}$ is symmetric and nonnegative definite with respect to $\mathbf{L} = (\mathbf{I};\mathbf{H})$. Thus, the iterative method converges to the vector $c$, which is a coefficient vector of the interpolating spline minimizing (4.1.5). This furnishes a computational algorithm of the hole filling like the following.

**Algorithm of spherical hole filling with $C^r(integer\ r \geq 0)$ continuity:**

step1. Determine the spherical triangulation of surrounding surface and mending surface which share common boundaries.

step2. Find a spherical spline to approximate the surrounding surface.

step3. Compute the $C^r-$ related boundary conditions $\mathbf{I}_{bc}\mathbf{c} = \mathbf{f_{bc}}$ as described in this section, here $\mathbf{c}$ denotes the coefficient vector, integer $r(\geq 0)$ denote the order of global continuity of the finalized surface.

step4. Calculate the interpolation conditions to satisfy the given data in the hole if there are any such data and assemble them into matrix form $\mathbf{I}_v\mathbf{c} = \mathbf{f_v}$. Otherwise we skip this step.

step5. Assemble $C^r$ smoothness conditions across the interior edges of mending surface into matrix form $\mathbf{Hc} = \mathbf{0}$.

step6. Calculate the energy functional on the triangulation $\Delta$ of mending surface and write it in form $\mathbf{c}^T\mathbf{Ec}$, where $\mathbf{E}$ is a diagonal block matrix and each block element is the energy functional on each triangle $T \in \Delta$.

step7. Apply iterative method described in Chapter 3 to solve the following linear system attained by Lagrangian multiplier method:

$$\begin{bmatrix} \mathbf{E} & \mathbf{I^T} & \mathbf{H^T} \\ \mathbf{I} & 0 & 0 \\ \mathbf{H} & 0 & 0 \end{bmatrix} \begin{bmatrix} \mathbf{c} \\ \eta \\ \gamma \end{bmatrix} = \begin{bmatrix} 0 \\ \mathbf{f} \\ 0 \end{bmatrix},$$

where $\mathbf{I}$ and $\mathbf{f}$ come from the combination $\mathbf{Ic} = \mathbf{f}$ of $\mathbf{I}_{bc}\mathbf{c} = \mathbf{f_{bc}}$ and $\mathbf{I}_v\mathbf{c} = \mathbf{f_v}$.

step8. Solve the linear system in step 6 to get $\mathbf{c}$.

step9. Visualize the surrounding surface and mending surface.

Numerical examples in Chapter 5 demonstrate that spherical splines are excellent for hole filling.

## 4.2 Spherical Splines for Point Cloud

In this section, we construct a spherical spline $C^r(r \geq 0)$ surface to interpolate the given data locations and their derivatives (if they are given like Satellite data, cf. [25]) by using

the minimal energy Hermite interpolation($l \geq 0$) method or minimal energy quasi-Hermite interpolation method.

Let $\mathcal{P}$ be a set of point cloud in 3D Euclidean space $\mathbf{R}^3$. Suppose that there is a 3D triangulation associated with the point cloud. That is, there exists a piecewise linear interpolation $\mathcal{I}$ which interpolates all the points in the point cloud. In order to use spherical splines for construct a smooth interpolation of the point cloud, we introduce a concept that the point cloud is **centralizable**.

DEFINITION 4.2.1. *We call the point cloud is* **centralizable** *if there exists a center* $O \in \mathbf{R}^3$ *such that for any point* $p \in \mathcal{I}$*, the ray from* $O$ *to* $p$ *does not intercept any other point in the piecewise linear interpolant* $\mathcal{I}$*.*

For example, in the following two figures, we are given a set of point cloud in the right hand side of the figure, and a triangulation associated with the point cloud is shown in the right of the figure. We show them from different viewing points.

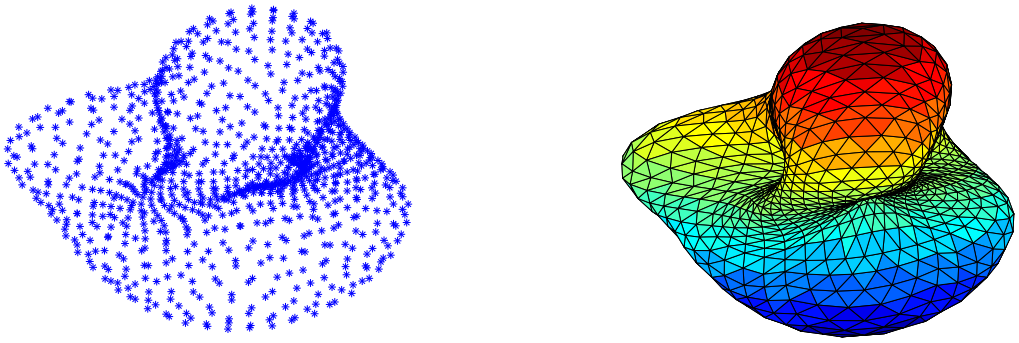

Figure 4.9: Original point cloud and a triangulation of the centralizable point cloud.

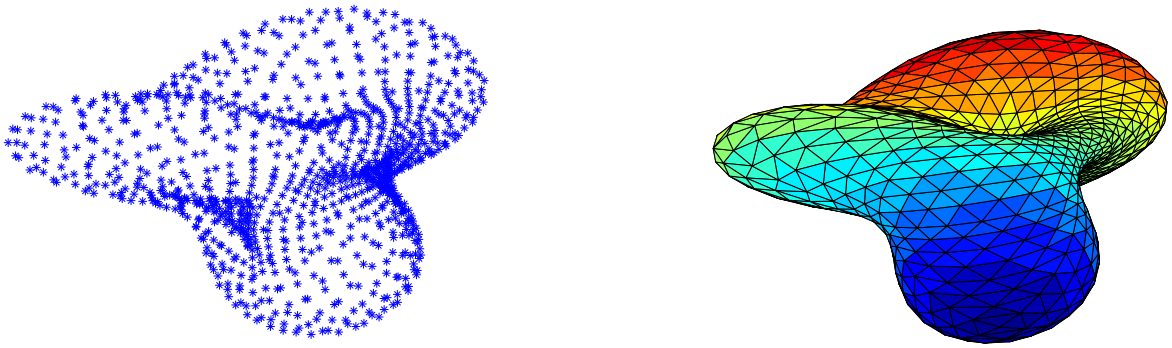

Figure 4.10: Original point cloud and a triangulation of the centralizable point cloud from a different point of view.

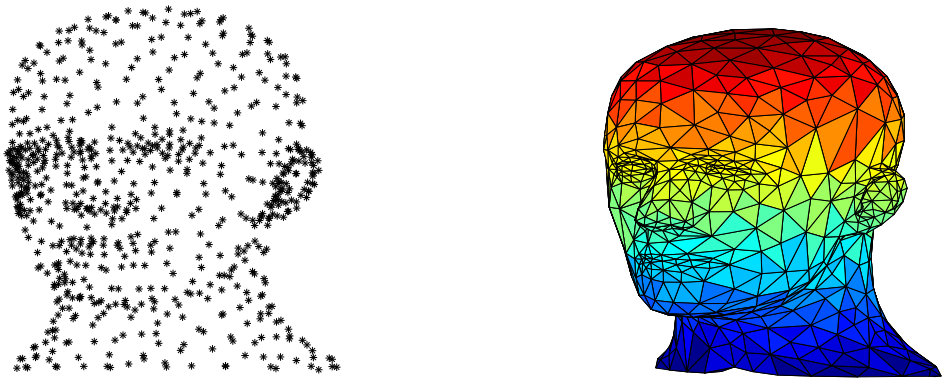

Figure 4.11: Original point cloud and a triangulation of the non-centralizable point cloud.

We shall focus on the centralizable point cloud. For a non-centralizable point cloud, we need cut off some data to make the modified data centralizable.

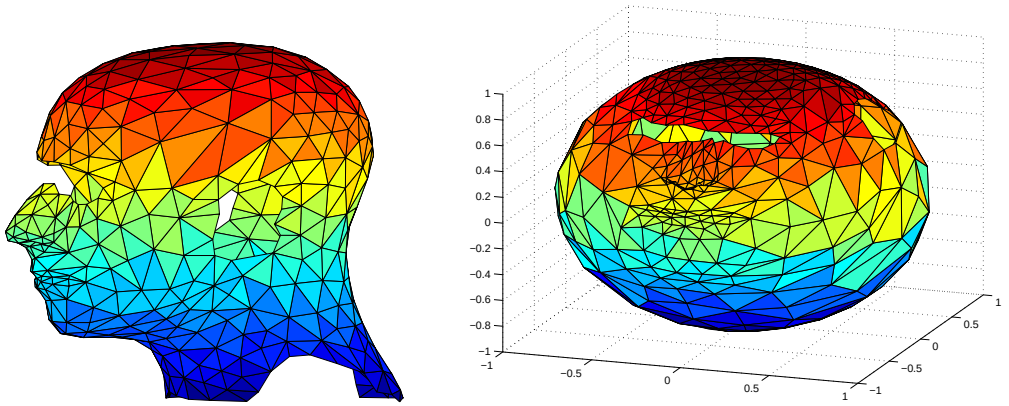

Figure 4.12: Modified head data(left) and a spherical triangulation $\Delta$(right).

For example, the point cloud in Fig. 4.11 is not centralizable near the areas of ears, eyes, and shoulders. After cutting off these areas, we have a modified point cloud as shown in the left of Fig. 4.12. A triangulation of the modified head data is shown in the right of Fig. 4.12.

When the point cloud $\mathcal{P}$ is centralizable, each point $p$ in the $\mathcal{P}$ can be projected onto the unit sphere $\mathbb{S}^2$ with center $O$ by the ray from $O$ passing through the point $p$. This induces point $v_i$ on the unit sphere and we can use the induced points $v_i$ to find a triangulation $\Delta$. Here $\Delta$ could be the whole sphere or a part of a sphere with or without holes. So we can use spherical splines over $\Delta$ to construct a smooth (continuously differentiable or $r-$th continuously differentiable) surface which interpolates the given points in $\mathcal{P}$ and their derivatives if they are given. Now let us give an algorithm for $C^r$(integer $r \geq 0$) point cloud to interpolate the given points and their derivatives if they are given by using the minimal energy Hermite interpolation method or the minimal energy quasi-Hermite interpolation method.

**Algorithm of spherical splines for $C^r(integer\ r \geq 0)$ centralizable point cloud**

step1. Find the center $O$ of the point cloud.

step2. Project the points in $\mathcal{P}$ to the unit sphere $\mathbb{S}^2$ with center $O$ and get a spherical triangulation $\Delta$ of these induced points.

step3. First we compute the interpolation conditions of locations. Express these conditions in terms of coefficient vector $\mathbf{c}$ described in Chapter 3 and assemble them into matrix form:

$$\mathbf{I}_v\mathbf{c} = \begin{bmatrix} f(v_1) \\ \vdots \\ f(v_N) \end{bmatrix},$$

where $f$ is the distance function of point $v \in \mathcal{P}$ from the center $O$, $i = 1, \cdots, N$, and $N$ is the number of points. Secondly we calculate the interpolated derivatives up to $l$-th($l \geq 1$) order at these points if it is necessary. Express these conditions in terms of coefficient vector $\mathbf{c}$ described in Chapter 3 and assemble them into matrix form:

$$\mathbf{I}_D\mathbf{c} = \mathbf{f_D}.$$

Finally, we combine above two conditions into matrix form $\mathbf{Ic} = \mathbf{f}$ for convenience of explanation.

step4. Assemble $C^r$ smoothness conditions across the interior edges of triangulation $\Delta$ into matrix form $\mathbf{Hc} = \mathbf{0}$.

step5. Calculate the energy functional on triangulation $\Delta$ and write it in form $\mathbf{c}^T\mathbf{Ec}$, where $\mathbf{E}$ is a diagonal block matrix and each block element is the energy functional on each triangle $T \in \Delta$.

step6. Apply iterative method described in Chapter 3 to solve the following linear system attained by Lagrangian multiplier method:

$$\begin{bmatrix} \mathbf{E} & \mathbf{I^T} & \mathbf{H^T} \\ \mathbf{I} & 0 & 0 \\ \mathbf{H} & 0 & 0 \end{bmatrix} \begin{bmatrix} \mathbf{c} \\ \eta \\ \gamma \end{bmatrix} = \begin{bmatrix} 0 \\ \mathbf{f} \\ 0 \end{bmatrix},$$

step7. Solve the linear system in step 6 to get $\mathbf{c}$.

step8. Visualize the $C^r$ spherical spline surface satisfying interpolatory conditions at points in $\mathcal{P}$ and their derivatives if they are given.

We shall show the numerical results in Chapter 5.

# Chapter 5

# Numerical Experiments

## 5.1 Numerical Experiments for Hermite Interpolation

Example 5.1.1. *We use spherical splines for Hermite data interpolation. For simplicity, we consider a standard triangulation* $\Delta_0$ *of the unit sphere consisting of eight congruent triangles with six vertices* $(1,0,0)$, $(0,1,0)$, $(0,0,1)$, $(-1,0,0)$, $(0,-1,0)$, *and* $(0,0,-1)$. *Then we refine uniformly* $\Delta_0$ *by dividing each triangle into four subtriangles using the midpoint of edges and denote resulting triangulation by* $\Delta_1$. *We continue the uniform refinement of* $\Delta_1$ *to get* $\Delta_2$ *and so on. We use the following test functions* $f_1(x,y,z) = 1 + 0.3x^8 + e^{0.2y^3} + z$, $f_2(x,y,z) = sin(9\theta)sin^9(\phi) + sin(\phi)$, $f_3(x,y,z) = 1 + 0.3x^8 + y^2 + z$ *and their derivatives. Then we find the spherical spline interpolation of the test functions.*

| $S_d^r(\Delta) \setminus f$ | $f_1$ | $f_2$ | $f_3$ |
|---|---|---|---|
| $S_5^1(\Delta_2)(H)$ | 0.0066 | 0.56347118414855 | 0.0054 |
| $S_5^1(\Delta_2)(L)$ | 0.0091 | 1.29355264798577 | 0.0078 |
| $S_5^1(\Delta_3)(H)$ | $5.4632e-004$ | 0.09049253039397 | $5.1111e-004$ |
| $S_5^1(\Delta_3)(L)$ | $6.4169e-004$ | 0.12874756706204 | $6.0932e-004$ |
| $S_5^1(\Delta_4)(H)$ | $3.3701e-005$ | 0.00792839967325 | $3.1337e-005$ |
| $S_5^1(\Delta_4)(L)$ | $4.1030e-005$ | 0.00982450777267 | $3.8608e-005$ |
| $S_5^1(\Delta_5)(H)$ | $2.0407e-006$ | $3.891376065110475e-004$ | $2.1941e-006$ |
| $S_5^1(\Delta_5)(L)$ | $2.4374e-006$ | $8.433571002092188e-004$ | $2.6213e-006$ |

Table 5.1: Maximal Errors of Hermite and Lagrange Interpolation with Second Order Energy Functional for $S_f \in S_5^1(\Delta)$.

| $S_d^r(\Delta) \setminus f$ | $f_1$ | $f_2$ | $f_3$ |
|---|---|---|---|
| $S_5^1(\Delta_2)(H)$ | 0.0026 | 0.29951914264812 | 0.0020 |
| $S_5^1(\Delta_2)(L)$ | 0.0110 | 2.07964802160888 | 0.0100 |
| $S_5^1(\Delta_3)(H)$ | $4.5779e-004$ | 0.06134015319020 | $4.1373e-004$ |
| $S_5^1(\Delta_3)(L)$ | 0.0017 | 0.11405534351457 | 0.0017 |
| $S_5^1(\Delta_4)(H)$ | $9.5467e-005$ | 0.00786475557904 | $8.4862e-005$ |
| $S_5^1(\Delta_4)(L)$ | $1.1594e-004$ | 0.01378199826989 | $1.8782e-004$ |
| $S_5^1(\Delta_5)(H)$ | $9.1351e-006$ | $4.236873067426927e-004$ | $8.5212e-006$ |
| $S_5^1(\Delta_5)(L)$ | $1.3884e-005$ | 0.00508637393995 | $2.0715e-005$ |

Table 5.2: Maximal Errors of Hermite and Lagrange Interpolation with Third Order Energy Functional for $S_f \in S_5^1(\Delta)$.

| $S_d^r(\Delta) \setminus f$ | $f_1$ | $f_2$ | $f_3$ |
|---|---|---|---|
| $S_5^1(\Delta_2)(H)$ | 0.0022 | 0.28173559207428 | 0.0024 |
| $S_5^1(\Delta_2)(L)$ | 0.0030 | 0.64677632399289 | 0.0035 |
| $S_5^1(\Delta_3)(H)$ | $1.8211e-004$ | 0.04524626519699 | $2.2747e-004$ |
| $S_5^1(\Delta_3)(L)$ | $2.1390e-004$ | 0.06437378353102 | $2.7118e-004$ |
| $S_5^1(\Delta_4)(H)$ | $1.1234e-005$ | 0.00396419983663 | $1.3933e-005$ |
| $S_5^1(\Delta_4)(L)$ | $1.3677e-005$ | 0.00491225388633 | $1.7166e-005$ |
| $S_5^1(\Delta_5)(H)$ | $6.8025e-007$ | $1.945688032555237e-004$ | $9.7525e-007$ |
| $S_5^1(\Delta_5)(L)$ | $8.1245e-007$ | $4.216785501046094e-004$ | $1.1651e-006$ |

Table 5.3: Relative Errors of Hermite and Lagrange Interpolation with Second Order Energy Functional for $S_f \in S_5^1(\Delta)$.

| $S_d^r(\Delta) \setminus f$ | $f_1$ | $f_2$ | $f_3$ |
|---|---|---|---|
| $S_5^1(\Delta_2)(H)$ | $8.6519e-004$ | 0.14975957132406 | $8.7162e-004$ |
| $S_5^1(\Delta_2)(L)$ | 0.0037 | 1.03982401080444 | 0.0045 |
| $S_5^1(\Delta_3)(H)$ | $1.5260e-004$ | 0.03067007659510 | $1.8413e-004$ |
| $S_5^1(\Delta_3)(L)$ | $5.7103e-004$ | 0.05702767175729 | $7.4299e-004$ |
| $S_5^1(\Delta_4)(H)$ | $3.1822e-005$ | 0.00393237778952 | $3.7730e-005$ |
| $S_5^1(\Delta_4)(L)$ | $3.8647e-005$ | 0.00689099913495 | $8.3505e-005$ |
| $S_5^1(\Delta_5)(H)$ | $3.0450e-006$ | $2.118436533713464e-004$ | $3.7875e-006$ |
| $S_5^1(\Delta_5)(L)$ | $4.6280e-006$ | 0.00254318696998 | $9.2075e-006$ |

Table 5.4: Relative Errors of Hermite and Lagrange Interpolation with Third Order Energy Functional for $S_f \in S_5^1(\Delta)$.

*We first consider the maximal errors. Table 5.1 and Table 5.2 are of the maximal errors between $S_f$ and $f$ for $f_1, f_2$, and $f_3$ with second order energy functional $E^2$ and third order energy functional $E^3$ respectively. The maximal errors are computed on almost equally-spaced points over the sphere. Table 5.1 and Table 5.2 demonstrate that the Hermite interpolation approximate the original function $f$ much better than Lagrange interpolation with the energy functionals both $E^2$ and $E^3$.*

*Second, we compare the relative error $\frac{\|s(w)-f(w)\|_\infty}{\|f(w)\|_\infty}$ in Table 5.3 with Energy functional $E^2$ and Table 5.5 with Energy functional $E^3$. These two tables also show the relative errors of the Hermite interpolation approximate the original function $f$ much better than Lagrange interpolation with the energy functionals both $E^2$ and $E^3$. Hence we can conclude that the Hermite interpolatory spline surface approximates original function values much better than Lagrange interpolatory spline surface under different energy functionals $E^2$ and $E^3$ in the same spherical spline spaces.*

EXAMPLE 5.1.2. *In this example, we consider the spherical splines for Hermite data interpolation under different energy functionals $E^2$ and $E^3$. We first construct the same spherical triangulation as Example 5.1.1. But we use the following test functions $f_1(x,y,z) = \frac{1}{1+x^2+y^4+z^6}$, $f_2(x,y,z) = 0.3x^8 + e^{0.2y^3} + z^3$, $f_3(x,y,z) = sin(9\theta)sin^9(\phi)$ and their derivatives. Then we find the spherical spline interpolation of the test functions.*

| $S_d^r(\Delta) \setminus f$ | $f_1$ | $f_2$ | $f_3$ |
|---|---|---|---|
| $S_6^1(\Delta_0)(E^3)$ | 0.22987953695775 | 0.28835856415728 | 3.17386786740602 |
| $S_6^1(\Delta_0)(E^2)$ | 0.25077741939099 | 0.29385403166936 | 2.97185896416610 |
| $S_6^1(\Delta_1)(E^3)$ | 0.02435446430443 | 0.04569622953948 | 2.30544327515634 |
| $S_6^1(\Delta_1)(E^2)$ | 0.05192221382849 | 0.09028894126441 | 2.08943150184926 |
| $S_6^1(\Delta_2)(E^3)$ | 0.00901424186606 | 0.00447771701237 | 0.300999855221215 |
| $S_6^1(\Delta_2)(E^2)$ | 0.01755117759007 | 0.00957941977496 | 0.61173496632118 |
| $S_6^1(\Delta_3)(E^3)$ | $8.507097138034103e-004$ | $8.483952232785086e-004$ | 0.03632526957430 |
| $S_6^1(\Delta_3)(E^2)$ | 0.00207573909188 | 0.00103445079261 | 0.09694695263925 |
| $S_6^1(\Delta_4)(E^3)$ | $1.447067891197085e-004$ | $1.002341249083383e-004$ | 0.00271119947541 |
| $S_6^1(\Delta_4)(E^2)$ | $1.455537539193363e-004$ | $6.509319827019411e-005$ | 0.00701754668327 |

Table 5.5: Maximal Errors of Hermite Interpolation with Second Order and Third Order Energy Functionals for $S_f \in S_6^1(\Delta)$.

*From the Table 5.5, we know that Hermite interpolation spline in $S_6^1(\Delta)$ with energy functional $E^3$ approximates the original function much better than the one with energy functional $E^2$.*

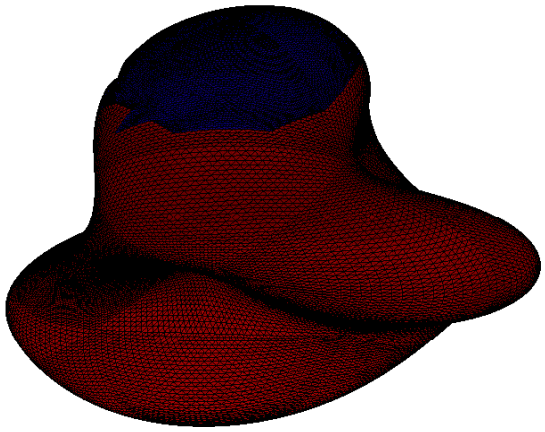

Figure 5.1: $C^1$ Hole filling in $S_5^1(\Delta)$ for data with one hole .

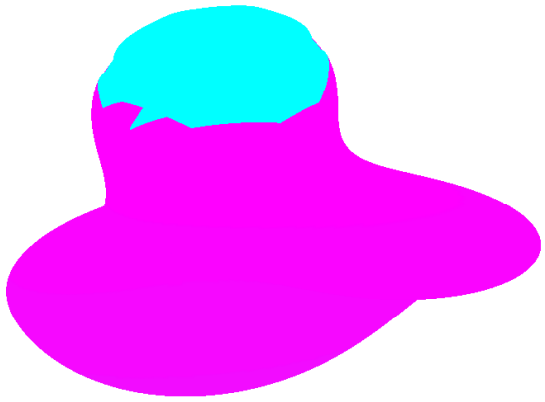

Figure 5.2: $C^2$ Hole filling in $S_8^2(\Delta)$ for data with one hole .

Example 5.2.1. *We consider centralizble data sets and fill one hole with $C^1$ and $C^2$ continuity, also do the same thing for two holes. First we consider one hole data sets. In Fig. 4.1 we show the original points, and in Fig. 4.2 we give one spherical triangulation of these points. To fill the hole, we first project these points to unit sphere to get the spherical triangulation. Then we can use the method in Chapter 4 to fill the hole with $C^r$ continuity.*

*The Fig. 5.1 shows $C^1$ filling hole, and Fig. 5.2 is the $C^2$ case.The spline surfaces look fair and smooth.*

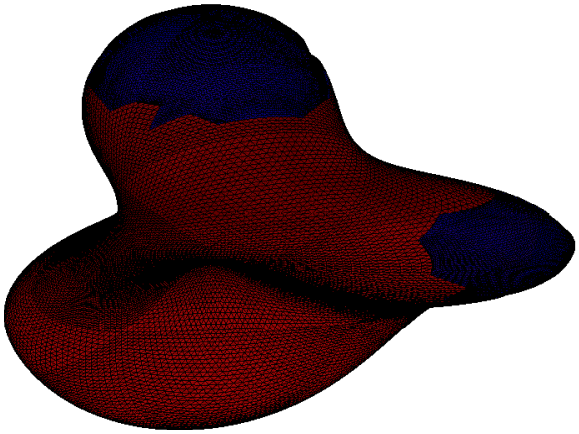

Figure 5.3: $C^1$ Hole filling $S_5^1(\Delta)$ for data with two holes .

*Second, we deal with data sets with two holes, see Fig. 4.3 for original data and Fig. 4.4 for spherical triangulation. And we show the $C^1$ hole filling in Fig. 5.3.*

EXAMPLE 5.2.2. *We consider filling holes of surfaces with different differentiable continuity. For noncentralizable data sets of head in Fig. 4.11, we preprocess them to get the cetralizable data sets as shown in Fig. 4.12.*

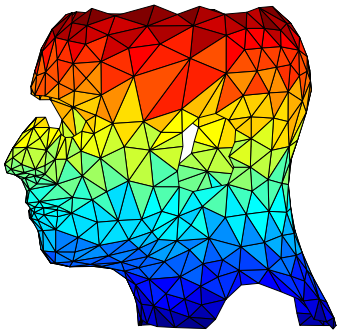

Figure 5.4: The modified head data with missing top.

*Then we first take off the top of the modified head data and get the triangulation with missing top as shown in Fig. 5.4.*

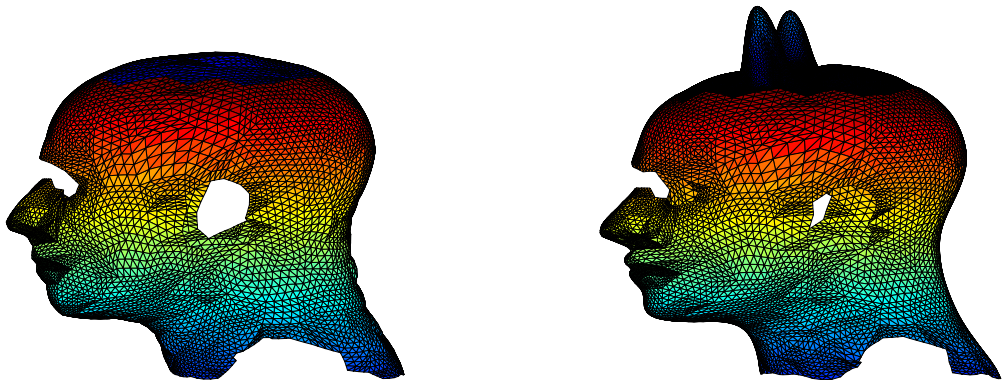

Figure 5.5: $C^0$ hole filling surface in $S_2^0(\Delta)$ (left) and a $C^1$ quintic spline hole filling with horns(right).

*In the left of Fig. 5.5 , we show $C^0$ hole filling using $S_2^0(\Delta)$ with partial interpolation of missing data points, the figure looks continuous. In the right of Fig. 5.5,we give a $C^1$ hole filling spherical spline surface with a few data values over the missing top to create two horns on the top of head. We repeat the experiments by using $C^2$ spline space $S_8^2(\Delta)$. For simplicity, we only show a $C^2$ spherical spline surface which interpolates the values and derivative values from the boundary of the missing top.*

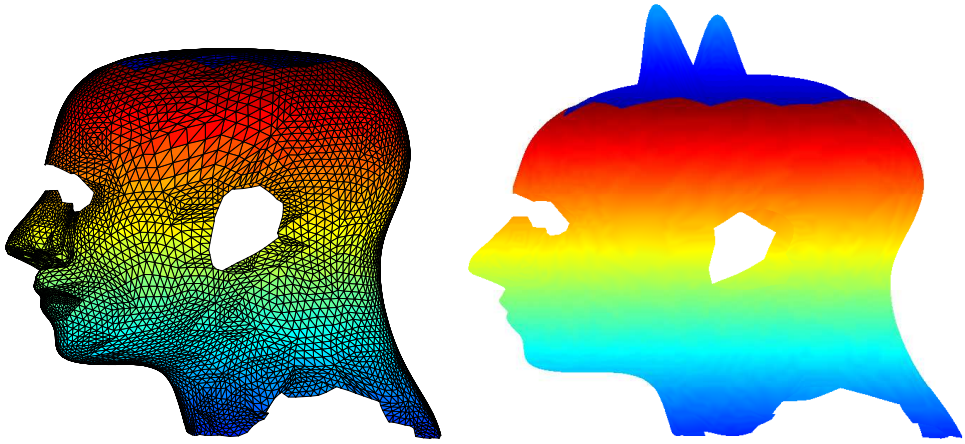

*Figure 5.6: A $C^1$ hole filling in $S_5^1(\Delta)$ without interpolation(left) and $C^2$ hole filling in $S_8^2(\Delta)$ with horns (right).*

## 5.3 Numerical Experiments for Point Cloud

Example 5.3.1. *In this example, we consider the modified head data and get global $C^1$ and $C^2$ surface. The spherical triangulation of the modified head data is shown in the right of Fig. 4.12. The following figures show the spherical spline surfaces to interpolate the modified head data with $C^1$ and $C^2$ continuity.*

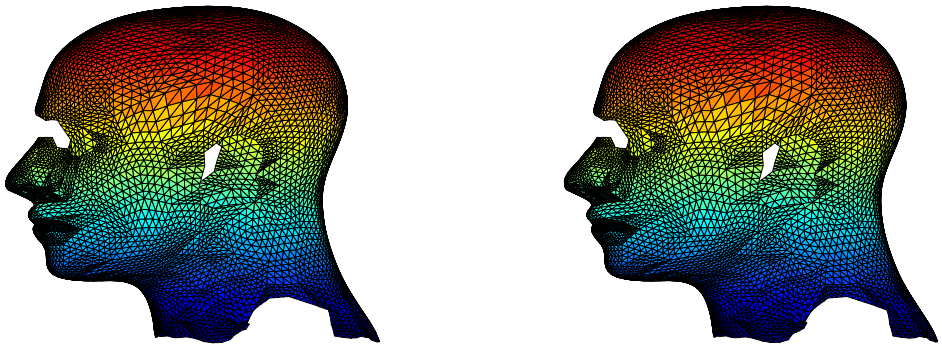

Figure 5.7: $C^1$ interpolatory spline surface in $S_5^1(\Delta)$(left) and $C^2$ interpolatory spline surface in $S_8^2(\Delta)$(right).

Example 5.3.2. *We consider centralizable data as shown in Fig. 4.9 and Fig. 4.10. Its spherical triangulation is shown in the following figure.*

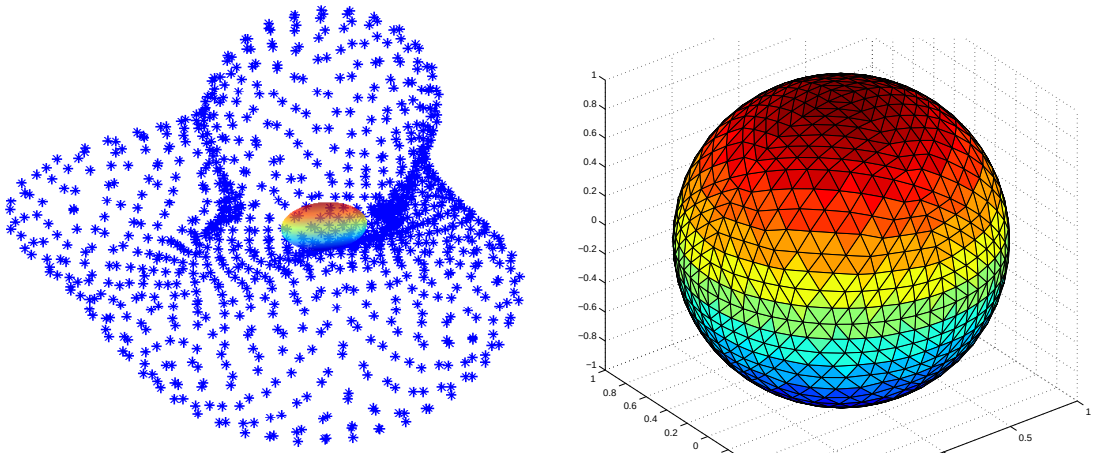


Figure 5.8: Original scattered data(left) and its spherical triangulation(right).

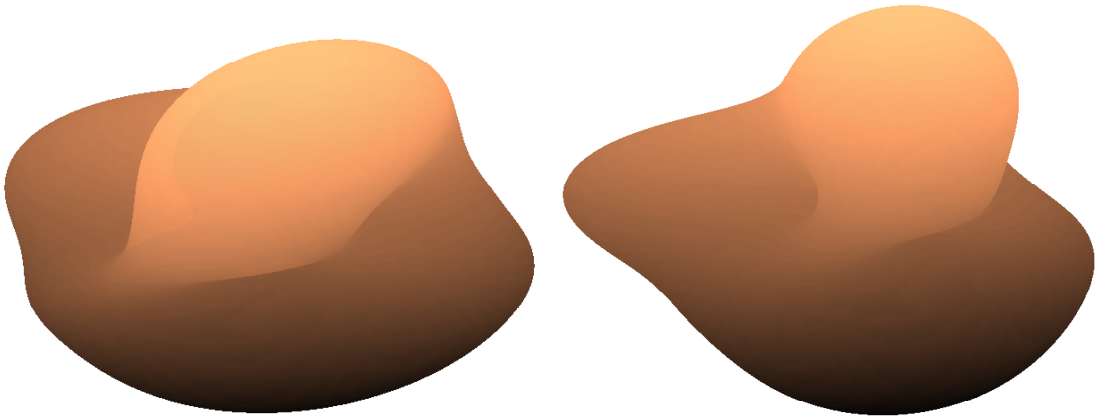

Figure 5.9: $C^1$ interpolatory spline surface in $S_5^1(\Delta)$ from different view points.

Figure 5.10: $C^1$ interpolatory spline surface in $S_5^1(\Delta)$ from different view points.

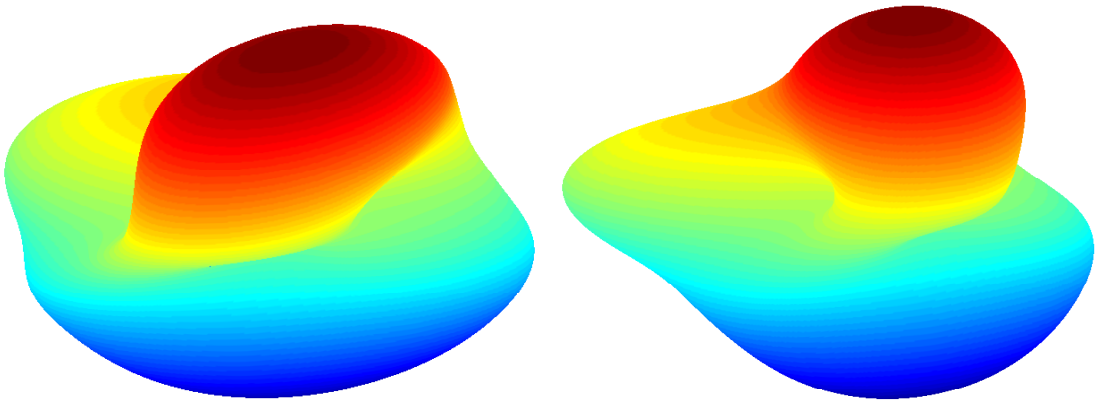

Figure 5.11: $C^2$ Hermite interpolatory spline surface with $l = 1$ in $S_8^2(\Delta)$ from different view points.

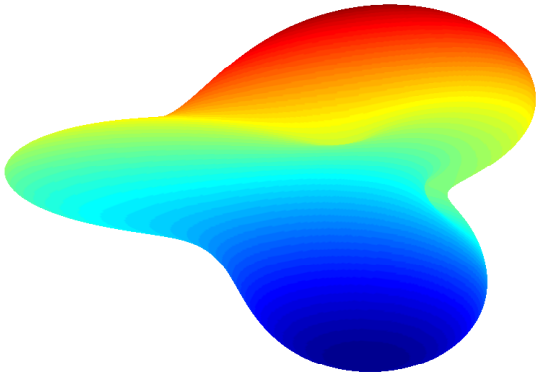

Figure 5.12: $C^2$ Hermite interpolatory spline surface with $l = 1$ in $S_8^2(\Delta)$ from different view points.

*Fig. 5.9 and Fig. 5.10 show the $C^1$ spline surfaces to interpolate the given data sets. And Fig. 5.11 and Fig. 5.12 are $C^2$ Hermite interpolatory spline surface to interpolate the given data sets and their first order derivatives. To ivestigate the global continuity, we draw the graphs of the derivatives of spline surfaces to see whether they are continuous or not. If they*

*looks continuous, then the spline surfaces are differentiable up to the given order derivatives. We show the figures of derivatives with repect to $\theta$ and $\phi$ like the following.*

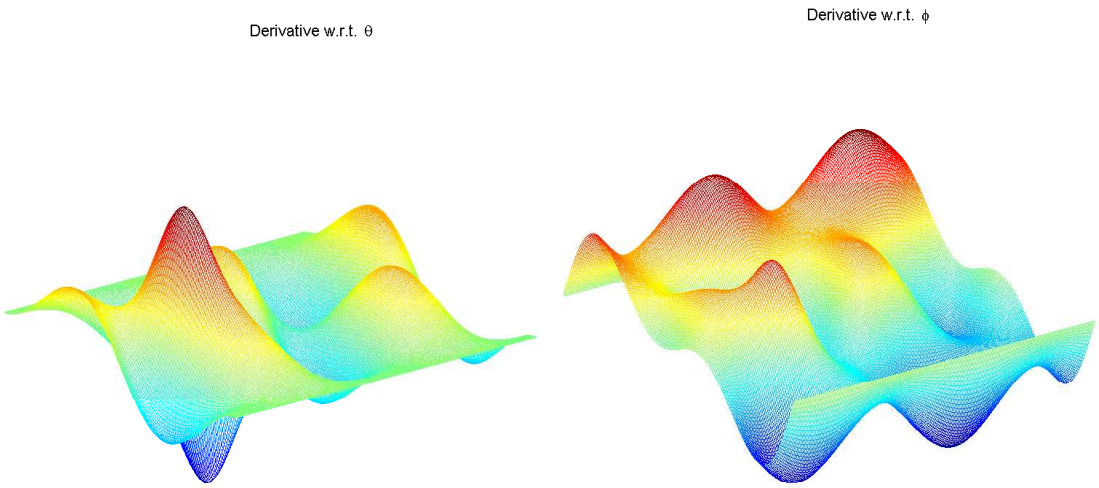


Figure 5.13: First order derivatives w.r.t. $\theta$(left) and w.r.t. $\phi$(right) for $C^1$ interpolatory spline surface in $S_5^1(\Delta)$ .

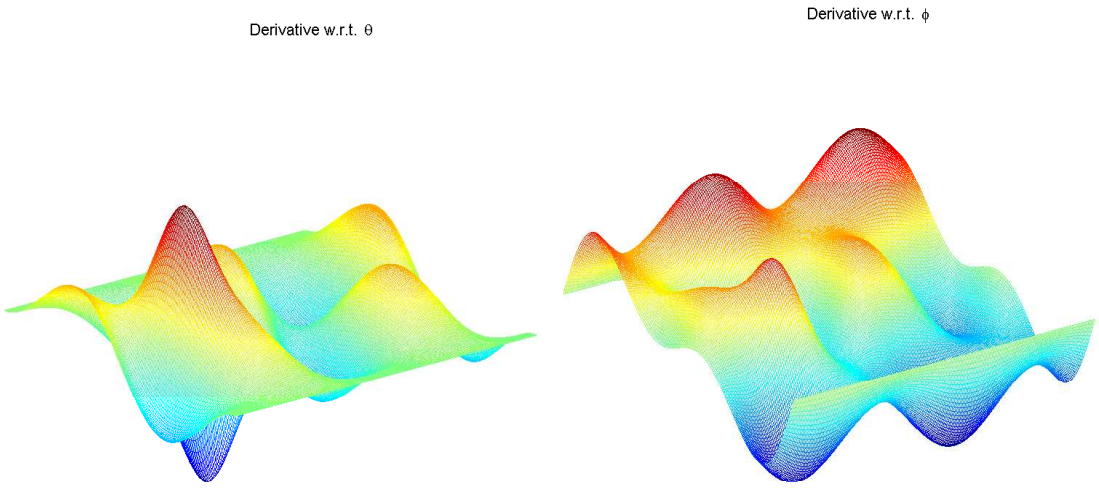


Figure 5.14: First order derivatives w.r.t. $\theta$(left) and w.r.t. $\phi$(right) for $C^2$ interpolatory spline surface in $S_8^2(\Delta)$ .

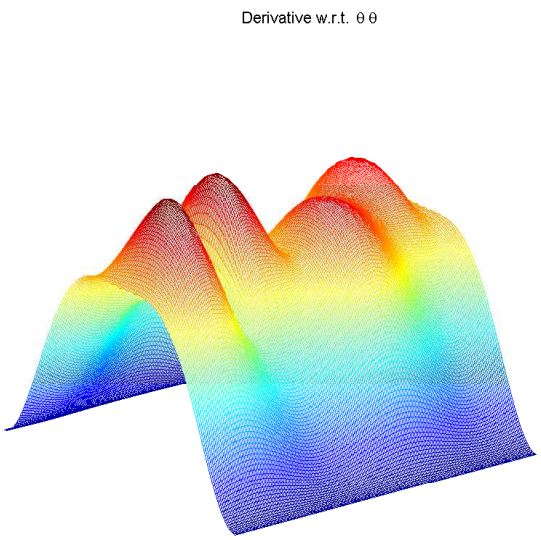


Figure 5.15: Second order derivative w.r.t. $\theta\theta$ for $C^2$ interpolatory spline surface in $S_8^2(\Delta)$ .

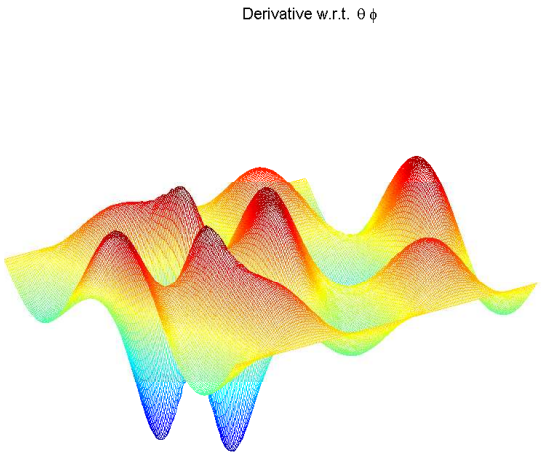


Figure 5.16: Second order derivative w.r.t. $\theta\phi$ for $C^2$ interpolatory spline surface in $S_8^2(\Delta)$ .

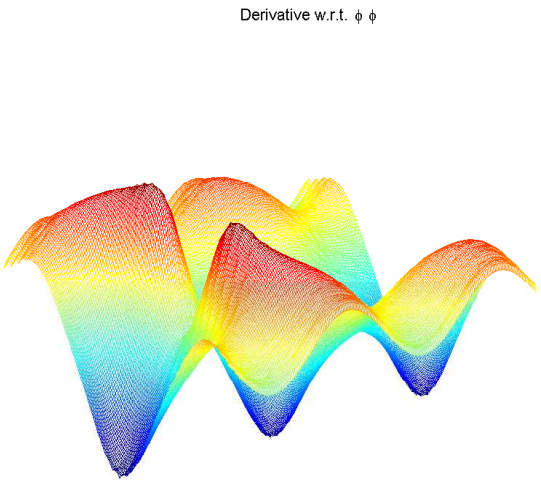


Figure 5.17: Second order derivative w.r.t. $\phi\phi$ for $C^2$ interpolatory spline surface in $S_8^2(\Delta)$ .

*From Fig. 5.13, we know the interpolatory spline surface is $C^1$. And Fig. 5.14, Fig. 5.15, Fig. 5.16 and Fig. 5.17 demonstrate the interpolatory spline surface is $C^2$.*

EXAMPLE 5.3.3. *In this example, we create a mushroom with $C^1$ continuity. Our spline surfaces are in $S_6^1(\Delta)$. We implement it by using the minimal energy Hermite interpolation method with $l = 1$. Our surfaces look smooth and fair.*

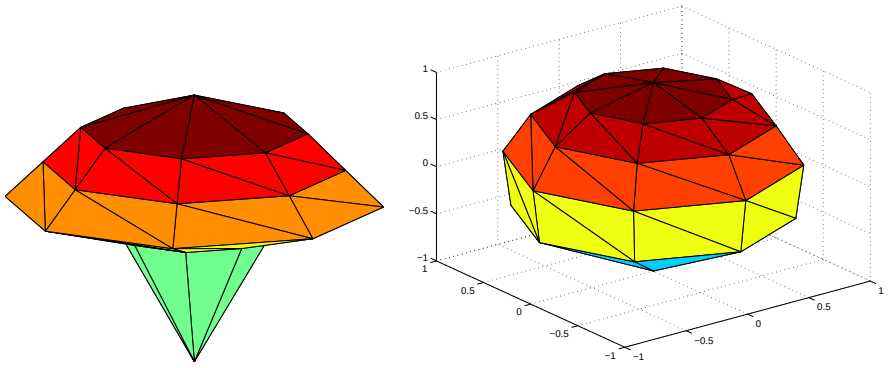


Figure 5.18: The mushroom data(left) and its spherical triangulation(right).

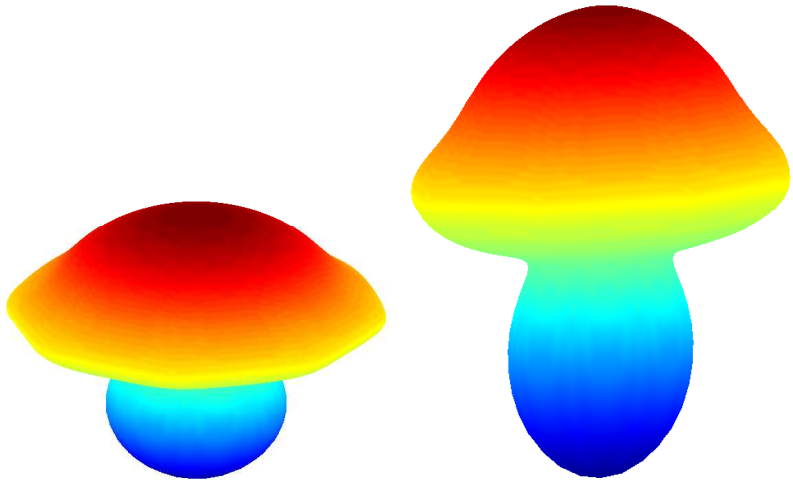

Figure 5.19: The $C^1$ interpolatory mushroom in $S_6^1(\Delta)$ from different point of view.

EXAMPLE 5.3.4. *In this example, we create a mushroom with $C^2$ continuity. Our spline surfaces are in $S_9^2(\Delta)$. We implement it by using the minimal energy Hermite interpolation method with $l = 2$. Our surfaces look smooth and fair.*

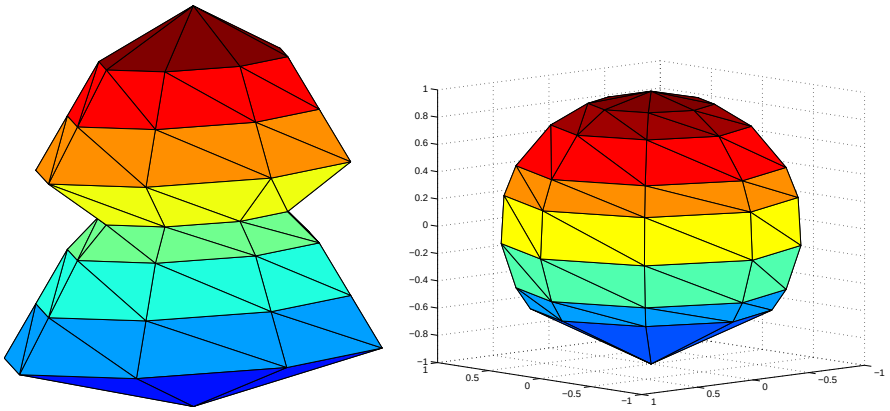


Figure 5.20: The gourd data(left) and its spherical triangulation(right).

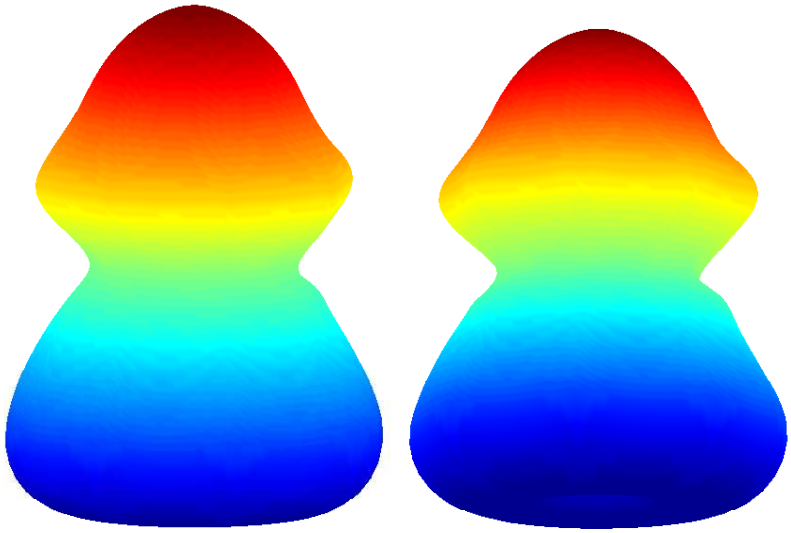

Figure 5.21: The $C^2$ gourd in $S_9^2(\Delta)$ from different point of view.

## 5.4 Conclusion and Future Work

For a spherical triangulation $\Delta$ which is a part of a sphere with or without holes, or the whole sphere and the domain bounded by $\Delta$ in general can not be converted to a planar domain, we get the following results:

(1) Given a set of scattered data with derivatives, we use minimal energy method to construct Hermite interpolation on spherical spline spaces over a spherical triangulation $\Delta$ of the scattered data locations. Then we show that the minimal energy method produces a unique Hermite spherical interpolation spline of given scattered data with derivatives. Finally we show that the Hermite interpolation spline converges to a given sufficiently smooth function $f$ in $L_2$ and $L_\infty$ norm if the values are obtained from this $f$. Hence the surface of the Hermite spherical interpolation spline resembles the given set of derivatives.

(2) For any integer $r \geq 0$, we first give a method of $C^r$ hole filling using the minimal energy quasi-Hermite interpolation over a spherical triangulation of polygonal holes on

the sphere. Then we have implemented several numerical experiments for $r = 0,\ 1,$ and $2$ to demonstrate our method.

(3) For any integer $r \geq 0$, we deal with centralizable point cloud by using the minimal energy Hermite interpolation method or quasi-Hermite interpolation method to get the surface with global $C^r$ continuity. Our surface can interpolate data locations and derivatives up to $r$th order if they are given. Also we implemented experiments for $r = 0,\ 1,$ and $2$ to show our method.

Some advantages are that all constrained conditions can be generalized to a solvable linear system and our method is applicable to $C^r$ case for any integer $r \geq 0$. The shape control is local although the solution is global. The figures look smooth and fair.

Our requirement of centralizable data may be too constrained for some application although it is good for data given on sphere $\mathbb{S}^2$. For non-centralizable data, we either divide it into several centralizable data sets with different centers or study the new methods to construct surfaces defined on surfaces. Hence it is necessary to study how to connect two sets of point clouds of different centers together, or the surfaces defined on surfaces(cf. [13]). We leave them to our future studies.

Another work we would like to do is to find some practical applications in global warming data process for our methods. Global warming refers to the increase in the average temperature of the Earth's near-surface air and oceans in recent decades and its projected continuation. It has aroused extensive interests of scientists and politicians. Scientists have studied global warming with computer models of the climate. These models are based on physical principles of fluid dynamics, radiative transfer, and other process, with some simplifications being necessary because of limitations in computer power. These models predict that the net effect of adding greenhouse gases is to produce a warmer climate ( cf. *http : //en.wikipedia.org/wiki/Global_warming* ). We hope to use our spherical spline methods developed in this dissertation to approximate climate model more accurately, deal with the collected temperature data more efficiently.

# Bibliography


[1] Adams, R., *Sobolev Spaces*, Academic Press, New York, 1975.

[2] Alfeld, P., M. Neamtu, and L. L. Schumaker, Circular Berstein-Bézier polynomials, in Mathematical Methods for Curves and Sorfaces, Morten Dæhlen, Tom Lyche, Larry L. Schumaker(eds), Vanderbilt University Press, Nashville & London, 1995, 11–20.

[3] Alfeld, P., M. Neamtu, and L. L. Schumaker, Berstein-Bézier polynomials on spheres and sphere-like surfaces, Comp. Aided Geom. Design. **13** (1996), 333–349.

[4] Alfeld, P., M. Neamtu, and L. L. Schumaker, Fitting scattered data on sphere-like surfaces using spherical splines, J. Comp. Appl. Math. **73** (1996), 5-43.

[5] Alfeld, P., M. Neamtu, and L. L. Schumaker, Dimension and local bases of homogeneous spline spaces, SIAM J. Math. Anal. **27** (1996), 1482-1501.

[6] Atkinson, K. E., *An Introduction to Numerical Analysis*, John Wiley and Sons, New York,1978.

[7] Aubin, T., *Nonlinear Analysis on Manifolds. Monge-Ampeòre Equations*, Springer-Verlag, 1982.

[8] Awanou, G. M. and M. J. Lai, On Convergence Rate of the Augmented Lagrangian Algorithms for Non symmetric Saddle Point Problems, Journal of Applied Numerical Mathematics, **54**(2005), 122–134.

[9] Awanou, G. M., M. J. Lai, and P. Wenston, The Multivariate Spline Method for Numerical Solution of Partial Differential Equations and Scattered Data Interpolation,

*Wavelets and Splines*, Edited by G. Chen and M. J. Lai, Nashboro Press, Brentwood, Tennessee, 2006, pp. 24–76.

[10] Baramidze, V. and M. J. Lai, Error Bounds for minimal energy interpolatory spherical splines, Approximation Theory XI, edited by C. K. Chui, M. Neamtu, and L. L. Schumaker, Nashboro Press, Brentwood, 2005, pp. 25–50.

[11] Baramidze, V., M. J. Lai, and C. K. Shum, Spherical Splines for Data Interpolation and Fitting, SIAM J. Scientific Computing **28**(2006), 241–259

[12] Baramidze, V., S. C. Han, M. J. Lai, C. K. Shum, and P. Wenston, Triangulated spherical splines for geo-potential reconstruction, submitted, 2006.

[13] Barnhill, R.E., Surfaces in computer aided geometric deign: A survey with new results, Comp. Aided Geom. Design. **2** (1985), 1–17.

[14] Böhm, Wolfgang, G. Farin and J. Jürgen, A survey of curve and surface methods in CAGD, Comp. Aided Geom. Design. **1** (1984), 1–60.

[15] Cao,Y. P., O. Terlyga, J. Van Laarhoven, J. B. Wu, G. R. Xue and P. Zhang, Web-spline finite elements, team2 report: IMA Mathematical Modeling Workshop (2006), Institute of Mathematical and Its Applications, to appear.

[16] Chui, C. K., M. J. Lai, Filling polygonal holes using $C^1$ cubic triangular spline patches,Computer Aided Geometric Design **17**(2000), 297–307.

[17] de Boor, C., A bound on $L_\infty$ norm of $L_2$ approximation by splines in terms of a global mesh ratio, Math. Comp. **30**(136) (1976), 765–771.

[18] Davydov, O., and L. L. Schumaker, On stable local bases for bivariate polynomial spline spaces, Constr. Approx. **18** (2001), 87–116.

[19] Evans, L. C., *Partial Differential Equations*, American Mathematical Society, 1998.

[20] Farin, Gerald, Triangular Bernstein-Bézier patches, Comp. Aided Geom. Design. **3** (1986), 83–127.

[21] Farmer, K. and M. J. Lai, Scattered data interpolation by $C^2$ quintic splines using energy minimization, Approximation Theory IX, edited by C. K. Chui, and L. L. Schumaker, Nashboro Press, Brentwood, 1998, pp. 47–54.

[22] Fasshauer, G. and L. L. Schumaker, Scattered Data Fitting on the Sphere, Mathematical Methods for Curves and Surfaces II, M. Daehlen, T. Lyche, and L. L. Schumaker (eds.), Vanderbilt Univ. Press, 1998, 117–166.

[23] Fasshauer, G. E. and L. L. Schumaker, Multi-patch parametric surfaces with minimal energy, Comp. Aided. Geom. Design **13** (1996), 45–79.

[24] Fasshauer, G. E., and L. L. Schumaker, Minimal energy surfaces using parametric splines, Comp. Aided Geom. Design. **13** (1996), 45–76.

[25] Freeden, Willi, V. Michel and H. Nutz, satellite-to-satellite tracking and satellite gravity gradiometry( Advanced techniques for high-resolution geopotential field determination), Journal of Engineering Mathematics **43** (2002), 19–56.

[26] von Golitschek, M., M. J. Lai, and L. L. Schumaker, Error bounds for minimal energy interpolatory splines, Numerishe Math., **93** (2002), 315–331.

[27] von Golitchek, M., and L. L. Schumaker, Bounds on projections onto bivariate polynomial spline spaces with stable local bases, Constr. Approx. **18** (2002), 241–254.

[28] von Golitchek, M., and L. L. Schumaker, Penalized Least Square Fitting, Algorithms for Approximation II, J.Mason and M. G. Cox (eds.), Chapman and Hall, London (1990), 210–227.

[29] Gomide, A., and J. Stolfi, Nonhomogeneous polynomial $C^k$ splines on the sphere $S^n$, Relatorio Tecnico IC-00-13, 2000.

[30] Gregory, J.A. and J.M. Hahn, A $C^2$ polygonal surface patch, Comp. Aided Geom. Design. **6** (1989), 391–410.

[31] Gregory, J.A. and J. Zhou, Filling polygonal holes with bicubic patches, Comp. Aided Geom. Design. **11** (1994), 69–75.

[32] Hahn, J., Filling polygonal holes with rectangular patches, in: Theory and Practice of Geometric Modeling (1989), 81-91.

[33] Höllig, Klaus, Finite element methods with B-splines, SIAM Society for industrial and applied mathematics, Philadelphia, 2003.

[34] Jones, A. K., Nonrectangular surface patches with curvature continuity, Comuter-Aided Design **20(6)**(1988), 325–335.

[35] Lai, M. J., and L. L. Schumaker, On the approximation power of bivariate splines, Adv. in Comp. Math. **9** (1998), 251–279.

[36] Lai, M. J. and P. Wenston, Bivariate Splines for Fluid Flows, Computers and Fluids 33(2004), pp. 1047–1073.

[37] Lai, M. J. and L. L. Schumaker, Spline Functions over Triangulations, Cambridge University Press, April 30, 2007.

[38] Le Gia, Q.T., Galerkin Approximation for Elliptic PDEs on Spheres, Journal of Approximation Theory **130** (2004), 123–147.

[39] Lions, J., and E. Magenes, *Non-Homogeneous Boundary Value Problems and Applications I*, Springer-Verlag, 1972.

[40] Neamtu, M., and L. L. Schumaker, On the approximation order of splines on spherical triangulations, Adv. in Comp. Math. **21** (2004), 3–20.

[41] Wahba, G., Spline interpolation and smoothing on the sphere, SIAM J. Sci. Statist. Comput. **2** (1981), 5–16.

[42] Wahba, G., Vector Splines on the Sphere with applications to the estimation of vorticity and divergence from discrete noisy data, Technical report no. 674, Department of Statistics, University of Wisconsin-Madison, 1982.

[43] Willmore, T.J., *Riemannian Geometry*, Oxford University Prtess, New York, U.S.A., 1997.

[44] Wu, J. B., L. Z. Ma, T. G. Jin and G. Z. Wang, The Construction of $G^2$ Continuous Surface on Irregular Topological Meshes, Progress in Natural Science, **8(2)** (1998), 142–149.

[45] Wu, J. B. and P. J. Zhang, Application of Circulant Matrix on Surface Modeling, Journal of Guangdong University of Technology, **15(1)** (1998), 83–89.

[46] Wu, J. B. and S. P. Wu, Nonhomogeneous Second Order Singular Hamiltonian Systems, Journal of Zhejiang University, **30(3)** (1996), 253–260.

[47] Wu, J. B. and P. J. Zhang. Necessary Conditions of Optimal Control under Mixed State-Control Constraints, Journal of Guangzhou Normal University, **20(7)** (1999), 12–17.

[48] Zhou, T., D. Han, M. J. Lai, Energy Minimization Method for Scattered Data Hermite Interpolation, accepted for publication in Applied Numer. Math. 2007.